

Low Temperature Active-Screen Plasma Surface Alloying of Precipitation Hardening Stainless Steels



University of Birmingham

A thesis submitted for the degree of

Master of Research (MRes)

By

Louise Cook

School Metallurgy and Materials
The University of Birmingham

June 2012

UNIVERSITY OF
BIRMINGHAM

University of Birmingham Research Archive

e-theses repository

This unpublished thesis/dissertation is copyright of the author and/or third parties. The intellectual property rights of the author or third parties in respect of this work are as defined by The Copyright Designs and Patents Act 1988 or as modified by any successor legislation.

Any use made of information contained in this thesis/dissertation must be in accordance with that legislation and must be properly acknowledged. Further distribution or reproduction in any format is prohibited without the permission of the copyright holder.

Synopsis

Precipitation hardening stainless steels are used for a variety of applications in a vast range of industries due to their combination of high mechanical properties, good corrosion resistance and an appropriate level of wear resistance for certain applications.

Despite this, the properties of these steels still need to be improved to fit the further requirements needed for more demanding applications. This work has investigated the response of 17-4PH and 17-7PH stainless steels to active screen plasma nitriding and active screen plasma carburising. The main focus was on mechanical properties, corrosion, wear resistance and the formation of the S-phase.

The active screen plasma nitriding treatments were conducted for 20 hours at 350°C, 390°C and 430°C in a gas mixture of 25%N₂ + 75H₂ and active screen plasma carburising treatments were conducted at 370°C, 410°C and 450°C in a gas mixture of 1.5%CH₄ and 98.5%H₂. The thickness of the plasma alloyed layer on both steels increase with the increase in the treatment temperature for both plasma nitriding and carburising.

The present work has shown for the first time that S-phase can be produced in the surface of 17-7PH stainless steel by active screen plasma nitriding at 350, 390 and 430°C and by active screen plasma carburising at 370 and 410°C. The plasma nitrided layer consists of S-phase, nitrogen containing martensite and Fe₃N while the plasma carburised layer is mainly composed of S-phase embedded with carbides.

Experimental results have demonstrated that active screen plasma nitriding and plasma carburising can effectively increase the surface hardness of 17-7PH by about 6-7 times and 17-4PH stainless steels by about 7-8 times over the untreated material.

The wear resistance of both materials has also been improved through these plasma treatments mainly due to the increase surface hardness and change of the change of wear mode from severe adhesive/delamination wear to mild oxidative wear. The 430°C nitriding and 410°C carburising produce the best improvement (~ 3.5 times) in wear resistance of 17-7 PH steel; the 390°C nitriding and 450°C carburising produce the best improvement (~ 100 times) in wear resistance of 17-4 PH steel.

The electrochemical corrosion and salt spray resistance of 17-7PH stainless steel can be improved by active screen plasma nitriding at 350, 390 and 430 °C. Plasma carburising at 370 and 410 °C can effectively enhance electrochemical corrosion resistance but their salt spray resistance is similar to or marginally lower than that of the untreated material. For 17-4PH steel, only plasma nitriding at 350°C and plasma carburising at 370°C can improve its corrosion resistance.

In short, it is possible to form S-phase in 17-7PH steel by low-temperature active-screen plasma surface alloying and to achieve combined improvement in surface hardness, tribological (wear and friction) properties and corrosion resistance of 17-4PH and 17-7PH stainless steels active-screen plasma surface alloying at low-temperature.

Contents

List of Tables	5
List of Figures.....	5
Chapter 1 – Introduction.....	11
Chapter 2 - Literature Review.....	13
2.1 Stainless Steel	13
2.1.1 Introduction	13
2.1.2 Alloying and classification	13
2.1.3 Precipitation hardening stainless steels	15
2.2 Wear and Corrosion	16
2.2.1 Wear of stainless steel.....	16
2.2.2 Corrosion	19
2.3 Surface Engineering.....	21
2.3.1 Introduction	21
2.3.2 Thermochemical treatment	22
2.3.3 The S-phase	25
2.3.4 Plasma treatment of PH stainless steels.....	28
Chapter 3: Experimental.....	30
3.1 Materials	30
3.2 Sample Preparation	31
3.3 Surface Treatments.....	31
3.4 Characterisation	32
3.4.1 Preparing cross-sections	32
3.4.2 Microstructure - SEM	32
3.4.3 Phase composition – XRD	33
3.4.4 Microstructure and phases – TEM	33
3.4.5 Chemical composition - GDOES.....	33
3.5 Mechanical Properties Assessment	34
3.5.1 Micro-hardness	34
3.5.2 Load bearing capacity.....	35
3.5.3 Wear testing.....	35
3.6 Corrosion Properties Assessment.....	35
3.6.1 Electrochemical testing.....	35
3.6.2 Salt Spray	36
Chapter 4 – Experimental Results.....	37

4.1 Surface morphology and Layer Structures	37
4.1.1 17-4PH stainless steel	38
4.1.2 17-7PH stainless steel	42
4.2 Chemical Composition	45
4.2.1 17-4PH stainless steel	45
4.2.2 17-7PH Stainless Steel	48
4.3 Phase Composition of the Surface Layers	52
4.3.1 17-4PH Stainless Steel	52
4.3.2 17-7PH stainless steel	53
4.3.3 TEM characterisation	59
4.4 Hardness and Layer Thickness	68
4.4.1 17-4PH	68
4.4.2 17-7PH	70
4.5 Friction and Wear	73
4.5.1 17-4PH	73
4.5.2 17-7PH	75
4.6 Corrosion Resistance	81
4.6.1 Salt Spray	81
4.6.2 Electrochemical corrosion	87
Chapter 5 – Interpretation and Discussion	96
5.1. Response of 17-4PH and 17-7PH to Low Temperature Active Screen Plasma Alloying	96
5.2 Towards Combined Wear and Corrosion Resistance by Low Temperature Active Screen Plasma Alloying.	99
5.2.1 The Nitriding Effect	99
5.2.2 The Carburising Effect	104
Chapter 6 – Conclusions	107
Chapter 7 – Further Work	110
References	111

List of Tables

- Table 3.1 Chemical composition of 17-4 and 17-7 PH stainless steels
- Table 3.2 Sample code and treatment conditions
- Table 4.6-1 The corrosion potential and pitting potential of untreated, plasma nitrided and plasma carburised 17-4PH samples.
- Table 4.6-2 The corrosion potential and pitting potential of untreated, plasma nitrided and plasma carburised 17-7PH sample.

List of Figures

- Figure 2.1 Optical microscopy shows ferrite stringers and fine carbide precipitates within the martensitic matrix. 17-7PH stainless steel (Totten, 2006)
- Figure 2.2 The microstructure of 17-4PH stainless steel plasma nitrided at 420°C (Esfandiari & Dong, 2007).
- Figure 3.1 Preparation of cross-sectional TEM sample a) Pre-thinning XTEM sample; b) SEM image of FIB preparing XTEM sample.
- Figure 4.1-1 SEM images of etched as-received a) 17-4PH and b) 17-7PH samples; c) plasma nitride and d) plasma carburized 17-4PH samples; e) plasma nitrided and f) plasma carburized 17-7PH samples.

- Figure 4.1-2 The layer structures of active screen plasma nitride 17-4PH stainless steel samples at various temperatures a) 4PN350 b) 4PN390 c) 4PN430.
- Figure 4.1-3 SEM images from plasma carburised samples of 17-4PH steel a) 4PC370 b) 4PC410 and c) 4PC450
- Figure 4.1-4 The layer structures of active screen plasma nitride 17-7PH stainless steel samples at various temperatures a) 7PN350 b) 7PN390 and c) 7PN420
- Figure 4.1-5 SEM images from plasma carburised samples of 17-7PH steel a) 7PC370 b) 7PC410 and c) 7PC450.
- Figure 4.2-1 Typical GDOES profile showing the composition of 430°C plasma nitrided 17-4PH stainless steel sample.
- Figure 4.2-2 GDOES profile showing the nitrogen content in plasma nitrided 17-4PH stainless steel samples, treated at 3 different temperatures.
- Figure 4.2-3 GDOES profile of plasma carburised 4PC410 sample.
- Figure 4.2-4 A GDOES carbon profile of plasma carburised 17-4PH stainless steel samples, treated at various temperatures.
- Figure 4.2-5 GDOES composition profiles of 7PN430 sample.
- Figure 4.2-6 GDOES profiles to show the nitrogen content within plasma nitrided 17-7PH stainless steel samples treated at various temperatures.

- Figure 4.2-7 The carbon content in 17-7PH stainless steel during plasma carburising treatments at various temperatures.
- Figure 4.3-1 XRD patterns of a) as received and plasma nitrided samples under varying conditions; b) plasma carburised 4PN430 sample with inserted possible phase reference lines.
- Figure 4.3-2 XRD patterns of a) as received and plasma carburised samples under varying conditions; b) plasma carburised 4PC450 sample with inserted possible phase reference lines.
- Figure 4.3-3 The XRD patterns of 17-7PH stainless steel samples a) as-received and plasma nitride samples under varying conditions; b) plasma nitride 7PN390 sample with inserted possible phase reference lines.
- Figure 4.3-4 The XRD patterns of as-received and plasma carburised 17-7PH stainless steel samples.
- Figure 4.3-5 TEM microstructure and SAD patterns of as-received a, b) 17-4PH steel sample (b=111), c, d & e) 17-7PH steel sample.
- Figure 4.3-6 a), c) BF and d), e) DF TEM microstructures and b) SAD pattern, taken from surface nitrided layer of 7PN350 sample.
- Figure 4.3-7 a) TEM microstructure and SAD patterns of b) top dark area in a), b=[101]_{ε-Fe₃C}; d) centre area in a), and c), d) index of b), c) from plasma carburised 7PC410 sample of 17-7PH stainless steel.
- Figure 4.3-8 a) BF XTEM microstructure of surface layer and b) DF XTEM of χ -Fe₅C₂ carbide taken by c) SAD pattern of χ -Fe₅C₂ diffraction spot

and d) index of c) from sample 4PC410 17-4PH stainless steel plasma carburised at 410°C.

Figure 4.3-9) a) Cross section DF TEM image taken by b) Cr₂₃C₆ carbide diffraction spots, as circled, from sample 4PC410 17-4PH stainless steel plasma carburised at 410°C.

Figure 4.4 -1 The surface hardness of plasma nitrided (PN) and carburised (PC) 17-4PH stainless steel samples as a function of treatment temperatures.

Figure 4.4-2 The layer thickness of plasma nitrided (PN) and carburised (PC) 17-4PH stainless steel samples as a function of treatment temperature.

Figure 4.4-3 The surface hardness of plasma nitrided (PN) and carburised (PC) 17-7PH stainless steel samples as a function of treatment temperature.

Figure 4.4-4 The thickness of plasma nitrided (PN) and plasma carburised (PC) 17-7PH stainless steel samples as a function of treatment temperature.

Figure 4.5-1 The friction coefficients of untreated (UT), plasma nitride (PN) and carburised (PC) 17-4PH stainless steel samples.

Figure 4.5-2 The wear volume loss of untreated (UT), plasma nitride (PN) and carburised (PC) 17-4PH stainless steel samples.

Figure 4.5-3 SEM microstructures of wear track on untreated sample

- Figure 4.5-4 SEM microstructures of wear track on 4PN390 sample
- Figure 4.5-5 SEM microstructures of wear track on 4PC 450 sample
- Figure 4.5-6 The friction coefficients of untreated, plasma nitrided and plasma carburised 17-7PH stainless steel samples.
- Figure 4.5-7 The wear volume loss of untreated, plasma nitrided and plasma carburised 17-7PH stainless steel samples.
- Figure 4.5-8 SEM micrographs of wear tracks n 17-7PH samples; a) untreated b)7PN 430 c) 7PC 410.
- Figure 4.5-9 a) SEM image of a wear track on 7PC410 sample and b) corresponding EDX analysis.
- Figure 4.6-1 Photographs of salt-spray tested 17-4PH samples: a) untreated (4UNT); plasma nitrided b) 4PN350, c) 4PN390 and d) 4PN430; and plasma carburised 4PC370 f) 4PC410 and g) 4PC450.
- Figure 4.6-2 The weight change of 17-4Ph stainless steel samples plasma nitrided (PN) and plasma carburised (PC) at various temperatures.
- Figure 4.6-3 Photographs of salt-sprayed 17-7PH stainless steel samples; a) untreated (UT); plasma nitrided b) 7PN350, c) 7PN390 and d) 7PN430; and plasma carburised e) 7PC410 and g) 7PC450.
- Figure 4.6-4 The weight changes of 17-7PH stainless steel samples plasma nitride (PN) and plasma carburised (PC) at various temperatures.
- Figure 4.6 -5 The potentiodynamic curves of 17-4PH stainless steel samples, plasma nitrided at various treatment temperatures.

- Figure 4.6-6 The potentiodynamic curves of 17-4PH stainless steel samples, plasma carburised using various treatment temperatures.
- Figure 4.6-7 SEM micrographs of corroded areas on plasma carburised a) 4PC370, b) 4PC410 and c) 4PC450.
- Figure 4.6-8 SEM micrographs of corroded areas on plasma carburised a) 4PC370 b) 4PC410 and c) 4PC450
- Figure 4.6-9 The potentiodynamic curves of 17-7PH stainless steel samples, plasma nitrided at various treatment temperatures.
- Figure 4.6-10 The potentiodynamic curves of 17-7PH stainless steel samples, plasma carburised at various treatment temperatures.
- Figure 4.6-11 SEM micrographs of corroded areas on a) UT b) plasma nitrided 17-7PH samples.
- Figure 4.6-12 SEM observations of corrosion tested areas on a) 7PC370 b) 7PC410 c) 7PC410 d) 7PC450
- Figure 5.1-1 The thickness of the treated layer on 17-4PH and 17-7PH stainless steel as a results of plasma nitriding at various treatment temperatures and nitrogen contents as well as varying plasma carburising temperature.

Chapter 1 – Introduction

Stainless steel has been used in a range of industries due to its desired corrosion resistance, superior mechanical properties and moderate wear resistance (Davis, 1994). Despite these desired properties, the wear resistance of stainless steel needs to be improved for tribological applications where this property is not sufficient.

Stainless steels are classified by their alloying elements and microstructures, described as austenitic, martensitic, ferritic or duplex or precipitation hardening stainless steel, which is based on the heat treatment that is used (Hong & Nagumo, 1997). 17-4PH and 17-7PH stainless steels, which were used in the present work, are precipitation hardening (PH) stainless steels.

Investigations have previously been carried out to improve tribological properties of stainless steel using surface alloying with both nitrogen and carbon. Both martensitic and austenitic stainless steels have been plasma nitrided in order to increase the wear resistance, with successful results showing a correlation of improvement with treatment temperature. Although the wear resistance has been found to improve after plasma nitriding, the corrosion resistance of these stainless steels decreased. For example, Brühl et al (2010) found that plasma nitriding could not maintain the corrosion resistance of martensitic stainless steel. Samples treated at higher temperatures of 450°C and 550°C demonstrated very poor corrosion resistance; whereas those treated at a lower temperature of 350°C demonstrated a certain degree of improvement in corrosion resistance (Xi et al, 2008).

This difference is due to the chromium content within the matrix of stainless steel. At higher treatment temperatures, CrN forms which subsequently depletes the chromium content from the surface resulting in poor corrosion resistance. At the lower treatment temperatures, chromium can remain in the matrix without precipitation of CrN. However, to date no systematic work has been conducted to study the response of precipitation hardening stainless steels to plasma alloying with carbon and nitrogen especially at relatively low temperature.

The aim of this research was to further extend knowledge within this area by conducting low temperature active screen plasma surface alloying for both 17-4PH and 17-7PH stainless steels with both carbon and nitrogen. The intention was to improve hardness, wear and corrosion properties as well as to investigate the possibility of forming S-phase in both these materials. The S-phase has previously been shown to have superior tribological properties, which in addition to the good corrosion resistance makes this material desirable.

Chapter 2 - Literature Review

2.1 Stainless Steels

2.1.1 Introduction

Stainless steels have previously been used in a range of diverse industries including the biomedical, chemical and food processing industries, and structural use for which it had been labelled the backbone of modern industry. In 1889, Riley of Glasgow discovered that the addition of nickel significantly enhanced the tensile strength of mild steel. 15 years after this discovery, observations showed that steels containing more than 9% chromium were more corrosion resistant. Confirmation of these results and research into possible applications took place over the following 15 years (Khatak & Raj, 2002).

Both the mechanical properties and the corrosion resistance and occasionally the wear resistance of a stainless steel must be considered when deciding the appropriate material for a particular application (Davis, 1994).

2.1.2 Alloying and classification

A steel contains more than 11% chromium, is considered a stainless steel and along with chromium, its principle alloying elements are nickel and molybdenum. Nickel promotes the formation of austenite phase and enhances toughness, ductility and weldability while molybdenum increases the resistance to pitting and crevice corrosion (Davis, 1994).

Stainless steels are historically classified by their microstructure and characteristic alloying elements. These are described as austenitic, martensitic, ferritic or duplex. In addition to these families of stainless steel, there is a fifth category

consisting of precipitation hardening stainless steels. This categorisation is based on the type of heat treatment used rather than the microstructure (Mannan & Lees, 2005).

In terms of usage and alloys, austenitic stainless steels, including the 200 and 300 grades, are the largest category of stainless steel (Campbell, 2008).

Austenitic stainless steels have excellent low temperature toughness, corrosion resistance and weldability (Kutz, 2002). Carbon forms chromium carbide that, when heated, precipitates on the austenite grain boundaries. The materials chromium content is tied-up as carbide, it is therefore important to limit the carbon within austenite (Kutz, 2002).

Precipitation hardening stainless steels, used in applications such as gears, contain nickel and chromium as well as other alloying elements such as copper or aluminium. These elements cause the precipitation hardening property allowing the stainless steel to have a high strength value (Mannan & Lees, 2005). Precipitation hardening stainless steels are those that have a name which demonstrates the level of chromium and nickel in their composition, such as 17-4PH or those in the 600 series. 17-4PH stainless steel was first produced in 1948, followed by 17-7PH. These alloys contain 11% to 18% chromium, 3% to 27% nickel and smaller amounts of additional metals, including aluminium, copper, molybdenum, titanium and tungsten (Cobb, 2010).

The chromium content of stainless steel causes its excellent corrosion resistance, making it very popular. Spontaneous reactions between the metal and oxygen

results in the formation of a thin, invisible, passivated surface layer which greatly decreases the corrosion rate and is easily maintained (Young, 2008)

2.1.3 Precipitation hardening stainless steels

Precipitation hardening (PH) stainless steels are iron-nickel-chromium alloys which contain one or more precipitation hardening elements such as aluminium, titanium, copper, niobium and molybdenum.

Precipitation hardening is achieved through aging treatments designed to obtain optimum ductility, strength, corrosion resistance and toughness (Nakagawa & Miyazaki, 1999).

The alloying elements in PH stainless steels may be balanced to produce martensite at room temperature, metastable austenite which can be converted readily to martensite or completely stable austenite (Krauss, 1989). Accordingly, these PH stainless steels can either be austenitic, martensitic or semi-austenitic. The type is determined by the martensite start temperature, which is a function of alloy composition (mainly Ni/Cr ratio) as well as austenitising temperature (Krauss, 1989). Tempering of martensitic or semi-austenitic PH stainless steels within the 480-620°C temperature range causes these particular alloys to undergo precipitation hardening by intermetallic phases.

The most common semi-austenitic alloy is 17-7PH stainless steel, which contains both a martensitic and austenitic microstructure as its chromium-nickel ratio prevents the formation of the fully austenitic phase. This 17-7PH stainless steel was developed to have corrosion resistance as well as significant mechanical strength but principally better stress corrosion resistance. The typical composition

of 17-7PH stainless steel is 0.07% C, 7% Nickel, 17% Cr and 1.1% Al, which is balanced so that austenite has a low thermodynamic stability. On cooling, its microstructure is predominantly austenite which is destabilised due to the increase of the Ms temperature of the matrix. This destabilisation occurs through the precipitation of carbides and intermetallic phases in the 750°C-950°C temperature range (Totten, 2006).

The most widely used martensitic PH stainless steel is 17-4 PH, which typically contains 0.04% carbon, 4% Ni, 16.5% Cr, 3.5% Cu and 0.3% Nb. The martensite transformation start temperature of 17-4PH stainless steel is around 105°C and 17-4PH stainless steel is composed of low-carbon lath martensite. There is an abundance of finely dispersed precipitates in the martensite lath after this treatment. The applications of this steel include turbine blades, tools and bearings (Esfandiari & Dong, 2007) (Davis, 1994).

2.2 Wear and Corrosion

2.2.1 Wear of stainless steel

Although stainless steel has good corrosion resistance, its poor wear resistance can become a design problem. Wear behaviour can be described as various contact conditions, including rolling and sliding at a range of applied loads (Davis, 1994).

Plasma nitriding changes the wear mechanisms taking place on the sample. Untreated samples degrade through abrasive wear and delamination whereas when treated, the main wear mechanism is oxidation (Sun & Bell, 1994).

Wear resistance of martensitic stainless steel may be improved by the formation of a composite surface, consisting of hard nitrided particles within the ferrite matrix. This is mainly because the formation of hard nitrides can effectively improve the hardness of the material via precipitation hardening (Corengia et al, 2006).

A study conducted by Sun & Bell (1998), investigated the sliding friction and wear behaviour of low temperature plasma nitrided austenitic 316 stainless steel. This was investigated under both dry and corrosive environmental conditions. The plasma nitriding temperatures were set at 450°C, 500°C and 550°C and it was found that plasma nitriding at these temperatures increases the wear resistance of 316 type austenitic stainless steel by more than two orders of magnitude. It was concluded that the degree of improvement is dependent on nitriding temperature.

A further study on 316 type stainless steel gave a better insight into the wear mechanisms that are involved in the wear behaviour as well as the effect that plasma nitriding has on these behaviours. Li & Bell (2004) plasma nitrided type 316 stainless steel samples at temperatures in the range of 420°C to 500°C and examined the SEM images of the surface to produce conclusions on the wear behaviour.

Li & Bell (2004), concluded that oxidation wear and micro-abrasion were the main wear processes involved on the plasma nitrided stainless steel, as was also concluded by Sun & Bell (1994). It was shown that two distinct areas are formed on the sample surface, a smooth area and another with the same appearance and hardness as the original nitrided surface.

The smooth area is built up from fine wear particles generated from the worn area, produced from the oxidation-scrape-reoxidation mechanism. Another possibility is that this smooth area could contain patched fine metallic particles that could then be oxidized during further sliding. The compacted smooth layer in both cases is supported by an extremely hard layer which as a result decreases the wear volume of the nitrided sample compared to the untreated sample (Li & Bell, 2004).

As previously mentioned with a focus on corrosion testing, Liang et al (2000), also studied the effect of plasma assisted nitriding on the wear behaviour of AISI 304 austenitic stainless steel. Similar to the findings of Li & Bell (2004), Liang et al (2000) concluded that the wear mechanism involved changed after the samples were plasma nitrided. Also agreeing with other studies, they found that the untreated sample suffered severe wear and this wear was mainly through adhesion, abrasion and plastic deformation. Once these samples had been nitrided, the surfaces revealed only very mild abrasive wear. On the other hand, the nitrided sample showed polishing of the grinding marks, producing a smooth oxidized surface with a rapid transition towards a mild oxidative wear mechanism. This is a similar conclusion to that of Li & Bell (2004).

Plasma nitrided samples show better wear resistance than those the untreated samples, due to the formation of an oxide layer on the surface of the material. This oxide layer prevents metal-to-metal contact by acting as a lubricant layer (Liang et al, 2000).

2.2.2 Corrosion

Corrosion resistance of plasma surface alloyed martensitic stainless steel is still problematic due to the formation of chromium nitrides and chromium carbides.

Corrosion is an electrochemical process of oxidation and reduction reactions, within which electrons are released and gained by elements in the corrosion solution and this forms the basis of electrochemical testing. During this type of testing, a polarisation cell is set up consisting of an electrolyte solution which resembles the potential material application. A reference electrode, a counter electrode and the metal sample (working electrode) of interest connected to a specimen holder are also used (Callister & Rethwisch, 2011).

In this solution, an electrochemical potential (voltage) is generated between various electrodes. The corrosion potential (E_{CORR}) is measured as an energy difference between the working electrode and the reference electrode. This method of testing is often used to evaluate/compare processing effects on corrosion properties, from processes such as plasma carburising and plasma nitriding.

Another method of corrosion resistance testing is the widely used salt-spray test method. This method has been criticised due to its failure to take into account various external factors that may be affecting corrosion rates. The basic procedure of this test is to expose the sample to a neutral salt solution at an elevated temperature (Appleman & Campbell, 1982).

Salt-spray and electrochemical testing carried out on 17-4PH stainless steel, plasma nitrided at 350°C demonstrated much poorer corrosion resistance, in

terms of significantly reduced corrosion potential, compared to the untreated sample (Esfandiari & Dong, 2007). These results confirmed that the samples treated at 350°C showed a decreased corrosion resistance. Those treated at 420°C or above showed significantly increased pitting corrosion resistance, highlighting a difference between the corrosion resistance in austenitic and precipitation hardening stainless steel (Esfandiari & Dong, 2006).

Another area of research looking at the corrosion resistance of stainless steel, carried out by Liang et al (2000), used plasma arc source ion nitriding to improve the hardness and corrosion resistance of 304L austenitic stainless steel. The steel was treated at 420°C for 70 minutes and the corrosion measurements were made by potential dynamic polarisation in which the electrolyte was 3.5% NaCl solution. The results of this research concluded that passivability and pitting resistance of 304 austenitic stainless steel was improved by the treatment. Scanning electron microscopy showed that corrosion pits appeared only on the untreated sample therefore confirming the conclusion that corrosion resistance can be improved by nitriding at a temperature below 450°C for austenitic stainless steels (Liang et al, 2000).

Abedi et al (2010) used plasma nitriding on 316 austenitic stainless steel to evaluate the effect on corrosion behaviour. The samples of stainless steel were nitrided at 450°C for 5 hours. The results demonstrated that the corrosion resistance was reduced by plasma nitriding due to the presence of sliding bands. These sliding bands may have been created due to the expanded austenite formation, providing an active site for the corrosion process.

The alloying elements within stainless steel can enhance the resistance to localised corrosion. Chromium can combine with oxygen to form a protective film, while nitrogen can react with H^+ to form NH_4^+ , which depresses oxidation inside the pit (Baba et al, 2002) (American Society for Metals, 1976).

Chromium provides corrosion resistance and this will decrease if chromium is depleted from the nitride layer through the formation of CrN. If this occurs, the passive film cannot be formed, which occurs in those samples treated at what are considered high temperatures (Czerwiec et al, 2000).

2.3 Surface Engineering

2.3.1 Introduction

Surface engineering describes a range of technologies designed to modify the surface properties of metallic and non-metallic components for engineering purposes. Surface engineering can be divided into two branches - surface modification and surface coating.

Problems such as erosion, corrosion and wear can be solved through the many different surface engineering techniques (Pine Do & Monterio, 2004) (Blawert et al, 1996).

Surface engineering techniques are very successful in improving the performance of a material. Choosing a surface treatment successfully must ensure that the important properties of the material are not affected detrimentally. These techniques create a composite system to provide an optimum performance from a material (Cotell C M and Sprague J A ,1994).

Surface modification shows potential in improving corrosion resistance as corrosion strongly depends on the microstructure and composition of the near-surface region (Menthe et al, 2000).

2.3.2 Thermochemical treatment

Thermochemical treatment involves the introduction of alloying elements (such as carbon and nitrogen) into the surface of steel through diffusion at elevated temperatures to produce a hardened surface case and a soft, tough and strong core within a steel. Thermochemical treatment processes mainly include nitriding and carburising.

Carburising

Carburising involves changing the carbon content of the surface, followed by a quenching process to convert the surface layers to martensite. There are different methods of carburising: gas carburising, salt bath carburizing and pack carburising (Phillip & Bolton, 2002)

Plasma carburising is normally carried out in a vacuum furnace at a temperature range of 950 to 1050°C by diffusion of deposited carbon ions on the surface. The carbon ion containing plasma is produced by glow discharge in a mixture of hydrocarbon plus hydrogen for dilution.

The same case depth can be achieved using this method as producing the required temperatures takes less time, making this method desirable. It also has closer control of the surface carbon and has no limitation on part size (Chattopadhyay, 2004).

Nitriding

Nitriding, a form of surface engineering, creates a case hardened surface by alloying nitrogen into the surface of a metal which are named after the medium which is used to donate the active nitrogen atoms. The three main types of nitriding are the salt bath method, gas nitriding and the latest method, plasma nitriding. These conventional nitriding, salt-bath method and gas nitriding processes have several disadvantages such as longer processing times and poor surface finish when compared to plasma nitriding (Rahman et al, 2005).

Plasma nitriding began in the 1920s as an alternative to conventional gas nitriding. After the Second World War, this method was used in countries such as Germany, Russia, China and Japan. The plasma nitriding process, however, was not introduced into the USA until 1950 and only been used in production over the last 25 years.

The plasma nitriding process commences with the sample being placed into a vacuum chamber, which is then evacuated to a desired vacuum pressure, usually 3-10bar (John, 2005). When this pressure is reached, the plasma nitriding unit is back-filled with a process gas to begin the pre-heating cycle, which is within temperature ranges of 450°C -550°C. After this initial preheating time, impurities are cleared from the sample surface through ion bombardment.

The next step is the introduction of a controlled flow of nitrogen and hydrogen into the chamber which is ionized by the voltage applied to the sample. This ionization forms a plasma which envelopes the sample surface which combined with heat and causes the gases to react with nitride which forms elements in the steel. A

wear resistant layer is formed as the gasses react with the elements present in the stainless steel. The composition of this layer will vary depending on the percentage of each gas in the chamber, which will be based on the future application of the sample. This nitriding cycle is continued for 2 to 72 hours, depending on the steel composition and the required depth, until the desired case depth is achieved (Rajan et al, 1994).

Yang et al (2011), compared gas nitrided and plasma nitrided steel samples and discovered that the layers formed are very similar. The two nitrided samples are both composed of an external compound layer which is much thicker in the sample that was plasma nitrided and unlike the gas nitrided sample, did not contain any pores. Both samples also have an underlying diffusion zone of approximately 110 μm in the plasma-nitrided layer, and 155 μm in the gas-nitrided sample (Yang et al, 2011).

Austenitic stainless steels are not normally thought to be suitable for nitriding due to the existence of an adherent oxide layer on the surface. The oxide layer on the surface of austenitic stainless steel causes slow diffusion of nitrogen and non-uniform hardening. This layer however is removed during plasma nitriding through the sputtering action of the energetic nitrogen and hydrogen ions within the plasma (Bell et al, 1985).

It should be highlighted that although conventional plasma nitriding can effectively increase the hardness and dry wear resistance of stainless steel, such improvements is at the price of its corrosion resistance (Dong 2010). When this treatment temperature is higher, the level of chromium at the surface of the material is depleted. During these treatments, the hardening process reduces the

level of corrosion resistance, due to the depletion of chromium in solid solution as precipitates of chromium nitride form. This chromium depletion layer is very prone to corrosion (Zhang & Bell, 1985). The formation of precipitates only occurs when plasma nitriding is carried out at temperatures above 500°C in order to accelerate nitrogen diffusion. This highlights the need to use lower treatment temperatures, successfully addressing this problem (John, 2005) (Zhao et al, 2008).

Attention has been paid to plasma nitriding at below 500°C in order to maintain the properties that already excel in this material, which is corrosion resistance, and improve those that do not perform so well. For stainless steel, this is the tribological and mechanical properties.

2.3.3 The S-phase

During the past decade, significant progress has been made in achieving combined improvement in tribological and corrosion properties of austenitic stainless steels due to the discovery of a new S-phase formed during low-temperature plasma nitriding and carburising (Dong, 2010).

“The S-phase can be defined as a thermodynamically metastable, nitrogen supersaturated solid solution with a distorted FCC structure” – Li, X.Y 2001.

The two most common names for this new phase are the S-phase or expanded austenite and is a super-saturated solid solution of nitrogen or carbon in the face centre cubic austenitic phase, proven to have high hardness and very good corrosion resistance (Marchev et al, 1998). The phase structure of the S-phase, although not fully understood, includes microstructure, crystallographic structure and atomic/ molecular structure (Dong, 2010)

The new phase was initially thought to be FCC structured and was first termed expanded austenite by Leyland et al, 1993. On the other hand, Marchev, et al, 1998, thought differently and proposed that the new phase was probably body centred tetragonal structured, similar to that seen to martensite in steel and it was therefore referred to as the M-Phase (Marchev et al, 1998).

This S-phase can form at low temperatures by introducing interstitials including nitrogen, carbon or a mixture into an FCC structured substrate. No nitrides/carbides form and the phase appears as a white layer on top of the substrate in the cross-sectional optical microstructure (Dong, 2010) (Ichii, 1986).

The super saturation of nitrogen in S-phase expands the FCC lattice of austenite, which is why the S-phase may also be called the expanded austenite. The S-phase has been found to be supersaturated with nitrogen up to approximately 22% which is much larger than the maximum solid solubility of nitrogen in FCC which is about 8.7% (Li, 2001). The lattice expansion shifts the XRD peaks to lower angles compared with those austenite peaks of the untreated sample, according to Bragg's law (Abedi et al, 2010). In the work of Li, 2001, XRD was used to identify the S-phase within 316 austenitic stainless steel. These specimens were plasma nitrided at temperatures between 380 °C and 500°C for 20 hours. Two main peaks were detected, named S1 and S2, both of which appeared at much lower angles and there was a degree of peak broadening for all the S peaks. The level of broadening depended upon the process temperature. Low temperature plasma nitriding produced phases that could not be identified in any of the existing ASTM X-ray diffraction index cards (Li, 2001).

There are several methods of observing the microstructure of this S-phase, including Transmission Electron Microscopy (TEM), Scanning Electron Microscopy (SEM) and X-ray phase analysis. Stroz & Psoda (2009) used two of these methods to study the structure of a layer formed during nitriding on 316 stainless steel. This material was treated at 440°C, which previously has been shown to produce an S-phase, also known as expanded austenite. An S-phase of 6µm was identified using X-ray diffraction after treatment and this expanded layer was due to the introduction of nitrogen atoms. A lot of defects were discovered within the single-cubic phase layer, such as stacking faults, twins, slip bands and dislocations. The formation of these slipping bands on the nitride sample surface caused the increase in surface roughness when the sample was nitrided (Abedi et al, 2010).

Li (2001), concluded through transmission electron microscopy that there are no new grains between the S-phase and the substrate and therefore the S-phase discovered in this study is in fact a diffusion zone without an intrinsic interface.

The main critical parameter in development of a precipitate-free S-phase has been recognized to be the process temperature and time. Wang et al (2006), observed that for a specific temperature there exists a critical time beyond which nitride formation occurs. For 673K this was 30 hours and for 703K this was 60 hours. Furthermore, Blawert et al, 1999 observed that nitrides formed at 683K or lower for treatment times of a few hours.

2.3.4 Plasma treatment of PH stainless steels

The formation of the S-phase has been recognized in studies involving austenitic stainless steels for many years but investigations have also been performed on plasma treatment of martensitic and precipitation hardening stainless steels.

Bruhl et al (2010), used plasma nitriding to modify the surface of three martensitic stainless steels. The XRD analysis performed on martensitic N695 and M240 stainless steel revealed that the white layer in martensitic stainless steel is a stressed structure which has been called "Expanded Martensite" (Bruhl et al, 2010).

The existence of this 'expanded martensite' was also suggested by Leyland et al (1993), despite there being limitations in this study. In 2003, Sun and Bell, also discovered supporting evidence of an 'expanded martensite' phase within 17-4PH martensitic stainless steel. They plasma nitrided this material for 20 hours in a temperature range of 350°C -450°C, discovering that when the process temperature was below 425°C, a featureless white layer could be produced.

The temperature dependency of the S-phase in austenitic stainless steel is also true of martensitic and precipitation hardening stainless steels. Plasma nitriding martensitic stainless steel in a narrow temperature range of 380°C-400°C supported evidence for the formation of the 'expanded martensite' at low temperatures. Over 420°C, XRD analysis discovered that the 'expanded martensite' has not been found to exist due to the formation of CrN (Manova, 2006).

The study conducted by Dong et al (2008) was one of the first studies to use both TEM and XRD for phase identification in low temperature surface alloying in martensitic PH stainless steels. This investigation used a temperature range of 350°C-500°C, time periods of 10-30 hours and a gas mixture of 25%N₂ and 75%H₂. The untreated sample was dominated by martensite with retained austenite.

Those samples treated at temperatures above 460°C were characterized by peaks of chromium nitride which supports the results found by previous investigations regarding high plasma nitride temperatures. The samples treated below 420°C, and therefore considered low temperature plasma nitride samples, needed both XRD and TEM in order to identify the present phases.

TEM analysis was necessary as it was difficult to use only XRD due to the possibility of having several over-lapping peaks. TEM analysis along with XRD analysis revealed that the plasma nitrided layer does not contain precipitates and has retained its original martensite structure but with larger lattice parameter. In all samples plasma nitrided at 420°C for 10 hours and those treated below 420°C for varying lengths of time, isolated S-phase grains were observed. It was therefore concluded from this study that the formation of the S-phase in the martensitic 17-4PH stainless steel is related to the conversion of the retained austenite in the original material.

To date no research work has been reported in the public domain on plasma surface alloying of 17-7 martensitic/austenitic precipitation hardening stainless steel.

Chapter 3: Experimental

3.1 Materials

The materials used in this research were 17-4PH martensitic precipitation hardening stainless steel and 17-7PH semi-austenitic stainless steel, which was provided by Dunkirk Speciality Steel. The chemical compositions of these two materials are shown Table 1. The 17-4 and 17-7 PH materials were furnished in the annealed condition, which is also called the solution heat treated condition or Condition A. Annealing is conducted by heat treating at approximately $1000\pm 50^{\circ}\text{C}$ and cooling to room temperature. In this condition, the 17-4 PH material possesses a martensitic structure and the 17-7 PH material possesses an austenite structure. However, it was found that the structure of 17-7PH is a combination of martensite and austenite and it will be detailed in section 4.

Table 3.1 Chemical composition of 17-4 and 17-7 PH stainless steels

COMPOSITION 17-4, wt%	COMPOSITION 17-7 , wt%
Carbon 0.07 max.	Carbon 0.09 max.
Manganese 1.00 max.	Manganese 1.00 max.
Phosphorus 0.040 max.	Phosphorus 0.040 max.
Sulphur 0.030 max.	Sulphur 0.030 max.
Silicon 1.00 max.	Silicon 1.00 max.
Chromium 15.00 - 17.50	Chromium 16.00 - 18.00
Nickel 3.00 - 5.00	Nickel 6.50 - 7.75
Copper 3.00 - 5.00	Aluminium 0.75 - 1.50
Columbium + Tantalum 0.15 - 0.45	
Iron balance	Iron balance

3.2 Sample Preparation

Small disc samples about 6.5mm in thickness were cut to from bars of 25 mm diameter using a struers cutter and labelled with both the type of steel (17-7PH and 17-4PH) as well as the treatment code. All the samples were grounded using SiC papers of 120, 240, 400, 800 and 1200 grades.

These grounded samples were then polished using polishing cloths, of grades 9µm, 6µm and 3µm, along with diamond paste, on a Struers grinding/polishing machine. These samples were then ultrasonically cleaned in acetone for 10 minutes at room temperature and dried under hot air in order to prevent water marks.

3.3 Surface Treatments

Plasma nitriding was carried out in an AS Plasma Metal 75kVA + 15kVA industrial scale active-screen plasma nitriding furnace for 20 hours. Three plasma nitriding treatments were undertaken, coded 4PN350, 4PN390, 4PN430, the details are shown in Table 2. These plasma nitriding treatments can be grouped into two sets: PN1, PN3 and PN5 were designed to investigate temperature effect with the same gas composition (25%N₂+75%H₂); PN6, PN3 and PN7 was used to study the effect of gas composition at 390 °C. There were also three active screen plasma carburising treatments (see Table 2 below), coded PC2, PC4 and PC6, designed to study temperature effect.

Table 3.2 Sample code and treatment conditions

Sample Code		Treatment type	Temperature (°C)	Gas composition (%)	Time (hour)
17-4	17-7				
4PN350	7PN350	Active Screen Plasma Nitriding	350	25% N ₂ , 75% H ₂	20
4PN390	7PN390	Active Screen Plasma Nitriding	390	25%N ₂ , 75% H ₂	20
4PN430	7PN430	Active Screen Plasma Nitriding	430	25%N ₂ , 75% H ₂	20
4PC370	7PC370	Active Screen plasma Carburising	370	1.5% CH ₄ , 98.5%H ₂	20
4PC410	7PC410	Active Screen plasma Carburising	410	1.5% CH ₄ , 98.5%H ₂	20
4PC450	7PC450	Active Screen plasma carburising	450	1.5% CH ₄ , 98.5%H ₂	20

3.4 Characterisation

3.4.1 Preparing cross-sections

Cross-sections of a representative amount of treated samples were cut and then mounted in conductive Bakelite using a MET-PREP PA 30 Mounting press. These cross-section samples were ground up to 1200 grit paper, polished up to 1µm and cleaned in acetone. The cross section samples were etched using Marbles reagent in order to highlight the microstructure.

3.4.2 Microstructure - SEM

A scanning electron microscope (SEM) was employed to study the cross-sectional morphology as well as measure the layer thickness of the nitrided stainless steel samples. SEM was also used for the post- observation of tested sample surfaces.

3.4.3 Phase composition – XRD

A Siemens D5000 X-ray diffraction (XRD) machine with Cu K α radiation (with a 40 kV accelerating voltage and a 30 mA filament current) was used for detailed study of surface phase composition of plasma nitrided stainless steels. A scan program was setup at standard $\theta/2\theta$ mode to produce different peaks. The crystalline phases present were identified by comparison with reference patterns from the Powder Diffraction File (PDF) from the International Centre for Diffraction Data.

3.4.4 Microstructure and phases – TEM

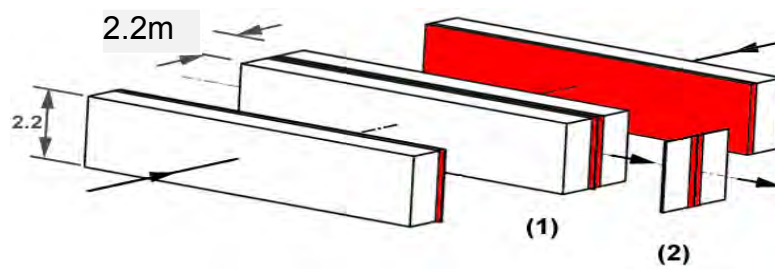
The transmission electron microscopy (TEM) samples prepared were in cross-section view. Two small slabs with a cross-section area of about 2.2x2.2 mm² were cut from the treated samples, which were then glued with the treated surfaces facing each other (Fig. 3-1a) This assembly was sliced to 1mm thick and then it was stuck on a bulk flat sample for grinding and polishing to around 80 μ m before it was fractured away from glued centre using tweezers. The pre-thinned slice was then transferred to a Quanta 3D FEG focused ion beam (FIB) miller for final thinning to 100nm (Fig. 3.1b).

A JEOL JEM-2100 LaB6 TEM and FEI Philips TECNAI F20 with the operating voltage of 200 kV was used to characterise the phase constituent and microstructure of the surface layers.

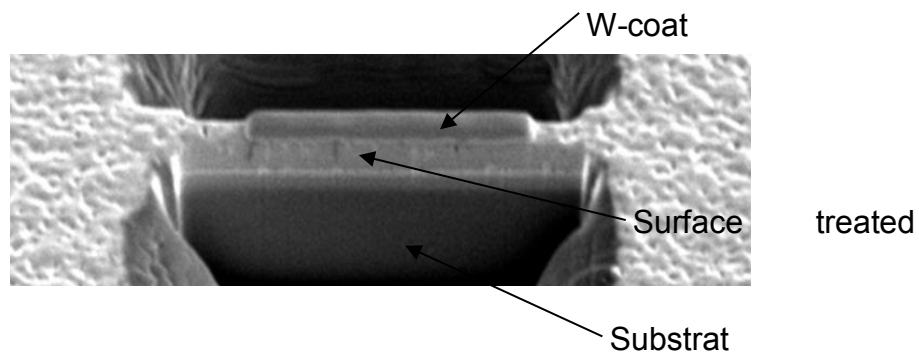
3.4.5 Chemical composition - GDOES

An atomic emission technique, glow discharge optical emission spectroscopy (GDOES) was used for surface analysis and depth profiling of chemical composition. The sample and GDOES sputtering hole were cleaned with ethanol

before loading, and the measurement then started. The measurement was stopped once the measurement of nitrogen or carbon had reached a stable level. Quantitative compositions were obtained after calibration using standard blocks of known composition.



a



b

Figure 3-1 Preparation of cross-sectional TEM sample, a) pre-thinning XTEM sample; b) SEM image of FIB preparing XTEM sample.

3.5 Mechanical Properties Assessment

3.5.1 Micro-hardness

A Vickers Mitutoyo (MVK-H1) hardness testing machine was used to measure the hardness values (Hv) of untreated and plasma nitrided stainless steel samples.

Each measurement was repeated four times and an average was taken in order to increase accuracy.

3.5.2 Load bearing capacity

A Vickers indenter was used to apply loads from 25g to 1000g to measure hardness as a function of the applied load – load bearing capacity. In order to avoid interference among adjacent indent points, there was a considerable distance between the indentations to ensure accuracy of results.

3.5.3 Wear testing

Samples of plasma nitrided and carburised 17-4PH and 17-7PH stainless steels were tested to evaluate their wear resistance. Sliding wear tests were carried out using a TE79 tribometer under a contact load of 10N in reciprocating sliding against an 8 mm WC/co ball in air without lubrication as.

The wear tracks created were measured and evaluated by a profilometer, whilst the wear volume loss was calculated by integrating the cross-sectional area of the wear track and then multiplying by the length of the wear track. This was carried out on a program called Ambios Profiler (XP-Plus Stylus).

3.6 Corrosion Properties Assessment

3.6.1 Electrochemical testing

Electrochemical corrosion tests were conducted in a solution of 3.5wt%NaCl at 23°C using a Gamry Ref 600 machine and a saturated calomel electrode (SCE) was used as a reference, and platinum as the counter electrode. The samples were immersed for 5 minutes during an open circuit potential (OCP) before testing

began. A scan rate of 1mVs^{-1} was used starting from -0.1V (Vs the OCP) to 1V (versus the reference). There were at least 3 tests carried out on each sample. The specimen electrode was polarised away from its equilibrium by imposing a changing DC potential difference between the specimen and reference electrode whilst recording the current response. .

3.6.2 Salt Spray

The salt spray test can be thought of as an accelerated lab test used to provide information regarding the corrosion-resistance of the stainless steel in a controlled corrosive environment. The solution used during this testing was 5%NaCl at a maintained temperature of 32°C . The exposure time was 100 hours for all samples. To analyse the effect of this salt spray testing, each sample was weighed before and after testing. The samples were photographed before and after the testing in order to see the effect that corrosion has on the surface of the material.

Chapter 4 – Experimental Results

4.1 Surface morphology and Layer Structures

SEM microstructures of as-received 17-4 and 17-7 PH samples were taken from transverse sections of received bar materials. It can be seen that 17-4 PH material reveals martensitic structure (Fig. 4.1-1a). Microstructure of 17-7PH steel shows austenite grains with some dark-etching islands of ferrite (Fig. 4.1-1b). However, within the austenite grains, martensite plates can be observed, which was confirmed by XRD and TEM analysis (see Sections of 4.3.2 and 4.3.3-1). The presence of martensite in solution treated condition of 17-7PH stainless steel is most probably caused by relatively low annealing temperature and/or short annealing time, which resulted in increased Martensite Starting (M_s) temperature above room temperature (Krauss, 1989).

Typical surface morphologies of as-treated samples were observed by SEM and the features are the results of interaction between the active species and the sample surfaces during active-screen plasma treatments (Corujeira Gallo and Dong, 2009). It can be seen that the plasma nitrided 17-4PH sample (Fig. 4.1-1c) shows original microstructural features, such as pre-austenite grain boundaries and martensite reliefs. Similarly, some original microstructural features of 17-7 PH steel can still be recognised from the plasma nitrided surface (Fig. 4.1-1e). On the other hand, however, very limited original microstructural features could be seen from the plasma carburised samples (Figs. 4.1-1 d & f). It was also noticed that fewer original microstructural features were observed from the plasma treated 17-

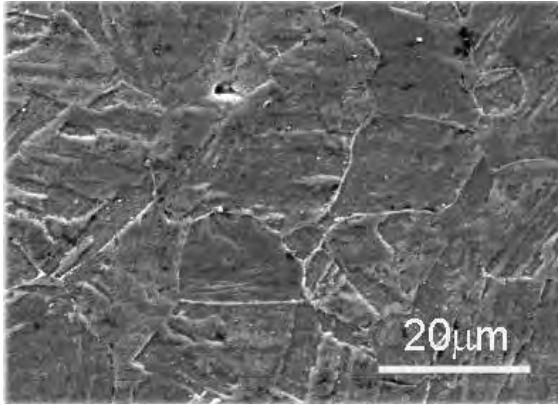
7PH samples (Figs.4.1-1 e & f) than from the 17-4PH samples (Figs.4.1-1 c & d) probably due to the finer microstructure for the former than for the latter.

The layer structures for plasma surface alloyed 17-4PH and 17-7PH stainless steels were investigated using SEM from the cross-sections, which allowed the surface layers produced through active screen plasma nitriding and carburising to be examined and measured.

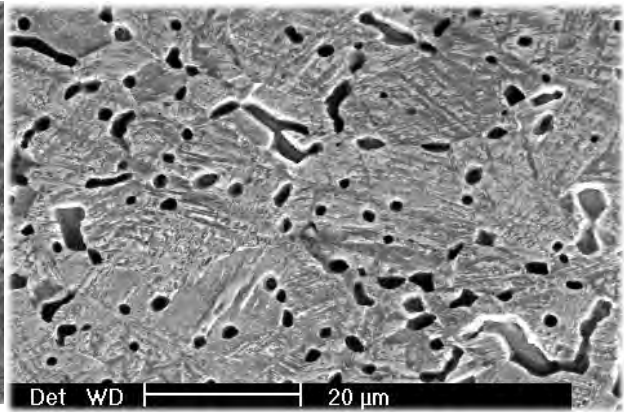
4.1.1 17-4PH stainless steel

The SEM images of cross-sections of plasma nitrided samples are shown in Figures 4.1- 2 a to c. It can be seen that a thin layer about 5 μm was formed on the sample treated at 350°C and the interface between the surface layer and the substrate of the material was not well defined (Fig.4.1-2a). When increasing the treatment temperature to 390°C, the interface became clearer and the surface layer became much thicker (c.a. 10 μm) as shown on Figure 4.1-2b. The 17-4PH stainless steel sample treated at the highest treatment temperature of 430°C showed the thickest layer of about 18 μm (Fig.4.1-2c). Within the layer, some apparent pre-austenite grain boundaries could be observed, indicating poor corrosion resistance along these areas.

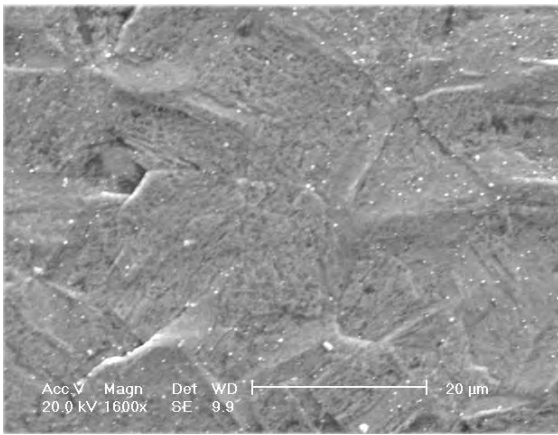
SEM images of active screen plasma carburised 17-4PH stainless steel samples are shown in Figure 4.1-3. The sample treated at 370°C shows a shallow surface layer. The interface between the layer and the substrate is very uneven and zig-zag in nature. The same interface characteristics can be seen on the 17-4PH stainless steel sample treated at 410°C and 450°C. However the surface layer is thicker in these cases.



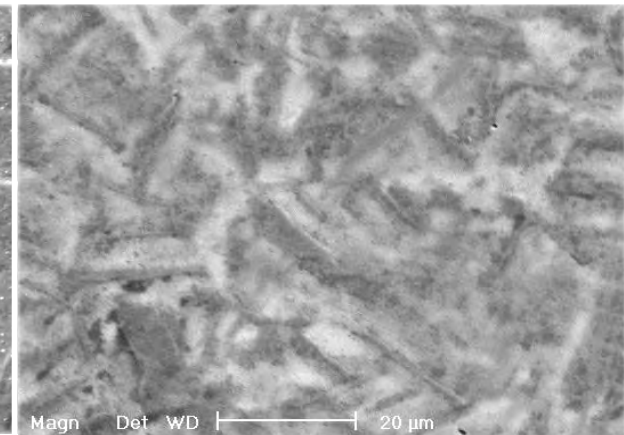
a) 17-4PH



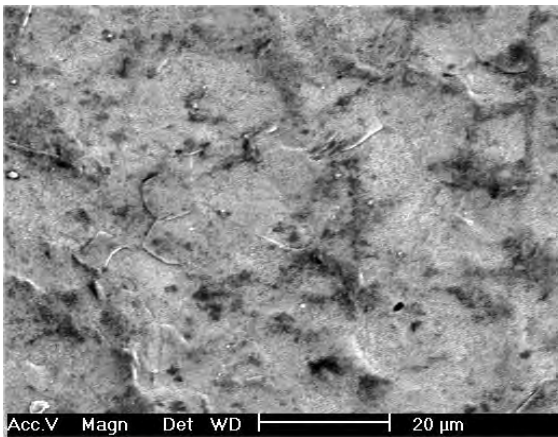
b) 17-7PH



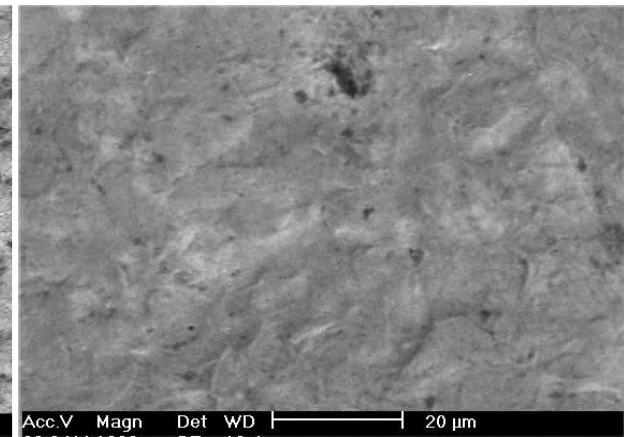
c) 4PN390



d) 4PC450

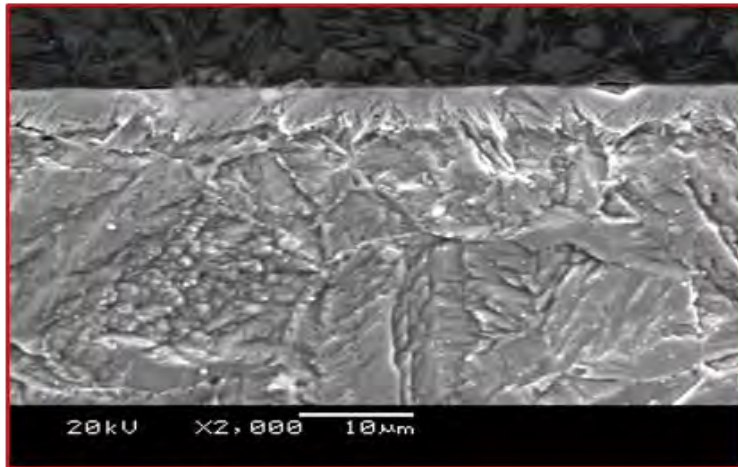


e) 7PN430

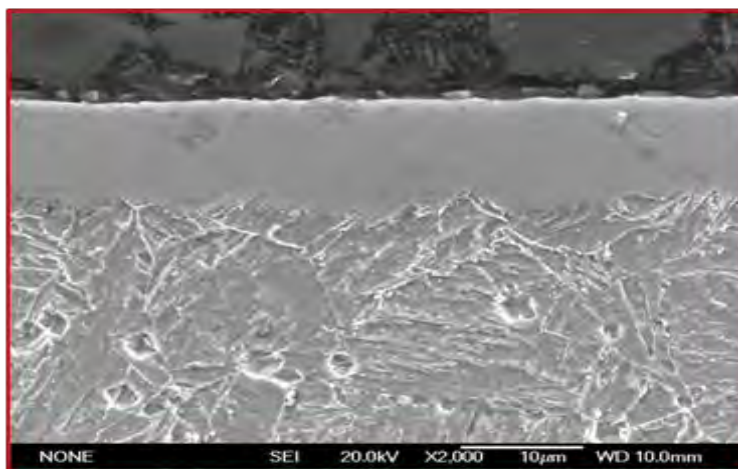


f) 7PC410

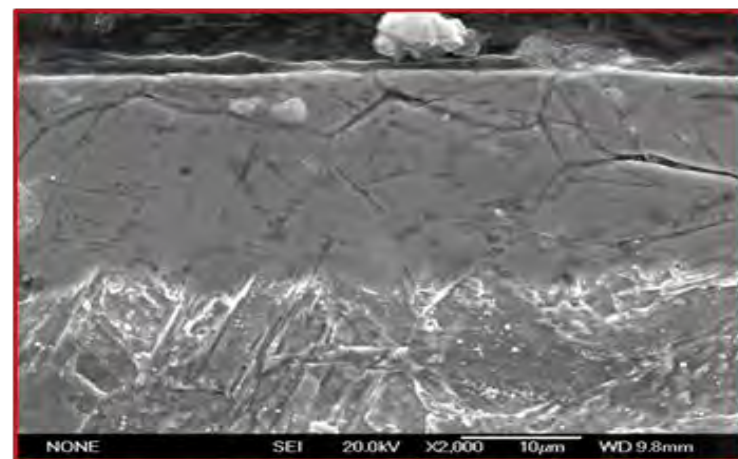
Figure 4.1-1 SEM images of etched as-received a) 17-4 PH and (b) 17-7PH samples; c) plasma nitrided and d) plasma carburised 17-4 PH samples; e) plasma nitrided and f) plasma carburised 17-7 PH samples.



a) 4PN350

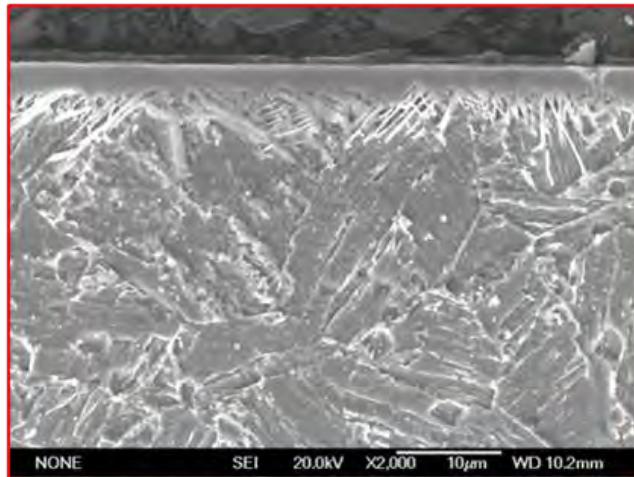


b) 4PN390

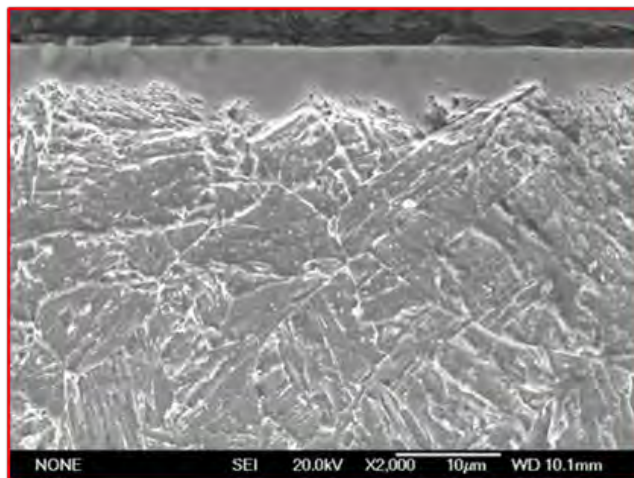


c) 4PN420

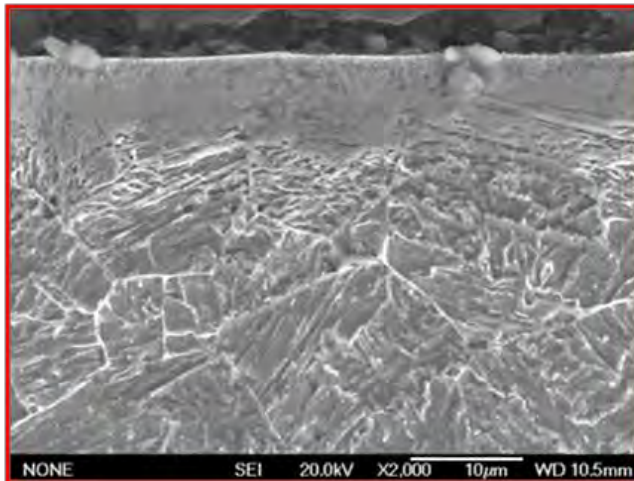
Figure 4.1 – 2 The layer structures of active screen plasma nitrided 17-4PH stainless steel samples at various temperatures a)4PN350; b)4PN390; c)4PN420.



a) 4PC370



b) 4PC410



c) 4PC450

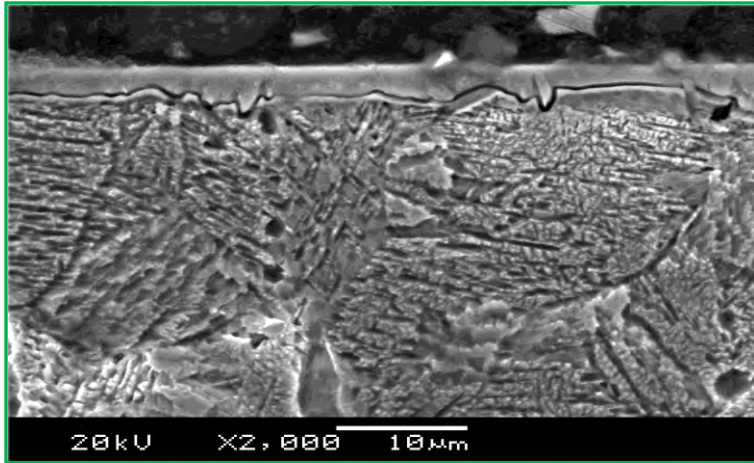
Figure 4.1-3 SEM images from plasma carburised samples of 17-4 PH steel

a) 4PC 370. b) 4PC410 c) 4PC 450.

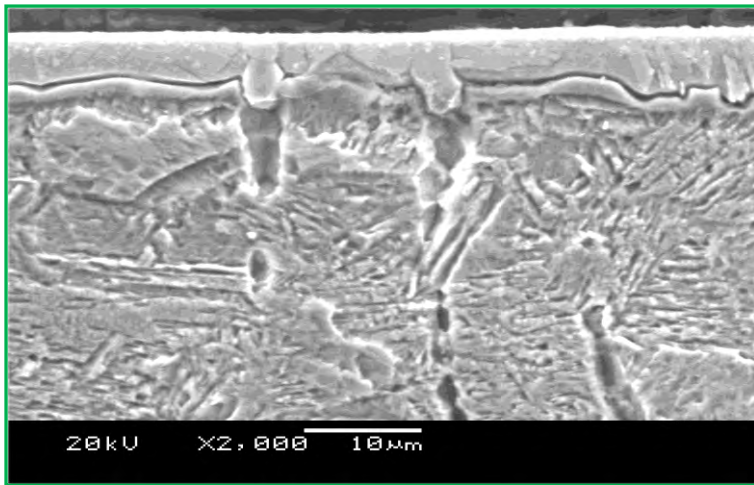
4.1.2 17-7PH stainless steel

During active screen plasma nitriding under different temperatures, a treated layer was formed on the surface of the 17-7PH stainless steel samples. It can be seen from Figure 4.1-4 that the interface between the surface layer and the substrate is largely even but with some tooth-shaped areas developed into the substrate. A crack-like deep etched line was observed just above the interface between the surface layer and the substrate. The thickness of the surface layer increased with increasing the temperature from 390 to 430°C.

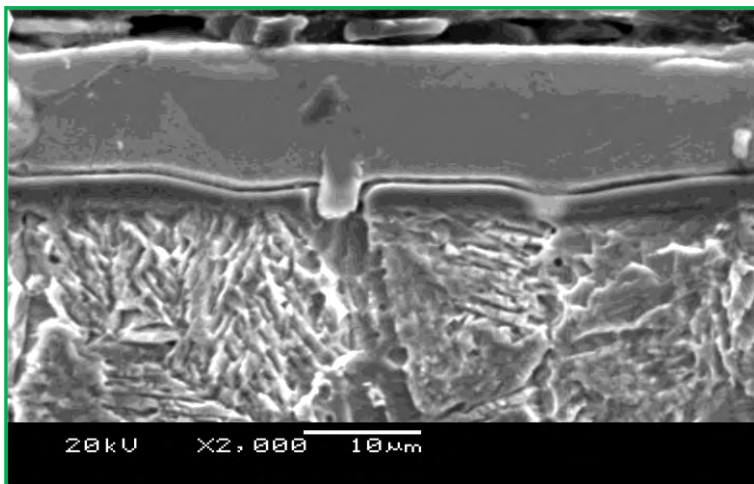
The 17-7PH stainless steel sample plasma carburised at 370°C created a surface layer with a very clear interface between this surface layer and the substrate (Fig. 4.1-5a), and increasing the treatment temperature to 410°C created a thicker layer (Fig. 4.1-5b). The 17-7PH stainless steel sample plasma carburised at the highest treatment temperature of 450°C revealed very different features, which can be seen in Figure 4.1-5c. The interfaces between the carburised surface layers and the substrate are relatively even. However, the surface layer appeared to be split into two sublayers. The top sub-layer is darker in appearance compared to the bottom sub-layer, an indication of reduced corrosion resistance probably due to carbides precipitation. In addition, some pillar-like features which extended from the bottom layer were observed within the top layer, which could be related to the initial duplex microstructures.



a) 7PN350

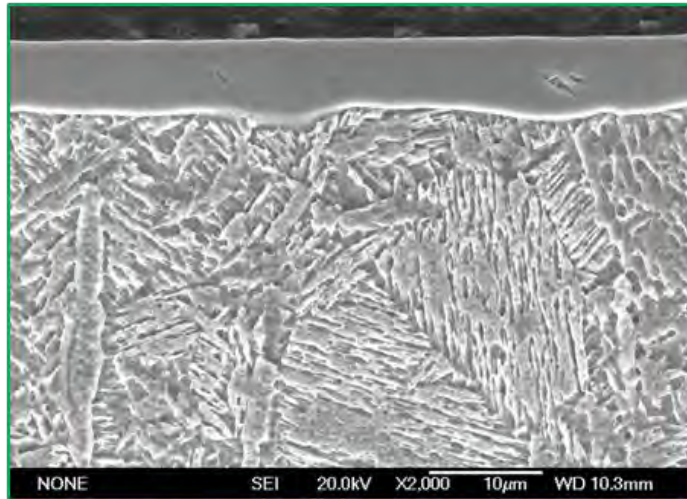


b) 7PN390

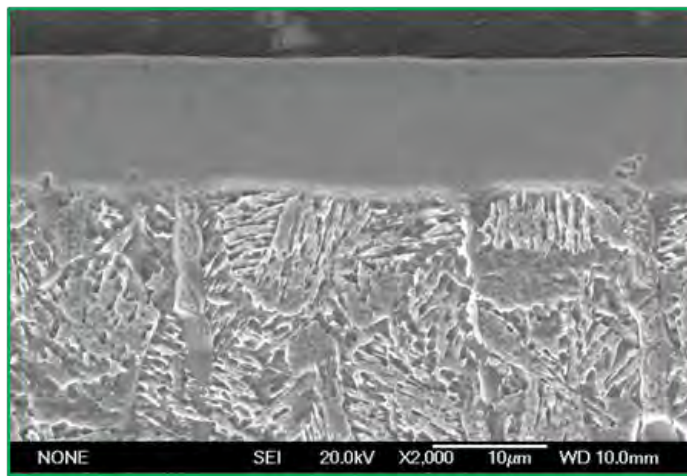


c) 7PN430

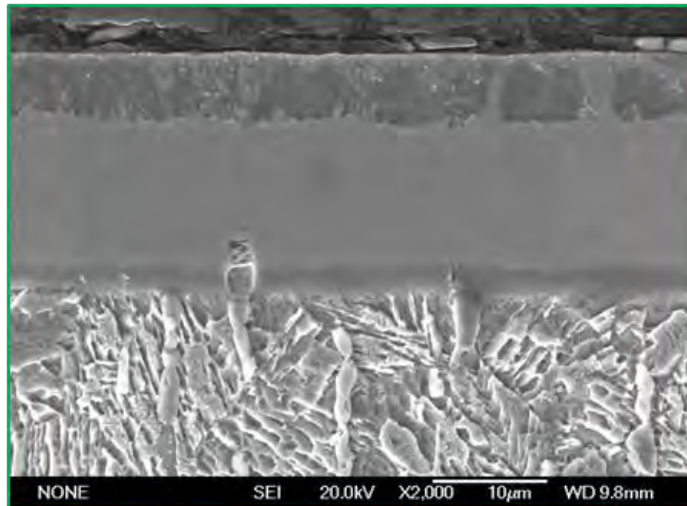
Figure 4.1-4 The layer structures of active screen plasma nitrided 17-7PH stainless steel samples at various temperatures: a)7PN350; b)7PN390; and c)7PN430.



a) 7PC370



b) 7PC410



c) 7PC450

Figure 4.1-5 SEM images from plasma carburised samples of 17-7 PH steel

a) 7PC 370. b) 7PC410 c) 7PC 450.

4.2 Chemical Composition

4.2.1 17-4PH stainless steel

The chemical composition of the surface modified layer can be analysed by glow discharge optical emission spectroscopy (GDOES). This technique was used to detect the distribution of nitrogen/carbon through the surface modified layers on those samples that were plasma surface alloyed with nitrogen and carbon. Because of the technical limitation of GDOES and surface roughness of the samples, the data collected from the outmost layer are not accurate and hence the following interpretation of the profiles neglects the initial data for the outmost layer (c.a. 0.5 μm).

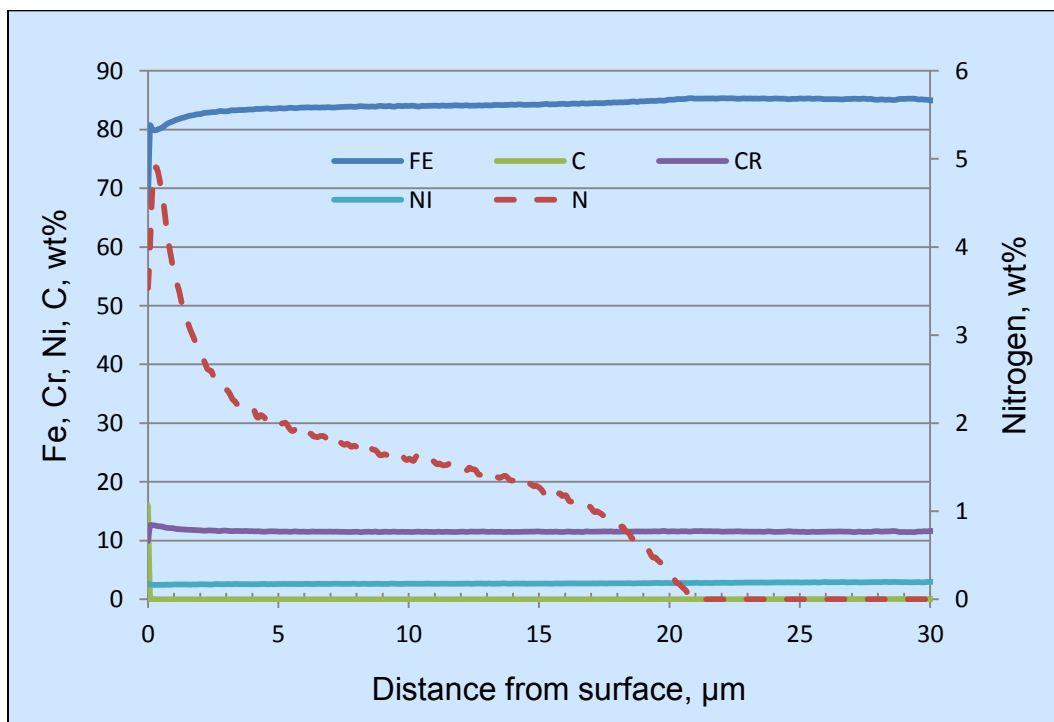


Figure 4.2-1 Typical GDOES full elemental composition profiles of 430°C plasma nitrided 17-4PH stainless steel

Figure 4.2-1 shows full elemental GDOES profiles of 17-4PH stainless steel plasma nitrided at 430°C for 20 h. It indicates the depth distribution of elemental composition of the 17-4PH stainless steel sample, which is comprised mostly of iron, along with carbon, chromium, nickel and then nitrogen after being plasma nitrided. The nitrogen content is about 5 wt% at the surface layer of the sample. This nitrogen content sharply decreased within the first 3-4 μm to a platform (5-15 μm) and then gradually decreases to zero within the substrate as it is not naturally present. The iron content is lower at the surface and then plateaus at approximately 85% within the surface modified case. The elements of Ni and Cr can be seen to be uniformly distributed throughout the sample.

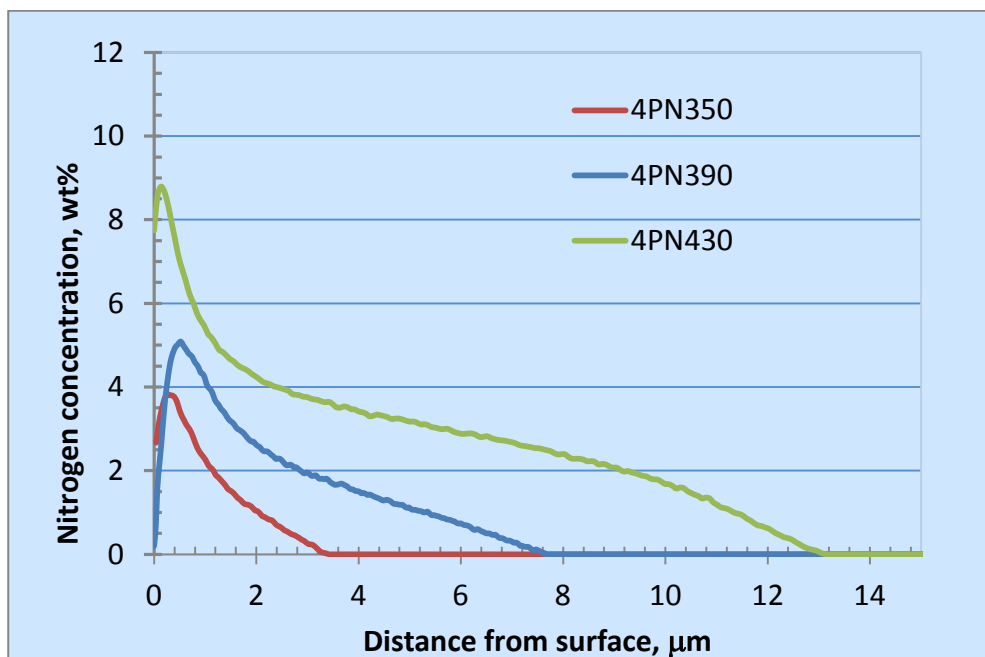


Figure 4.2-2 GDOES profiles showing the nitrogen content in plasma nitrided 17-4PH stainless steel samples treated at three different temperatures.

It can be seen from Figure 4.2-2 that the plasma nitriding temperature affected the distribution of nitrogen through the 17-4PH stainless steel samples. In general, the

higher the treatment temperature, the higher the nitrogen content and deeper the nitrided layer thickness. The thickness of the nitrided case increased from about 3.5 μm for PN350 (350°C) through about 8 μm for PN390 (390°C) to around 13.5 μm for PN430 (430°C). Typical GDOES profiles of plasma carburised samples are exemplified in Figure 4.2-3. It can be seen that the carbon level is high at the surface, which sharply decreases in correlation with the sharp initial increase in iron, which is at its lowest at the surface. The other elements of Cr and Ni remain constant throughout the whole depth of the sample. Figure 4.2-4 presents carbon depth profiles of plasma carburised three samples as a function of the treatment temperature. It can be seen that all samples show a high carbon content at the surface and drop to 2, 1 and 0.3 wt% for 450, 410 and 370°C treated samples, respectively. The carbon contents then reduced gradually except for 4PC450 sample, which showed a valley at a depth about 2.5 μm . It is difficult to determine the layer thickness produced through plasma carburising from the GDOES results alone, as seen on Figure 4.2-4. SEM results would be more accurate in this case as carbon is present within untreated stainless steel.

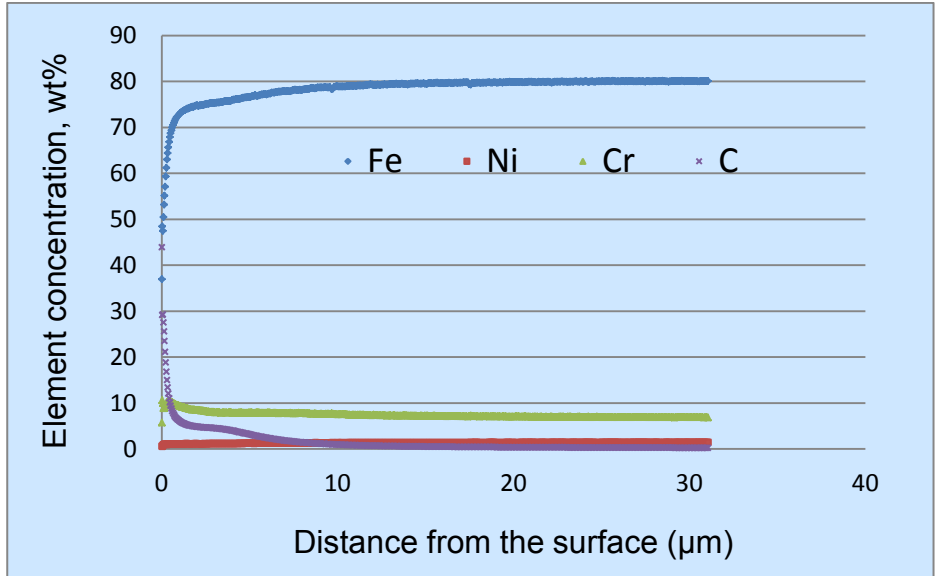


Figure 4.2-3 GDOES profiles of plasma carburised 4PC410 sample.

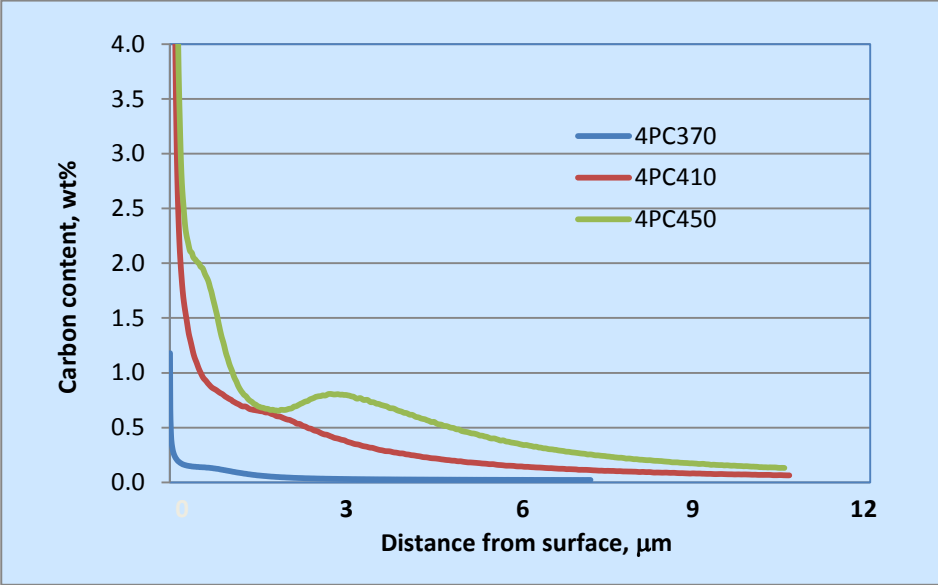


Figure 4.2-4 GDOES carbon profiles of plasma carburised 17-4 samples treated at various temperatures.

4.2.2 17-7PH Stainless Steel

Figure 4.2-5 shows typical GDOES depth profiles of plasma nitrided 7PN430 sample. The elemental distribution in the plasma nitrided 7PN430 (17-7PH steel)

is similar to plasma nitrided 4PN430 sample (17-4PH steel) but with a thinner surface layer (Fig 4.2-1). Figure 4.2-6 shows GDOES nitrogen depth profiles of all 17-7PH stainless steel samples which were active screen plasma nitrided at varying temperatures. As can be seen, the treatment temperature has an important effect on the nitrogen distribution through the stainless steel samples. This implies that higher temperature treatment introduced more nitrogen content and nitrogen diffused deeper in high temperature treated than in low temperature treated samples. The surface layer thickness of the plasma nitrided 17-7PH samples estimated from the GDOES profiles is about 2.5, 4.2 and 13.3 μm for 7PN350 (350°C), 7PN390 (390°C) and 7PN430 (430°C), respectively.

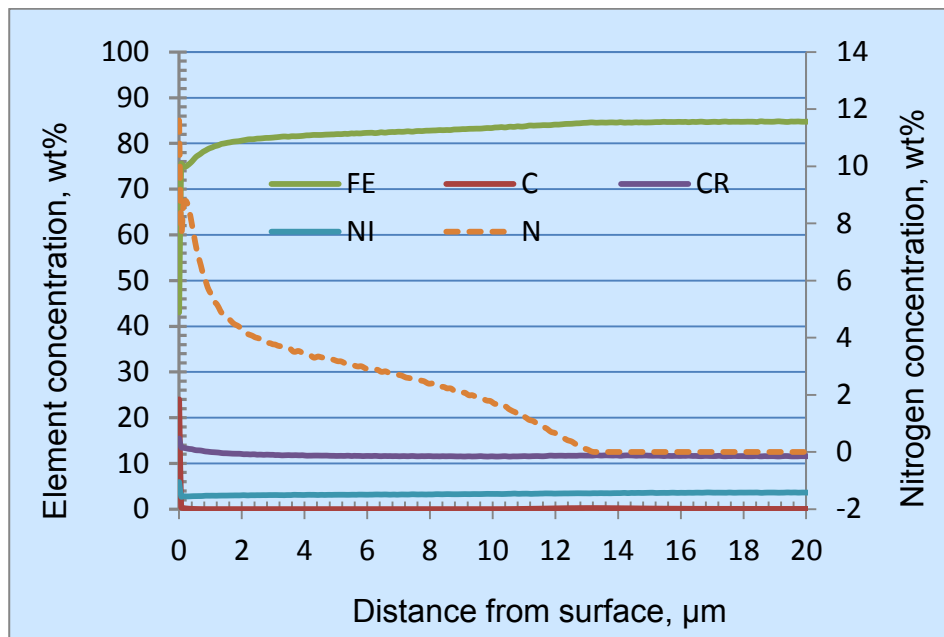


Figure 4.2-5 GDOES composition profiles of 7PN430 sample

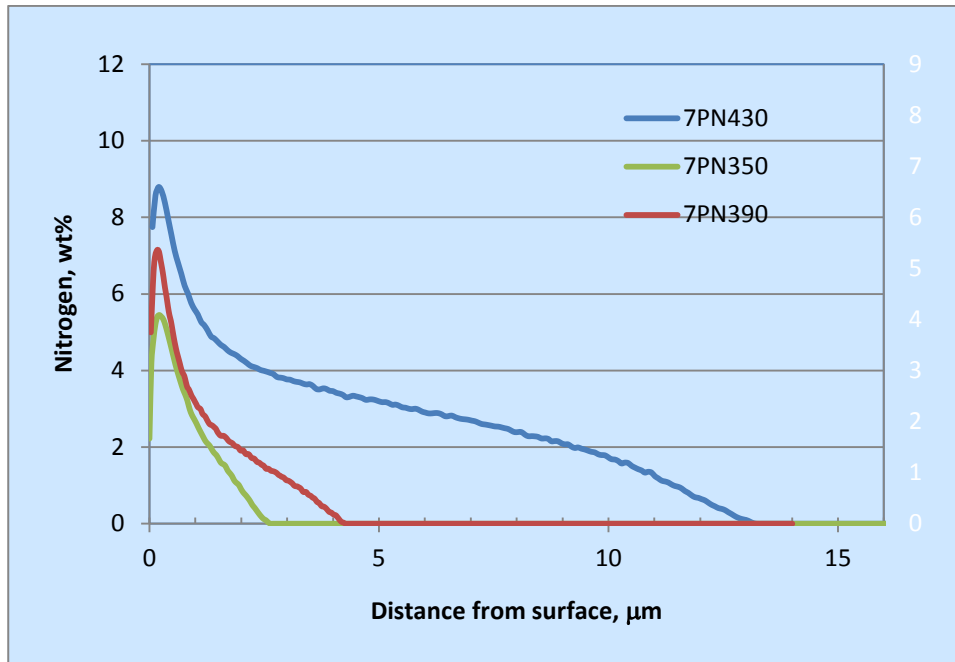


Figure 4.2-6 GDOES profiles to show the nitrogen content within plasma nitrided 17-7PH stainless steel samples treated at various temperatures.

Carbon depth profiles of plasma carburised 17-7PH samples are shown in Figure 4.2-7. It can be seen that for carburising temperature below 450°C, about 0.7 wt% carbon content was introduced to the 7PC370 and 7PC410 sample surfaces with a deeper thickness for 7PC410 than for 7PC370 sample. It is interesting to see that the carbon profile of 7PC450 sample has a lower carbon content of about 0.48 wt% within 5μm surface layer and then increases to a peak content of about 0.85 wt% before it decreases gradually, which could be correlated with the two sub-layer structure observed in SEM image (Fig 4.1-5).

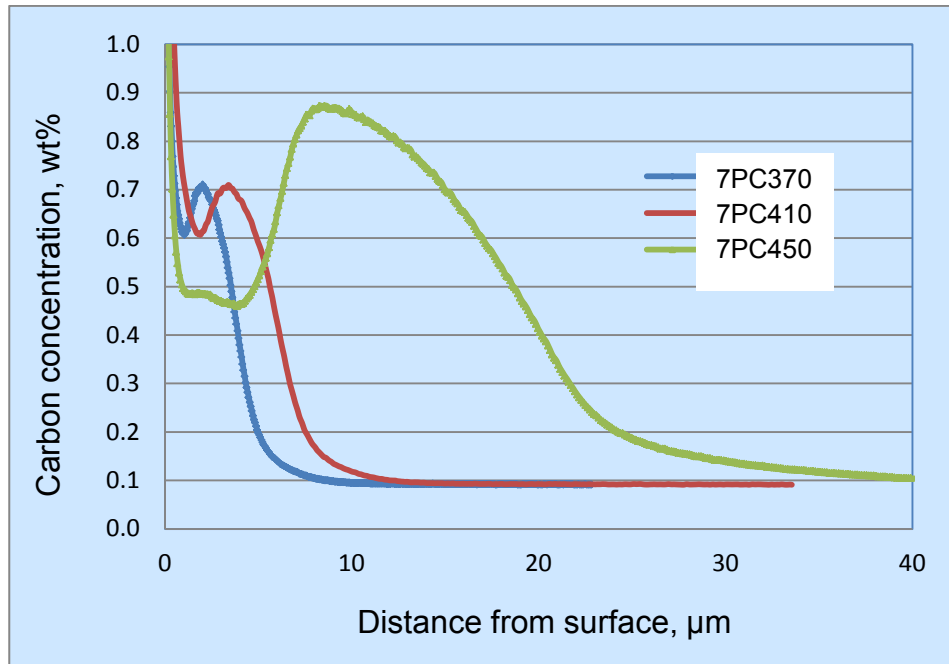


Figure 4.2-7 The carbon content in 17-7PH Stainless Steel during Plasma Carburising treatments at various temperatures.

4.3 Phase Composition of the Surface Layers

Phase compositions of all surface treated samples were studied by XRD and some of these samples were further characterised by TEM. The XRD patterns of plasma nitrided and carburised 17-4 and 17-7 PH stainless steel samples showed different phase compositions and the results of the detailed analysis are reported in this section.

4.3.1 17-4PH Stainless Steel

XRD patterns from the untreated 17-4PH stainless steel and plasma nitrided samples are shown in Figure 4.3-1. It can be seen that the untreated sample shows a set of martensite (α') peaks, while patterns of plasma nitrided 4PN350, 4PN390 and 4PN430 samples show broadened peaks around $2\Theta=20^\circ$ and 35° , corresponding to α' martensite (110) and (211) planes. A peak at $2\Theta 19^\circ$ and more peaks between $2\Theta 16\sim 20^\circ$ can be seen for sample 4PN390 and 4PN430 respectively in Figure 4.3-1a. Figure 4.3-1b shows a calculated pattern for 4PN430, based on the scanned pattern by X'pert Highscore software, fitted with possible nitrides phases of Fe_3N , Fe_4N , Cr_2N and bcc/fcc iron. It can be seen that many peak reference lines of these phases fit within two broaden peaks around $2\Theta 19^\circ$ and 35° , indicating the possibility of the formation of nitrides during the plasma treatments.

XRD patterns from untreated 17-4PH stainless steel and plasma carburised samples are shown in Figure 4.3-2 a. It can be seen that the plasma carburised 4PC370, 4PC410 and 4PC450 samples showed broaden peaks around $2\Theta=20^\circ$, 35° and 41° , corresponding to the α' martensite (110), (211) and (220) planes, which may be attributed to carbon-containing expanded martensite. For 450°C

carburised 4PC450 sample (Fig 4.3-2b), some new peaks were detected the peak reference lines of Fe_2C_5 and Cr_{23}C_6 carbides can be fit into the broaden peaks. However, because of the peak overlapping, it is difficult, if not impossible, to identify the phases produced during plasma carburising, which necessitated TEM investigation of the phase composition of the plasma carburised surface layer.

4.3.2 17-7PH stainless steel

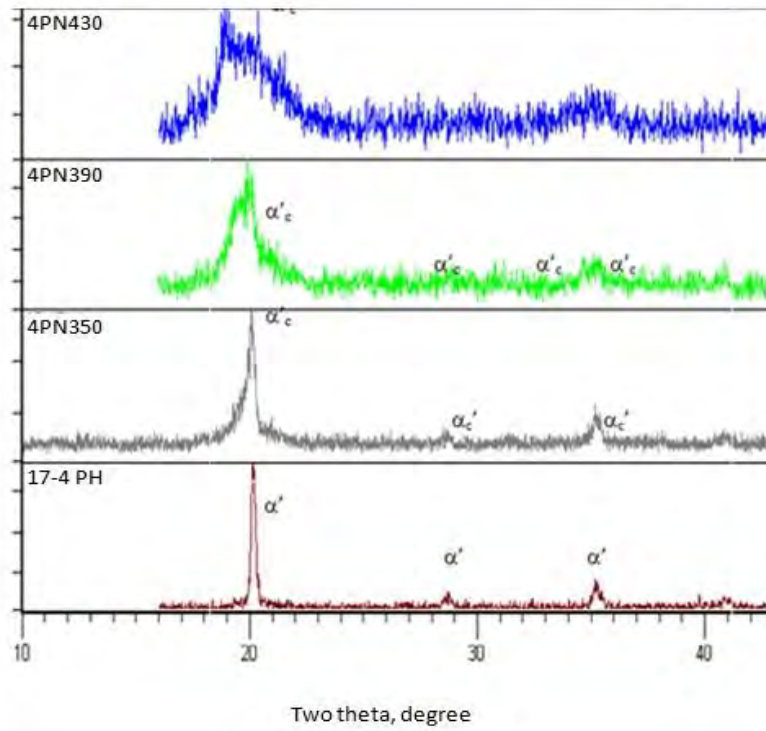
Figure 4.3-3 shows XRD patterns of as-received and plasma nitrided samples of 17-7PH stainless steel. As can be seen from Figure 4.3-3a, the as-received 17-7PH stainless steel sample contains martensite (α') and austenite phases. When plasma nitrided at 350 (7PN350) and 390°C (7PN390), the XRD patterns showed one main broad peak at $2\theta=19.5^\circ$, a very weak peak at $2\theta=22^\circ$ and austenite peaks. Because of the surface layers produced for 7PN350 and 7PN390 are very thin (4 and 7 μm , Fig. 4.4-4), the detected austenite phase was contributed from the substrate. More detailed XRD analysis suggested that both Fe_3N nitride and S-phase (or expanded austenite) could be formed in the surface of 7PN350 and 7PN390 samples (Fig.4.3-3b).

For 7PN430 sample two broad peaks around $2\theta=18$ and 20.8° were detected, which could not be assigned to any known nitrides but are analogous to the S-phase found in austenitic steel after low temperature plasma nitriding (Li X Y, 2001). Because of the thick surface nitrided layer (15 μm), no peaks from the substrate could be detected and the S-phase peaks were contributed from the surface layer.

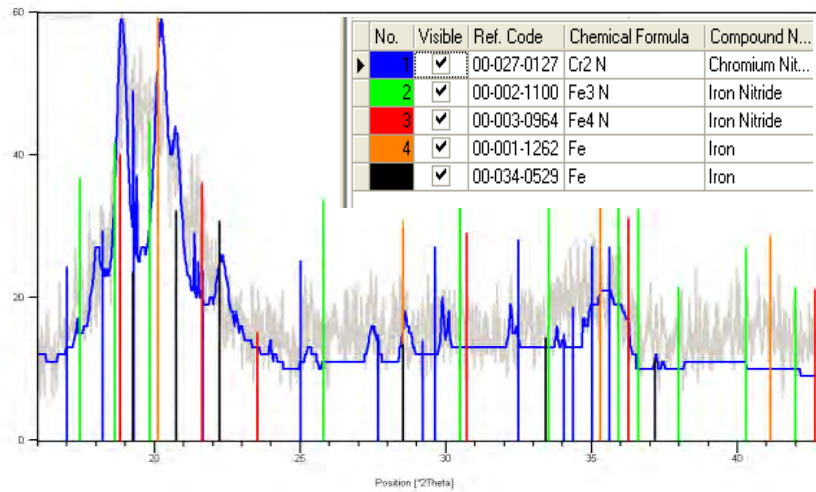
Figure 4.3-4 shows the XRD patterns for as-received and plasma carburised 17-7PH stainless steel samples treated at three different temperatures. It can be seen that austenite peaks were detected from 7PC370 (370°C) and 7PC410 (410°C) samples, marked with red lines in the figure, which was contributed from the substrate since the surface layer is only 6 and 11µm respectively. A set of broadened fcc peaks at the left side of austenite peaks could be an indication of the formation of carbon S-phase during plasma carburising. However, the very broad peaks and rough background character of the XRD patterns (especially for 7PC410), could not rule out the potential formation of other phases.

The XRD pattern for 7PC450 differed greatly from that for the low-temperature treated 7PC370 and 7PC430 samples in that apparent three broad peaks between 2 theta 18.5 and 23° were detected. This may be to some extent related to the formation of dark top sublayer as shown in Figure 4.1-5c. Indexing of these peaks revealed possible formation of carbides Fe_5C_2 , Cr_7C_3 and Cr_{23}C_6 as marked with green, blue and amber reference lines in Figure 4.3-4.

Because of the peak broadening and the very close d-spacing values for those carbides, it is impossible to determine conclusively the phase composition by XRD analysis alone for the plasma carburised surface layers. Consequently, further TEM work was carried out to identify any small amount of carbides in the carburised surface layers.



a



b

Figure 4.3-1 XRD patterns of a) as-received and plasma nitrided 17-4 PH samples under varying conditions; b) plasma nitrided 4PN430 sample with inserted possible phase reference lines.

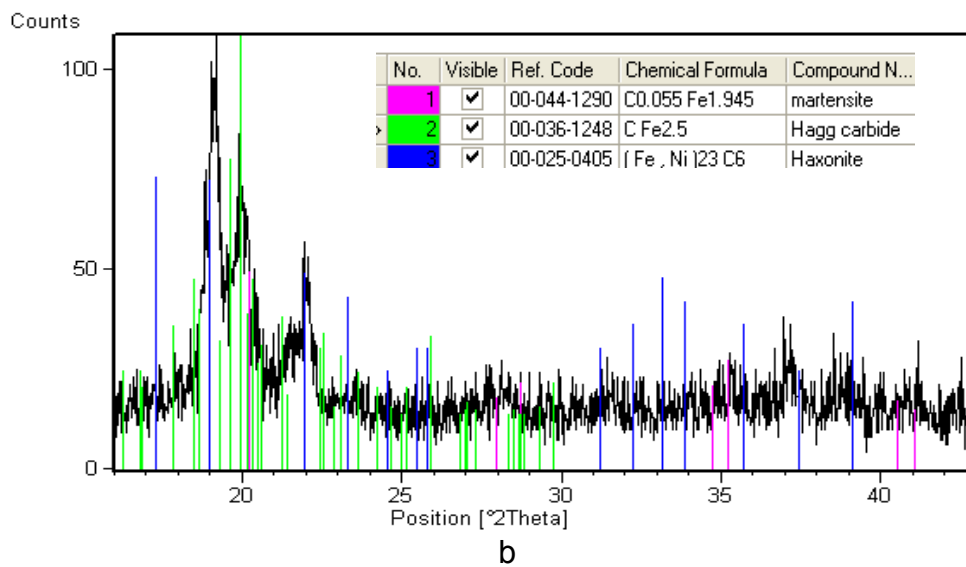
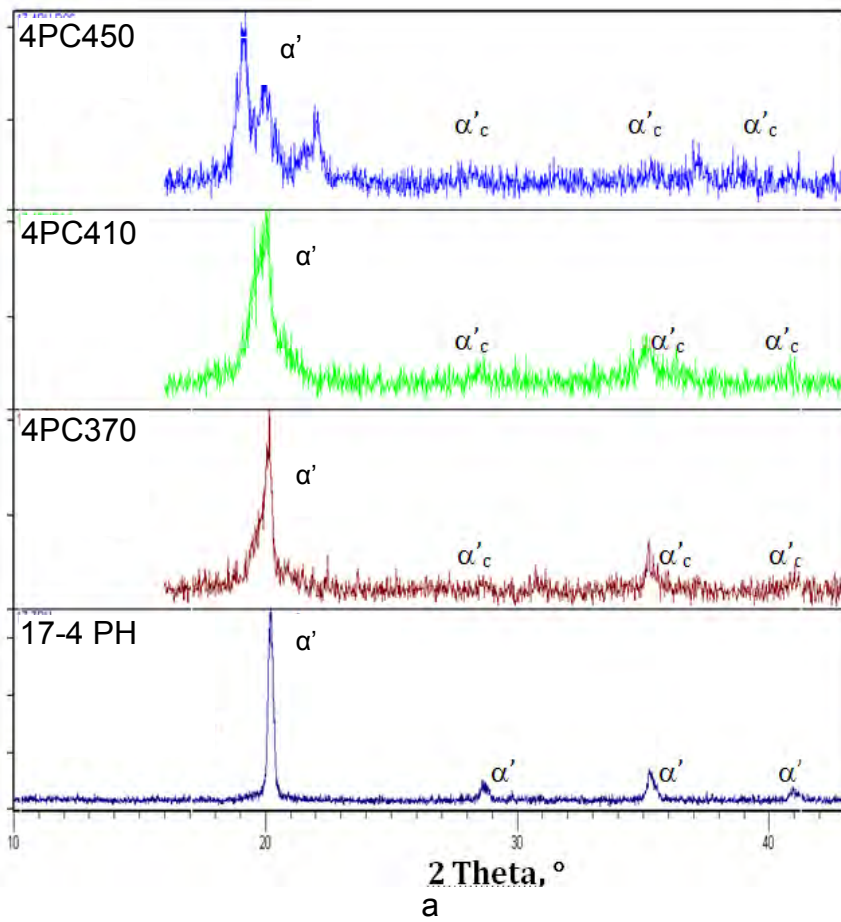
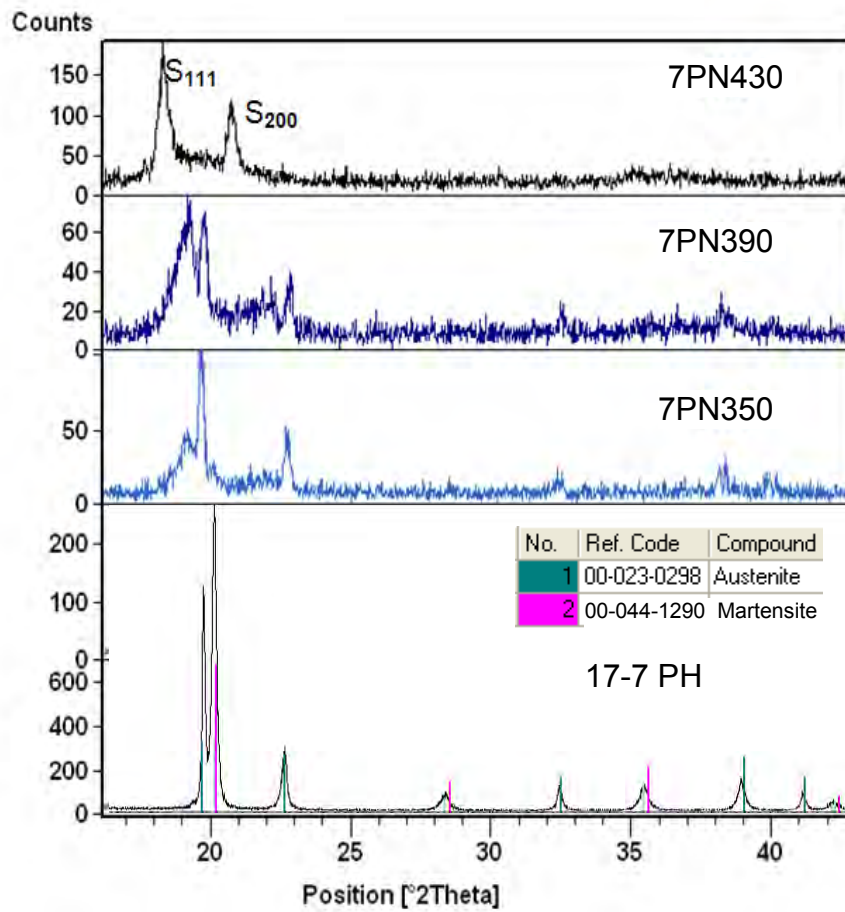
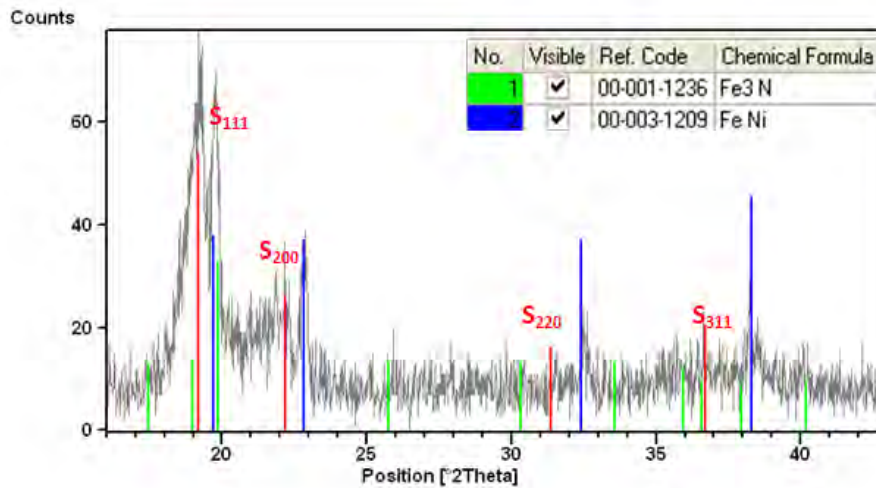


Figure 4.3-2 XRD patterns of a) as-received and plasma carburised samples under varying conditions; b) plasma carburised 4PC450 sample with inserted possible phase reference lines.



a



b

Figure 4.3-3 The XRD patterns of 17-7PH stainless steel a) as-received and plasma nitrided samples under varying conditions; b) plasma nitrided 7PN390 sample with inserted possible phase reference lines.

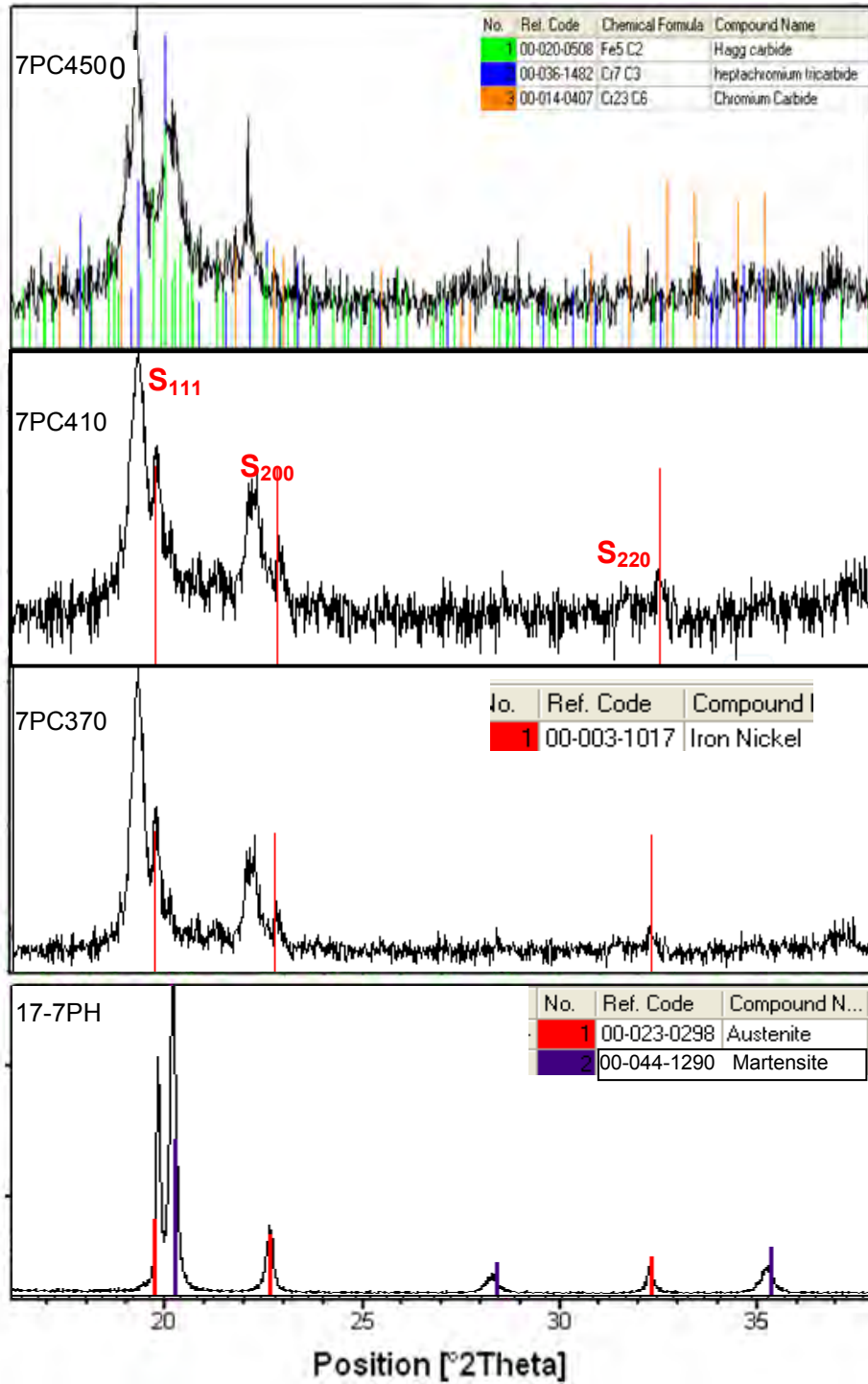


Figure 4.3-4 The XRD patterns of as-received and plasma carburised 17-7PH stainless steel samples.

4.3.3 TEM characterisation

As have been seen in Figures 4.3-1 to 4.3-4, most of the XRD peaks are broad and many of them are overlapped, it is difficult, if not impossible, to index the phase constitution of plasma alloyed surfaces by XRD alone. Hence TEM work has been carried out to further investigate the microstructures of some selected samples.

The microstructure of as received 17-4PH and 17-7PH stainless steels were observed by TEM and the typical microstructures are shown in Figure 4.3-5. It can be seen that 17-4 PH sample is dominated by lath martensite (Figs 4.3-5 a, b) while - 17-7PH sample contained austenite (Figs 4.3-5 c, d) and martensite (Fig. 4.3-5 c, e) together with a trace of ferrite.

4.3.3-1 7PN390 sample

Cross-sectional TEM microstructures of surface nitride layer for sample 7PN390 are shown in Figures 4.3-6. It can be seen that the surface layer consists of plenty of needle like precipitates. SAD patterns from the surface layer revealed super imposed spots patterns and they were identified as b.c.c nitrogen martensite, f.c.c S-phase and nitride Fe_3N . Dark field TEM image taken by $\epsilon\text{-Fe}_3\text{N}$ and S-phase diffraction spots as circled in solid and dotted lines in Figure 4.3-6b revealed needles of nitride growth from austenite (S-phase) grain boundaries. Three phases presented preferred orientations of

$$[011] \alpha'_N, // [100]_{S_N} // [001]_{\text{Fe}_3\text{N}}; \quad (1-11) \alpha'_N // (020)_{S_N} // (100)_{\text{Fe}_3\text{N}}.$$

Spots patterns from nitrogen martensite and S-phase are faint and distorted, indicating high residue stress of the surface layer. This is caused by the phase

change by introducing nitrogen during the plasma treatment, resulting in compressive residue stress within the surface layer.

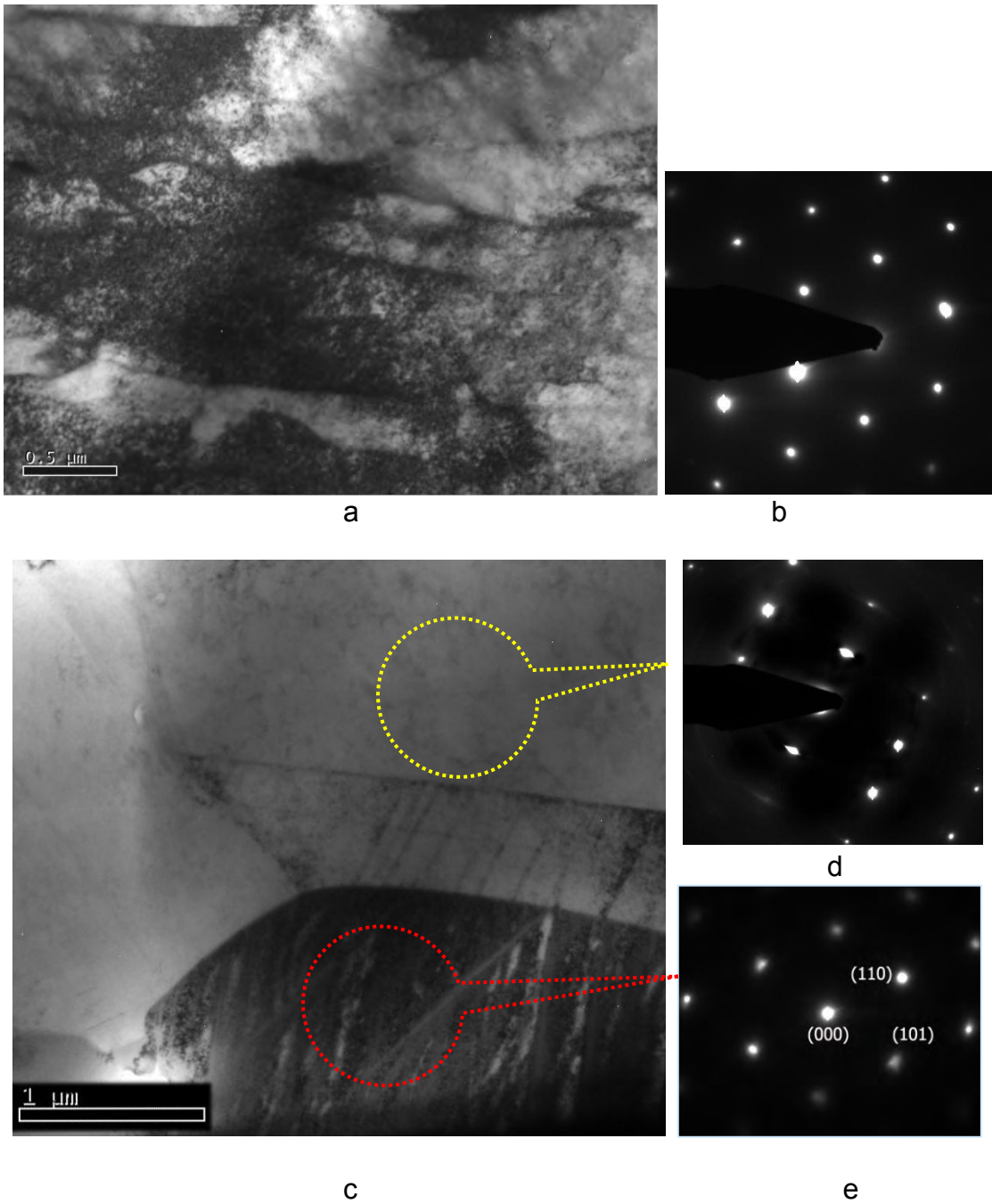


Figure 4.3-5 TEM microstructure and SAD patterns of as-received a, b) 17-4PH steel sample (b=111), c, d & e) 17-7PH steel sample.

4.3.3-2 7PC410 sample

TEM surface layer microstructure of 410°C plasma carburised 17-7PH sample (7PC410) is shown in Figure 4.3-7a. It can be seen that thin, long intersect colonies of platelets were formed in the matrix. SAD patterns in Figures 4.3-7 b and c were taken from top dark area and centre area circled by solid and dotted line in Fig 4.3-7a, respectively. Indexing of the patterns identified matrix structure of Sc-phase (Fig 4.3-7b, $b=[101]_{Sc}$) on the top layer of dark contrast, while those long, thin, intersected colony platelets were indexed as *Hägg*-Fe₅C₂ (χ)carbide. As evidenced in Figures 4.3-7d,e, three set of χ carbide patterns of [-281], <-492> were indexed on the matrix of martensite [013] pattern. The carbide appears with large aspect ratios, typically featuring a short dimension of ≈ 100 nm and a long dimension up to tens of micrometers, which were growing from the surface to the substrate following carbon diffusion front during plasma carburising.

As observed in XRD patterns, weak martensite peaks were detected in 17-7PH steel when plasma nitrided and carburised at 7PN390 and 7PC410 conditions (Figures 4.3-3 and 4.3-4). TEM observation proved the transformation of martensite to austenite in treated surface layers during plasma surface alloying and S-phase was formed from the austenite structure. However, this transformation was not in 100% and trace martensite was observed (Figure 4.3-6).

4.3.3-3 4PC410 sample

As shown in Figure 4.3-5 a,b, lath martensite was revealed for untreated 17-4 PH sample. After plasma carburising, TEM observation found that the martensite matrix was retained in this sample, as evidenced in Figure 4.3-8 d, $b=[133]$, and

SAD pattern superimposed with the precipitated carbide. χ -Fe₅C₂ carbide was identified as the dominant carbide (Figure 4.3-8d) precipitated from martensite in surface hardened layer during plasma carburising. The shape of the χ -Fe₅C₂ carbide is similar to that in 7PC410 sample, appearing as long, thin, intersected colony platelets with large aspect ratios (Figs. 4.3-8 a b). However, detailed TEM analysis in the areas close to the outmost surface found that Cr₂₃C₆ carbide formed at χ -Fe₅C₂ carbide intersect nodes, as can be seen in Figure 4.3-9a, which is a dark filed image taken by circled Cr₂₃C₆ sports in Fig.4.3-9b. This finding may explain the higher hardness of 17-4 PH 4PC410 sample than 17-7PH 7PC410 sample (see Chapter 5).

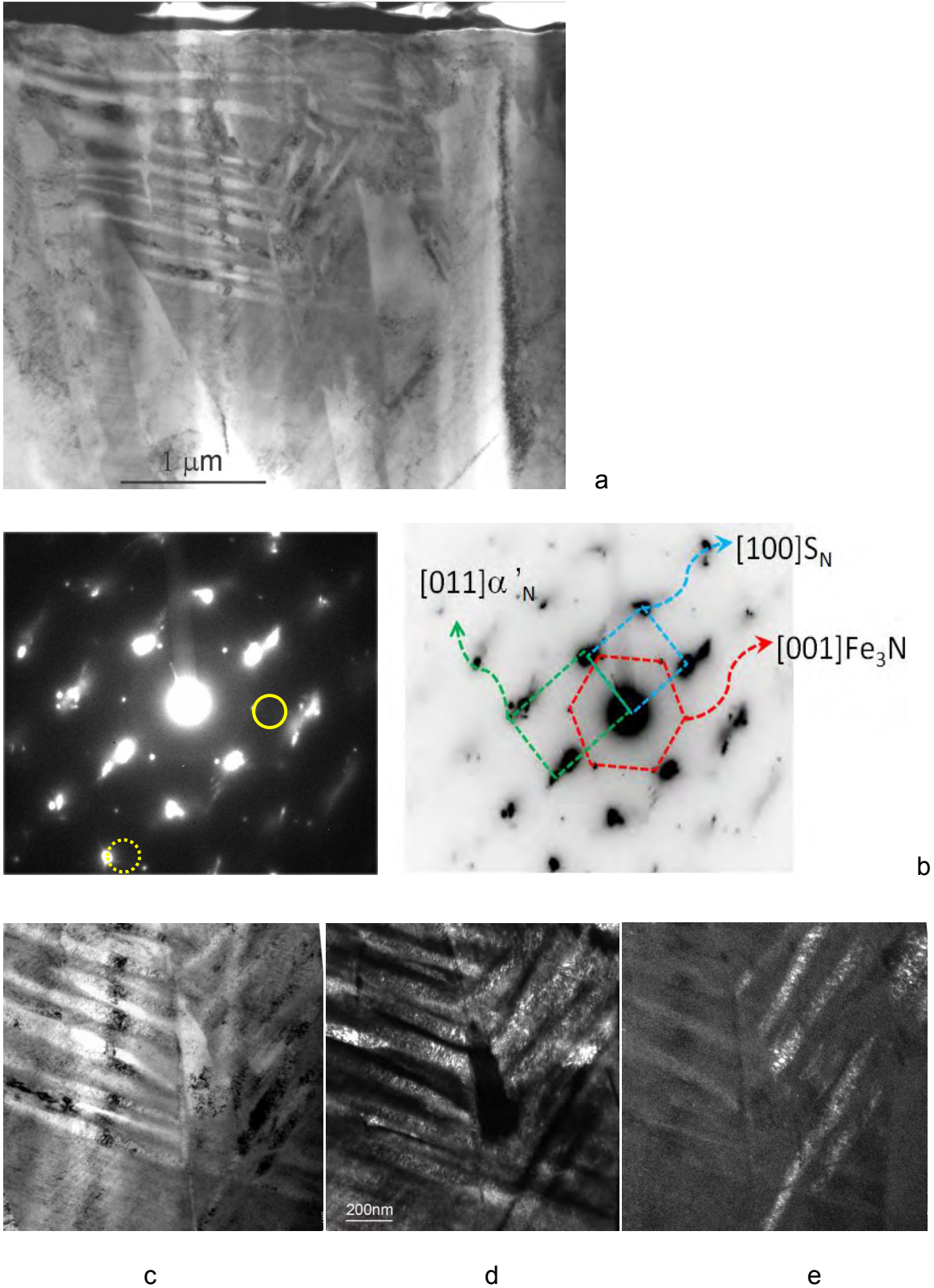
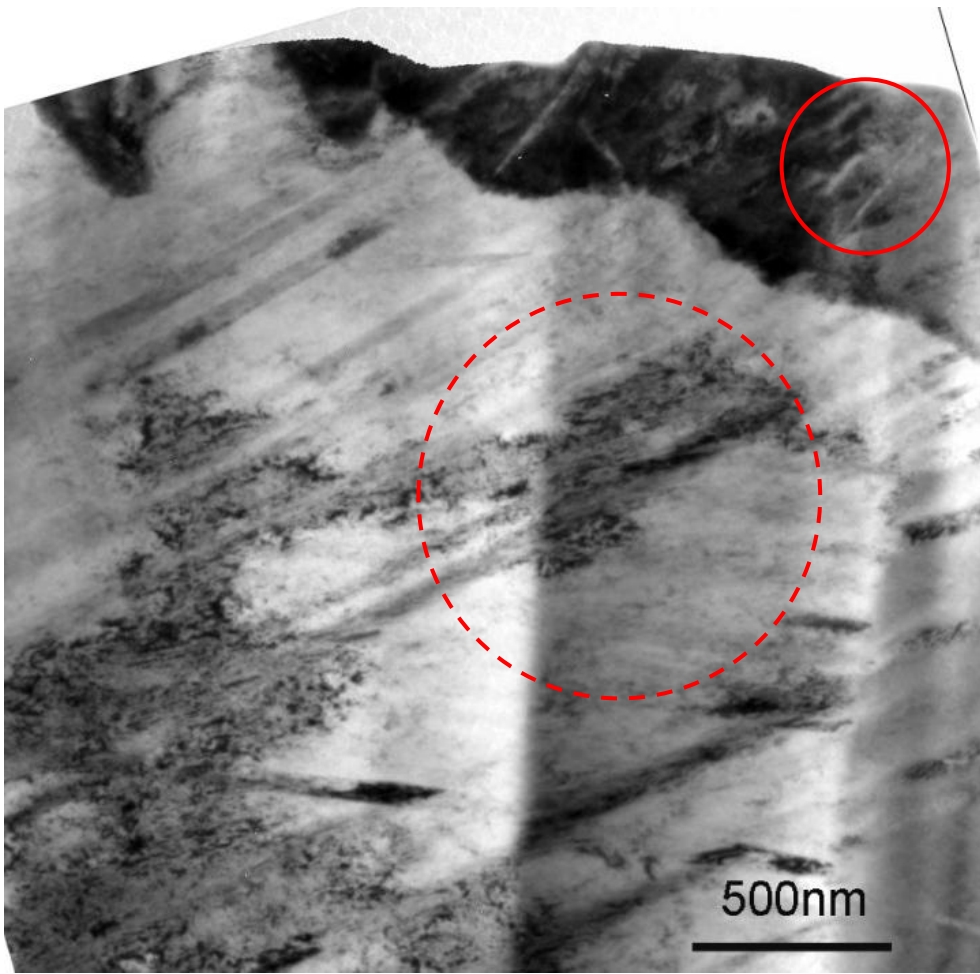
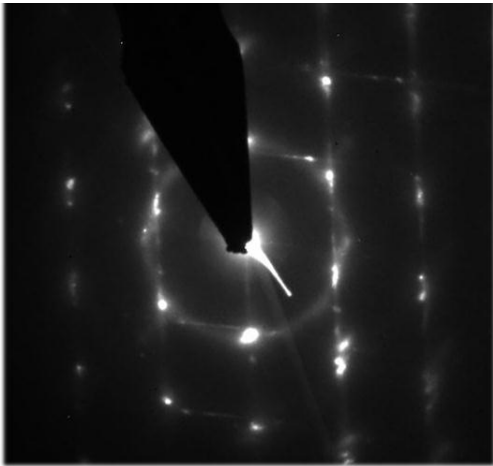


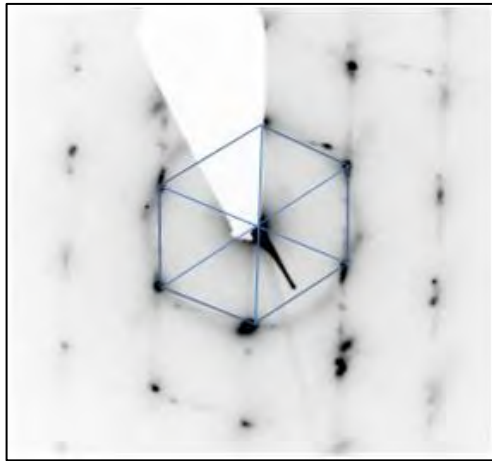
Figure 4.3-6 a),c) BF and d), e) DF TEM microstructures and b) SAD pattern, taken from surface nitrided layer of 7PN390 sample.



a



b



c

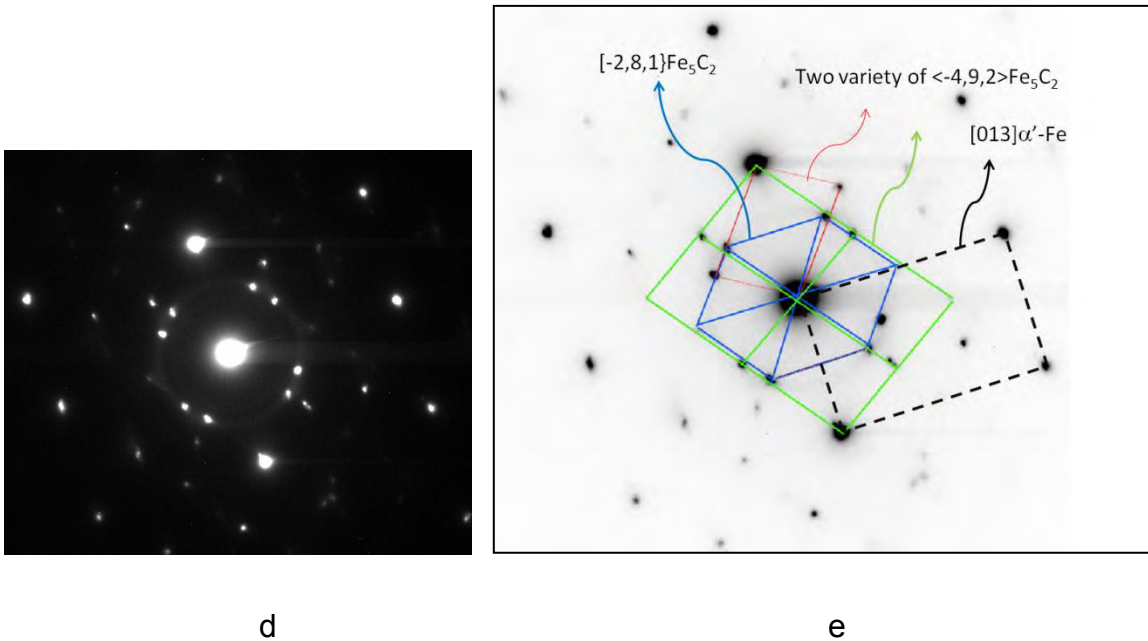


Figure 4.3-7 a) TEM microstructure and SAD patterns of b) top dark area in a), $b=[101]Sc$; d) centre area in a), and c), d) index of b),c) from plasma carburised 7PC410 sample of 17-7PH stainless steel.

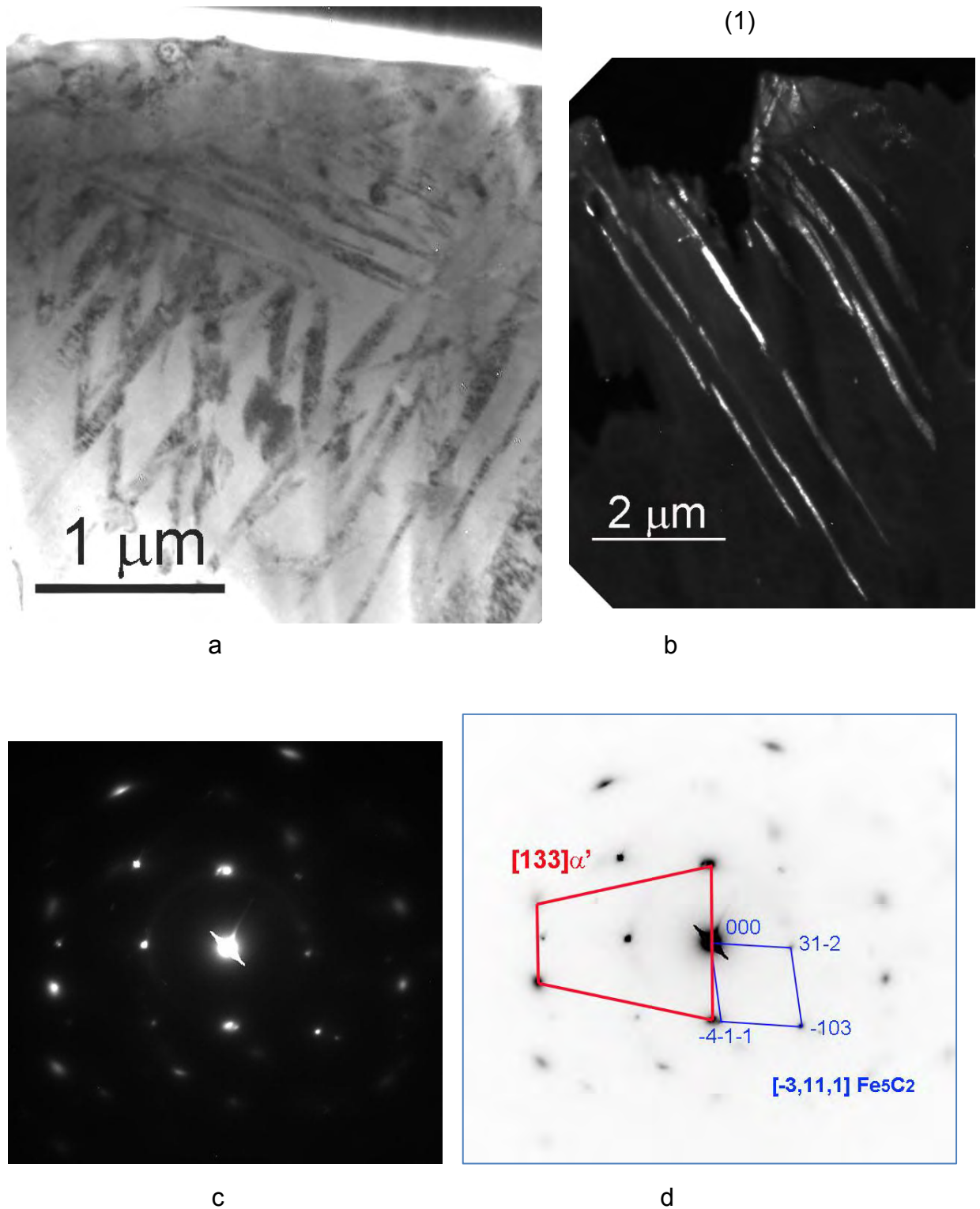


Figure 4.3-8 a) BF XTEM microstructure of surface layer and b) DF XTEM of χ -Fe₅C₂ carbide taken by c) SAD pattern of χ -Fe₅C₂ diffraction spot and d) index of c) from sample 4PC410 of 17-4PH stainless steel, plasma carburised at 410°C.

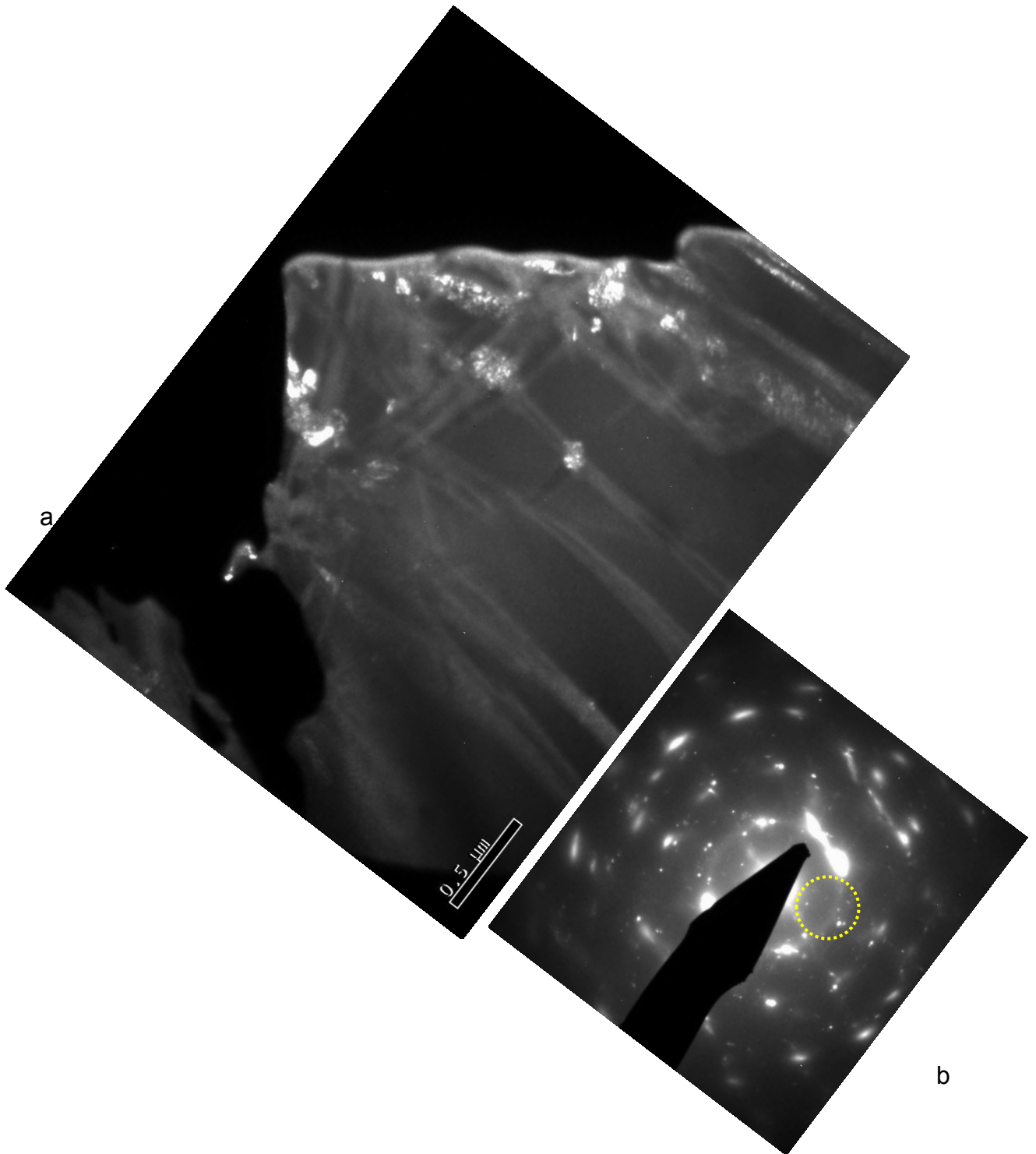


Figure 4.3-9) a) Cross section DF TEM image taken by b) Cr₂₃C₆ carbide diffraction spots, as circled, from sample 4PC410 of 17-4PH stainless steel, plasma carburised at 410°C.

4.4 Hardness and Layer Thickness

The surface hardness is related to other properties such as the wear resistance of a material, and therefore is important when assessing the benefit of surface modification treatments on both mechanical and tribological properties.

4.4.1 17-4PH

After active screen plasma treatments, all samples have showed a significant increase in surface hardness dependent on the treatment conditions. It can be seen from Figure 4.4-1 that, the surface hardness increased from 1201 to 1591HV_{0.05}) when plasma nitrided at 350°C (4PN350) and 390°C(4PN390). However, further increase in temperature to 430°C led to a decrease from 1,591 to 1,326HV_{0.050}(Figure 4.4-1). The mechanism involved will be discussed in Chapter 5.

The thickness of the modified layers produced through plasma nitriding of 17-4PH stainless steel increased with the treatment temperature, as shown in Figure 4.4-2. The transition between 350°C to 390°C showed an increase from 4µm to 11µm on 17-4PH stainless steel, whereas from 390°C to 430°C there was a much larger increase to a modified layer thickness of 24µm. This is in agreement with Fick's diffusion law as it is well-known that the diffusion coefficient of nitrogen increases with temperature. The kinetics and activation energy of the diffusion of nitrogen will be discussed in Chapter 5.

Plasma carburising at 370, 410 and 450°C for 20 hours produced surface hardness values of 915, 1180 and 1413HV_{0.050}, respectively, highlighting a positive temperature dependency (Figure 4.4-1). The same dependency, shown in

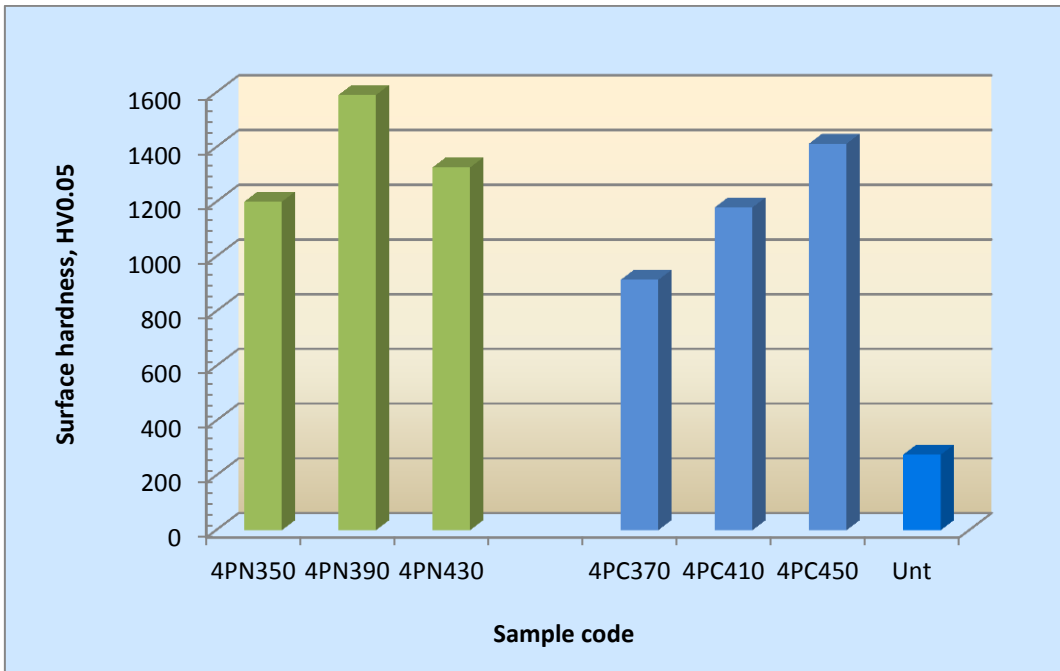


Figure 4.4 -1 The surface hardness of plasma nitrided (PN) and carburised (PC) 17-4PH stainless steel samples as a function of treatment temperature.

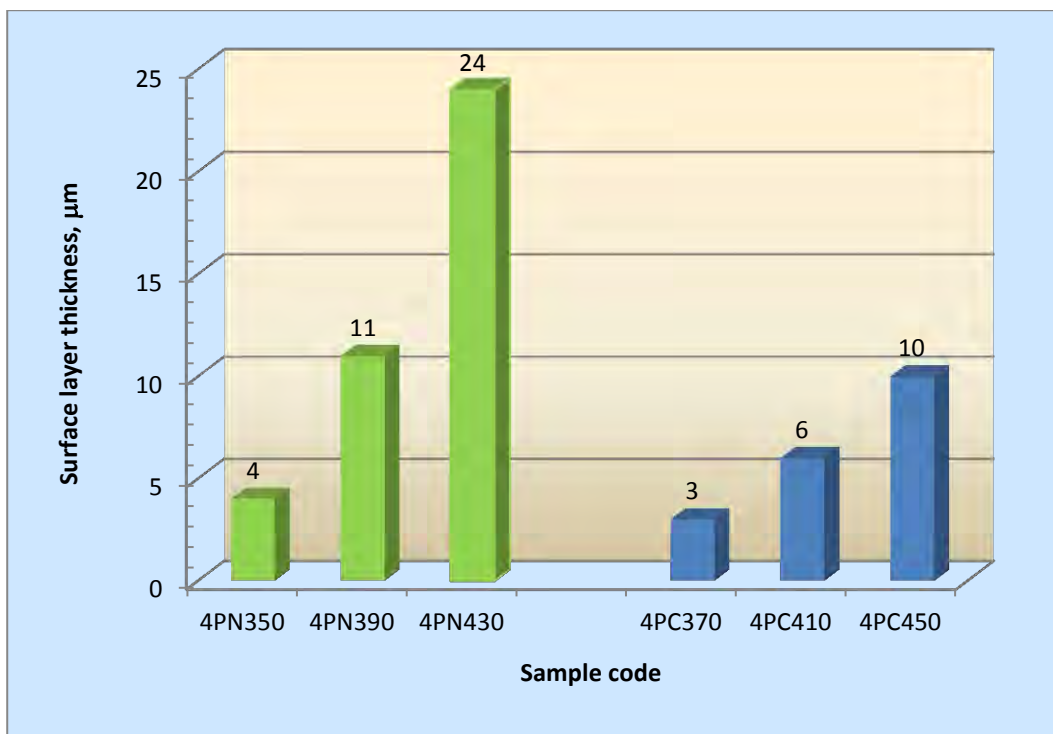


Figure 4.4-2 The layer thickness of plasma nitrided (PN) and carburised (PC) 17-4PH stainless steel samples as a function of treatment temperature.

Figure 4.4-2, occurs for the thickness of the carburised surface layer, producing 3, 6 and 10 μ m respectively for 370, 410 and 450°C treated samples.

Clearly, effective hardening of 17-4PH stainless steel has been achieved by active screen plasma surface alloying with N (nitriding) or C (carburising) as evidenced by the significantly increased surface hardness from about 240HV0.05 for untreated material to 1591HV0.05 for nitrided 4PN390 and 1413 for carburised 4PC450 samples, representing about 5 times improvement.

4.4.2 17-7PH

Similar to 17-4PH, the surface hardness of plasma alloyed 17-7PH stainless steel also depends on the treatment temperature. However, different from plasma nitrided 17-4PH steel (Fig. 4.4-1), the surface hardness of 17-7PH stainless steel increased with increasing the treatment temperature. 17-4PH steel has a substrate surface hardness value of 204HV0.050, which increased to 422, 582 and 1428HV0.050 when treated at 350°C, 390°C and 430°C, respectively. Except for PN430 treatment, the hardening response to plasma nitriding of 17-7PH is not so strong as 17-4PH at relatively low temperatures of 350 and 390°C.

Plasma carburising can also be used to improved the surface hardness of 17-7PH stainless steel, producing values of 508, 857 and 1230HV0.050. However, it is clear by comparing Fig. 4.4-3 with Fig. 4.4-1 that the hardening response to plasma carburising is weaker for 17-7PH than for 17-4PH although both showed the same temperature dependence of hardness.

There is a clear connection between the temperature of the plasma surface alloying treatment of 17-7PH steel and the thickness of the surface modified layer

(Figure 4.4-4), which is very similar to the trend observed for plasma alloyed 17-4PH steel (Fig. 4.4-2). However, it is of interest to find that when treated under the same conditions, whilst the plasma nitrided layer is thicker formed on 17-4PH than on 17-7PH, the opposite occurred for the plasma carburised layer (Fig. 4.4-2 vs Fig.4.4-4).

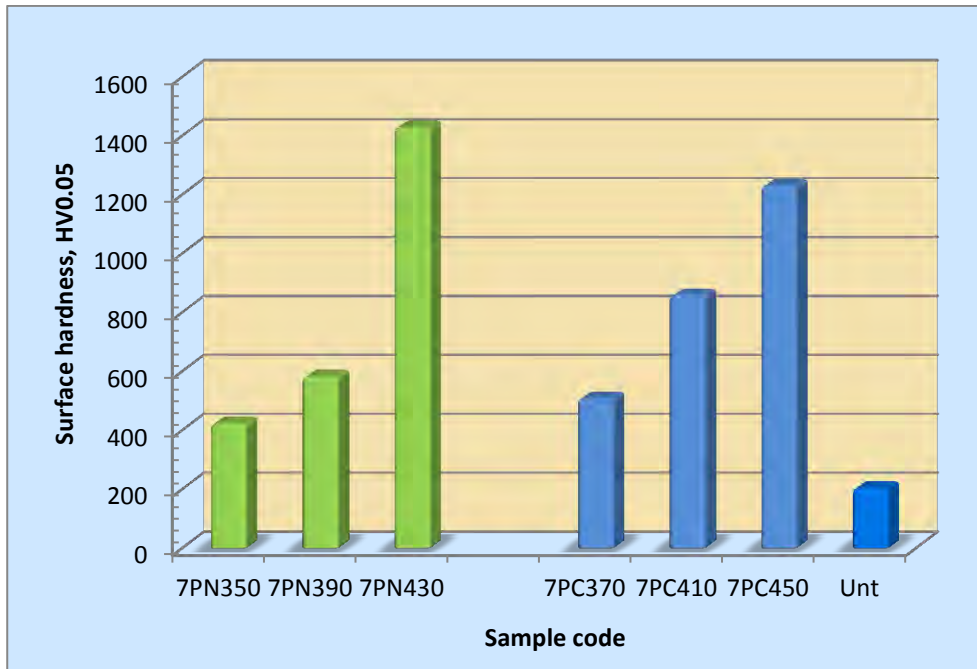


Figure 4.4-3 The surface hardness of plasma nitrided (PN) and carburised (PC) 17-7PH stainless steel samples as a function of treatment temperature.

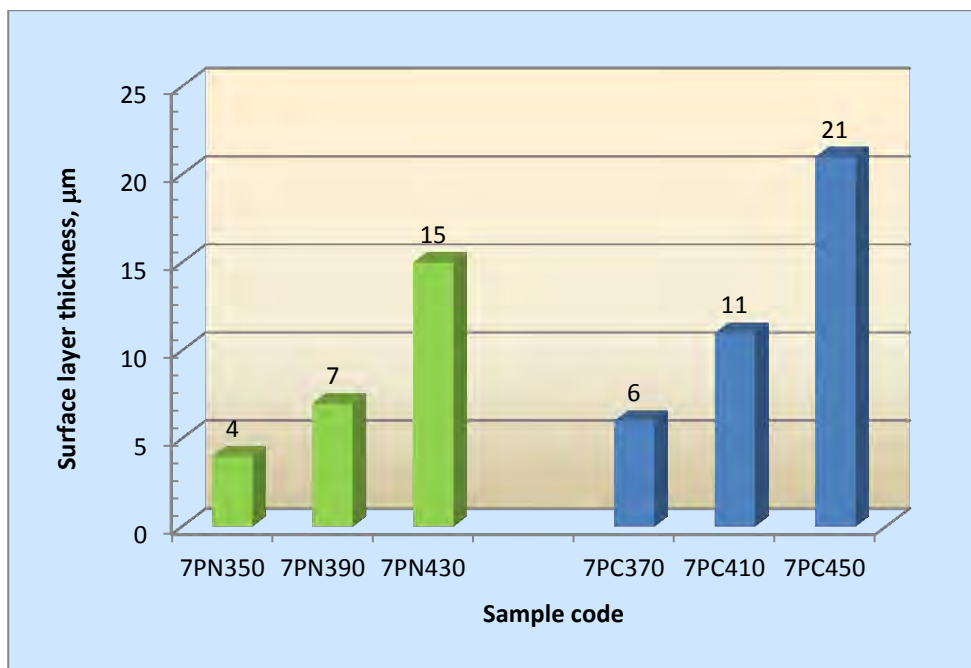


Figure 4.4-4 The thickness of plasma nitrided (PN) and carburised (PC) 17-7PH stainless steel samples as a function of treatment temperature.

4.5 Friction and Wear

In order to evaluate the effect of plasma surface alloying on the tribological properties of 17-4PH and 17-7PH stainless steels, the friction coefficients and wear loss on both untreated and treated 17-4PH and 17-7PH stainless steel samples were tested using a reciprocating tungsten carbide (WC/Co) ball for 4 hours in un-lubricated conditions under a contact load of 10N.

4.5.1 17-4PH

As shown in Figure 4.5-1, plasma surface alloying treatments can effectively reduce the friction coefficient of 17-4PH stainless steel from 0.51 for the untreated sample to between 0.14 and 0.33, representing a reduction of 35.3-72.5%.

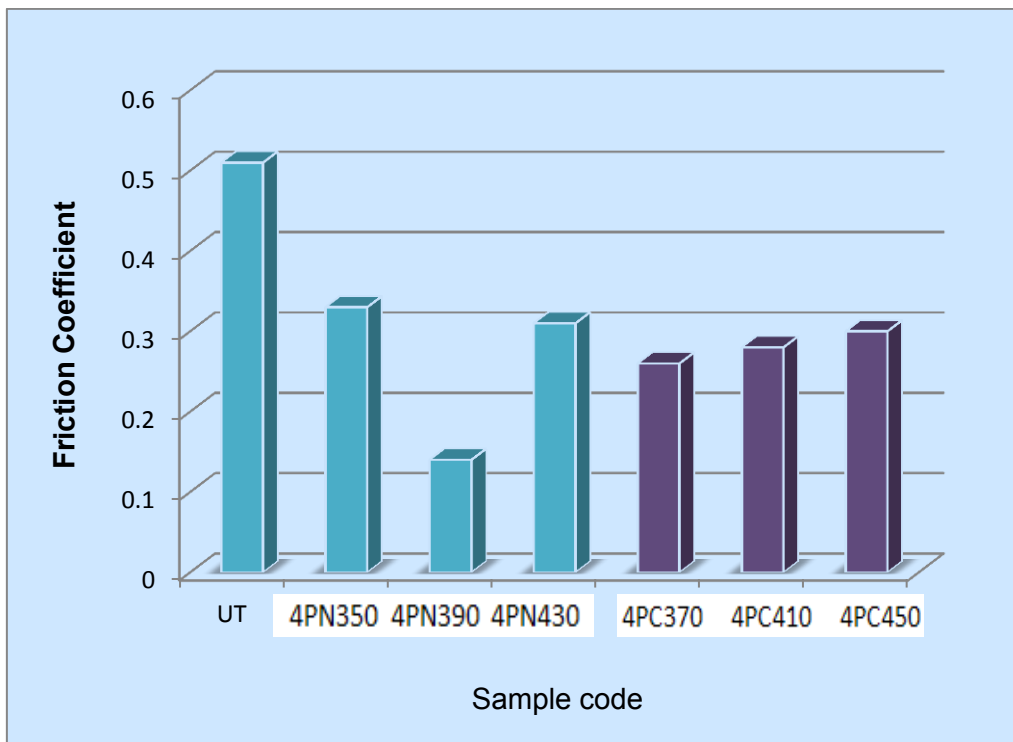


Figure 4.5-1 The friction coefficients of untreated (UT), plasma nitrided (PN) and carburised (PC) 17-4PH stainless steel samples.

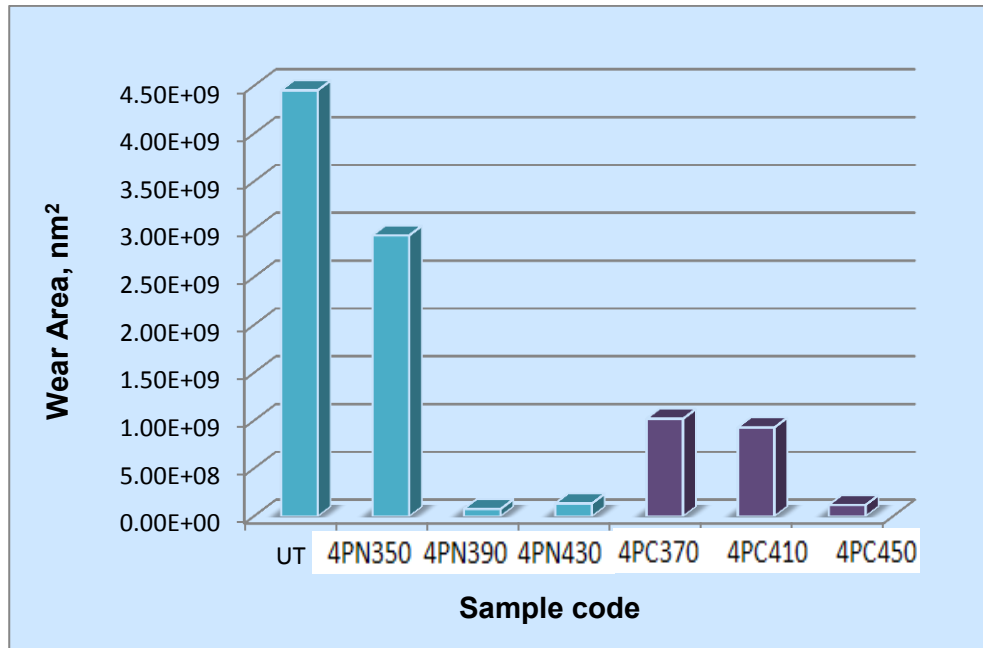


Figure 4.5-2 The wear loss of untreated (UT), plasma nitrided (PN) and carburised (PC) 17-4PH stainless steel samples.

Figure 4.5-2 shows the wear area loss dependent on varying plasma treatments. Untreated 17-4PH stainless steel produced a wear loss of $4.45 \times 10^3 \mu\text{m}^2$; however when nitrided at 350°C for 20 hours, this was reduced to $2.94 \times 10^3 \mu\text{m}^2$. This was further reduced to $76.7 \mu\text{m}^2$ and $1.34 \times 10^2 \mu\text{m}^2$ for 390°C and 430°C nitrided samples respectively. The optimal treatment parameters for plasma nitriding is 390°C (4PN390) which produced a wear loss of only $76.7 \mu\text{m}^2$ which is about 2 orders of magnitude less than that that occurred for the untreated sample.

Active screen plasma carburising can also be used to improve the wear resistance of 17-4PH stainless steel, as can be seen from Figure 4.5-2. The pattern can be described as an increase in wear resistance with increasing treatment temperature. The 4PC450 sample performed the best in terms of wear resistance

among carburised samples and similar to plasma nitrided samples of 4PN390 and 4PN430.

Post-test SEM observation was conducted to study on the wear track of untreated (Fig. 4.5-3), plasma nitrided (Fig. 4.5-4) and plasma carburised samples (Fig. 4.5-4) to study the wear-reduction mechanisms involved for the plasma surface treated samples. It can be seen from Figure 4.5-3 that the untreated 17-4PH revealed severe delamination and abrasive wear as evidenced by larger craters and coarse grooves on the wear track surface. In the contrast, the wear tracks formed in the plasma treated 17-4PH were characterised by mild oxidative and abrasive wear, which is supported by the evidences of fine and dark wear debris (Fig. 4.5-4) and very fine scratches (Fig. 4.5-4).

4.5.2 17-7PH

For plasma nitrided 17-7PH stainless steel samples, the friction coefficient decreased with increasing treatment temperature. The 350, 390 and 430°C plasma nitrided samples produced friction coefficient values of 0.17, 0.16 and 0.10 respectively as shown in Figure 4.5-6. Clearly, plasma nitriding is more effective in reducing friction coefficient for 17-7PH than for 17-4PH steel (Figs. 4.5-1 vs 4.5-6).

Plasma carburising of 17-7PH stainless steel also caused a decrease in friction coefficient with increasing temperature (Fig. 4.5-6), although this decrease is not so effective as plasma nitriding. With the rise in temperature from 370°C to 450°C when plasma carburising 17-7PH stainless steel, the coefficient of friction decreases from 0.49 in the untreated sample to 0.29, 0.25 and 0.24 respectively.

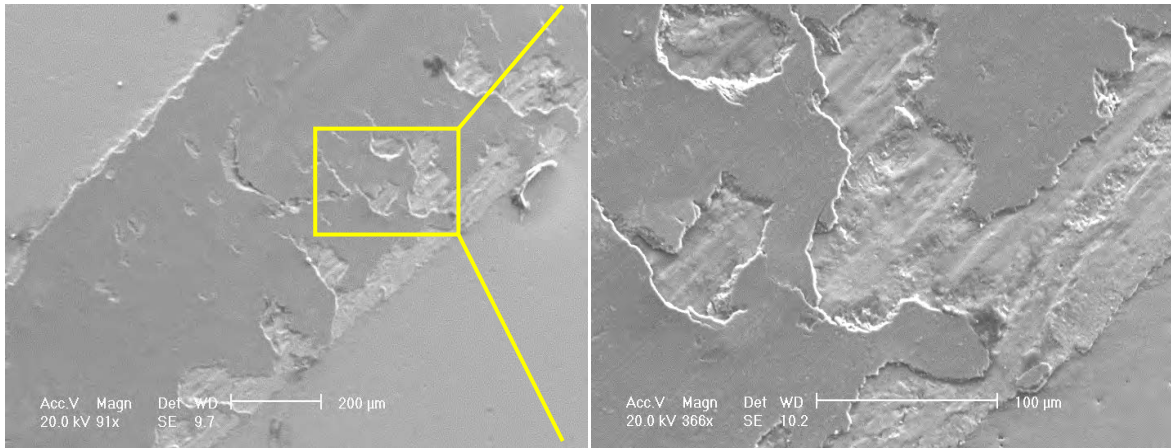


Figure 4.5-3 SEM microstructures of wear track on untreated sample

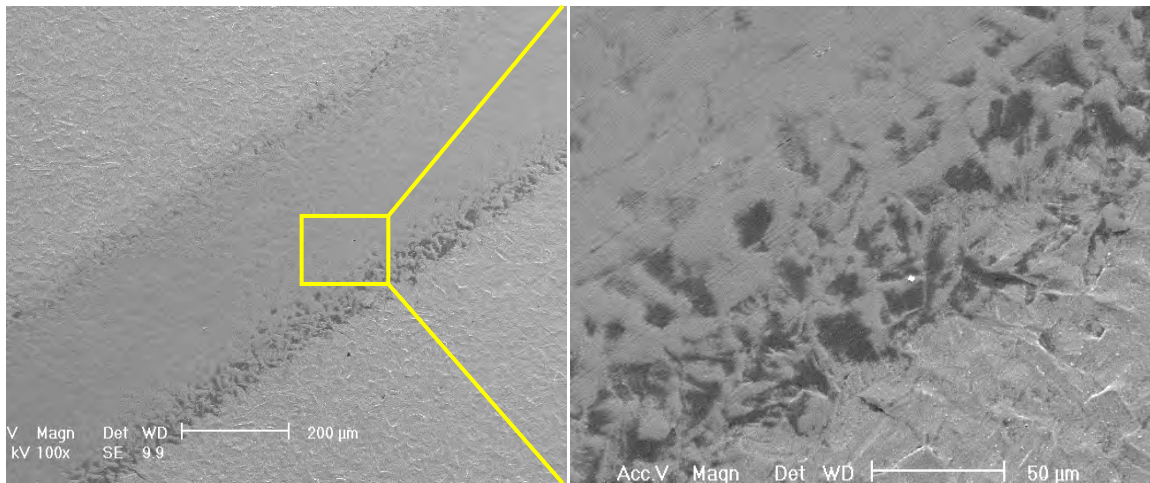


Figure 4.5-4 SEM microstructures of wear track on 4PN390 sample

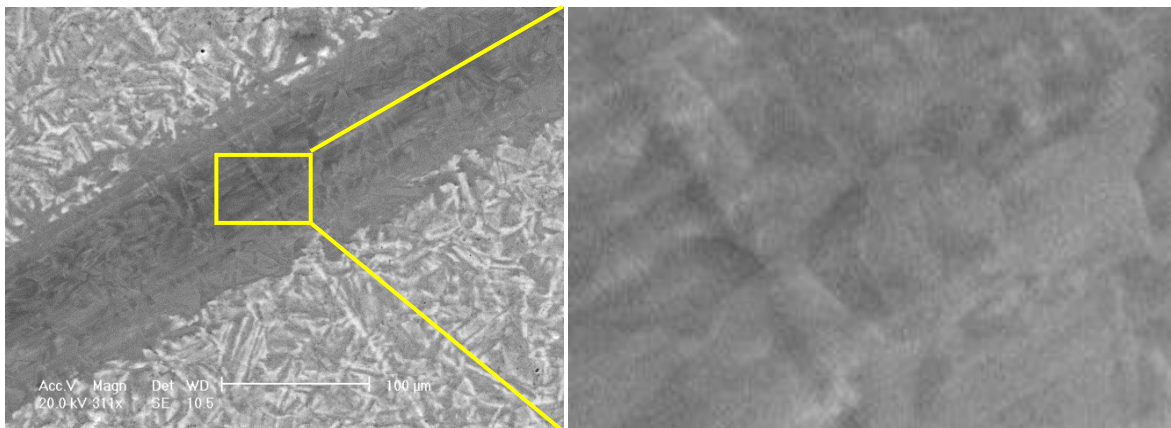


Figure 4.5-5 SEM microstructures of wear track on 4PC450 sample

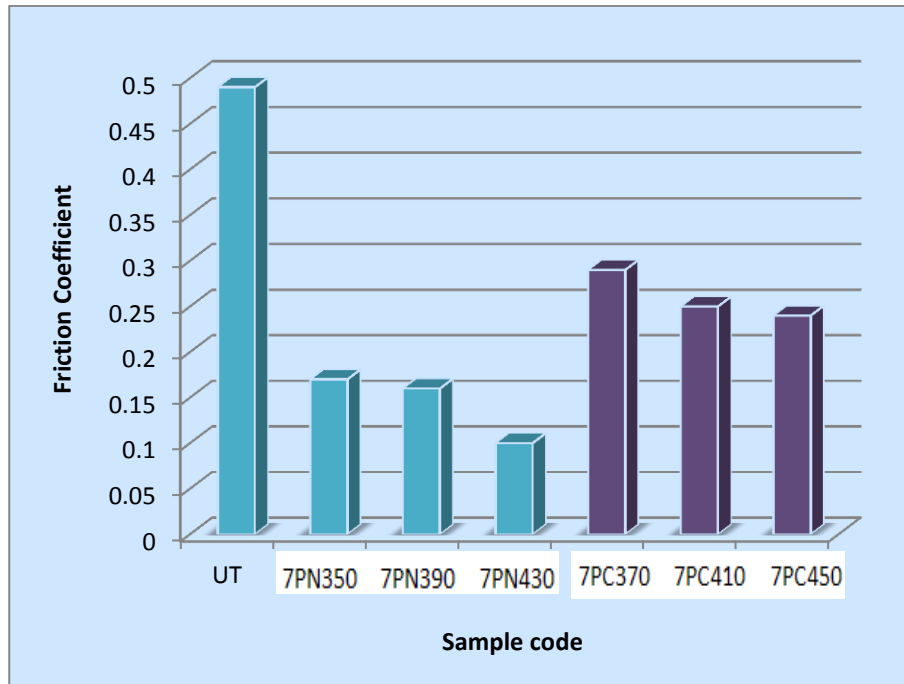


Figure 4.5-6 The friction coefficients of untreated (UT), plasma nitrided (PN) and carburised (PC) 17-7PH stainless steel samples.

As seen from Figure 4.5-7, in the case of 17-7PH stainless steel, the area loss due to wear on the untreated sample decreased from 4.08×10^3 to 2.6×10^3 , 1.16×10^3 and $6.06 \times 10^2 \mu\text{m}^2$ after plasma nitriding at 350°C , 390°C and 430°C , respectively. The trend is very clear: the higher the treatment temperature, the lower the wear loss.

Wear resistance of 17-7PH stainless steel can also be improved through active screen plasma carburising (Figure 4.5-7). Treating the 17-7PH stainless steel at 390°C (7PC390) decreased the wear loss from 4.08×10^3 to $2.6 \times 10^3 \mu\text{m}^2$. This figure is further reduced to $1.16 \times 10^3 \mu\text{m}^2$ when plasma carburised at 410°C (7PC410). This pattern is reversed when treated at 450°C (7PC450) as it

increased the wear loss to $1.00 \times 10^3 \mu\text{m}^2$, which however is smaller than that of untreated sample.

Severe delamination and abrasive wear and accumulated debris can be seen on the untreated samples (Fig. 4.5-8). The best performed 7PN430 and 7PC410 samples have similar wear loss measurements (Figure 4.5-7); SEM observation reviewed more debris cover of 7PC410 than 7PN430 sample (Figs 4.5-8b vs 8c).

EDX analysis on the surface cover layer of the wear tracks indicated high oxygen, tungsten and surface layer elements such as Fe, Cr, N, etc and an example of it is shown in Figure 4.5-9.

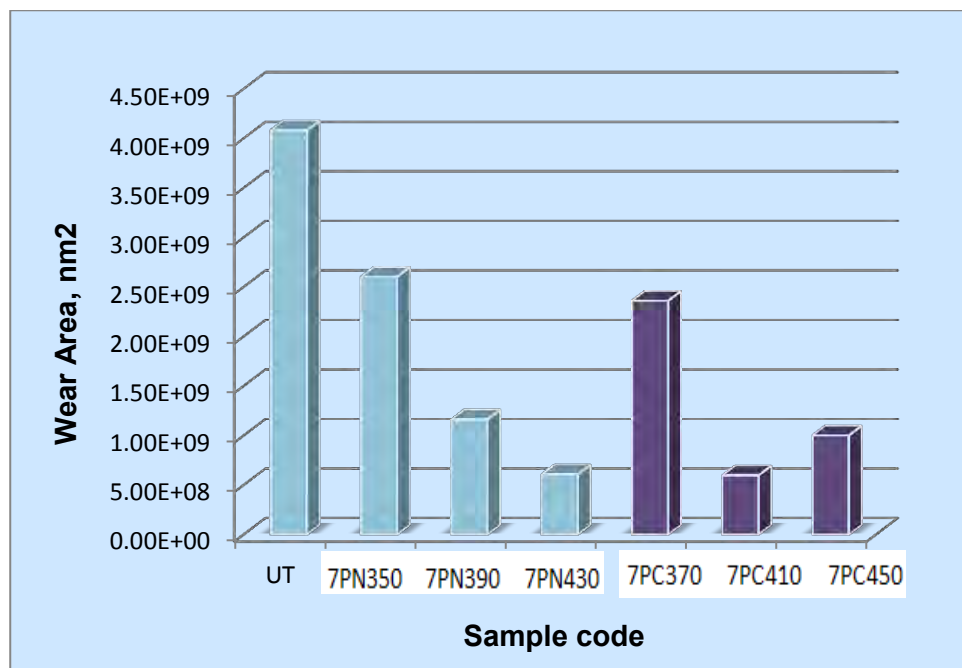


Figure 4.5-7 The wear loss of untreated (UT), plasma nitrided (PN) and carburised (PC) 17-7PH stainless steel samples.

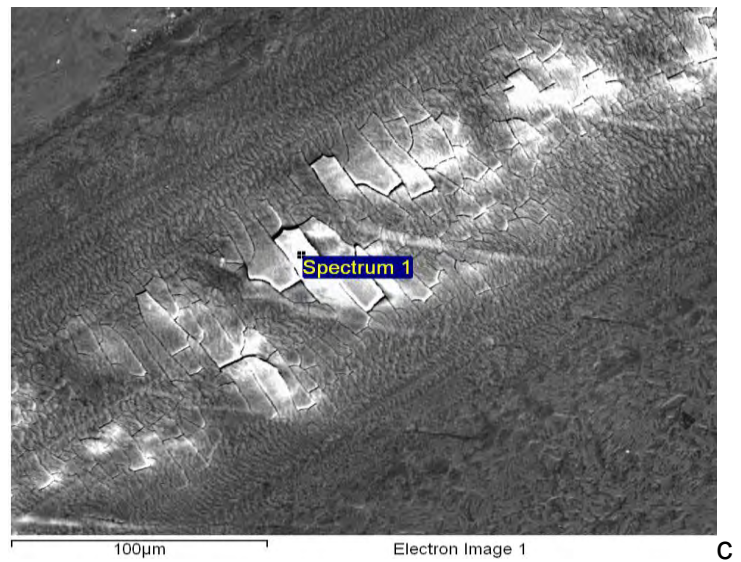
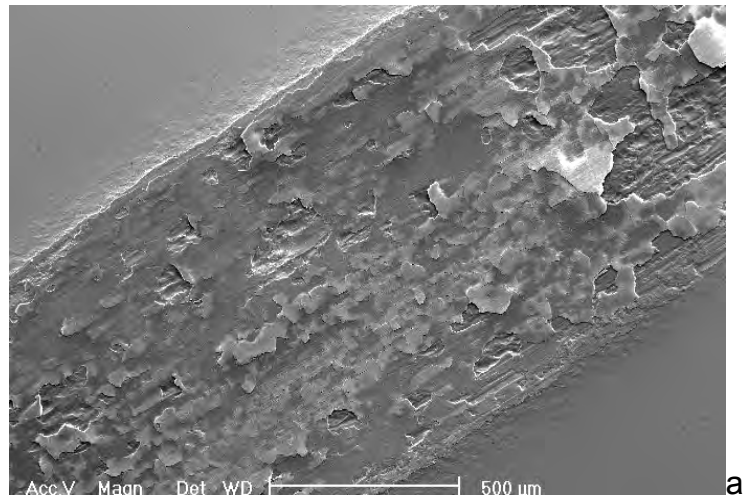
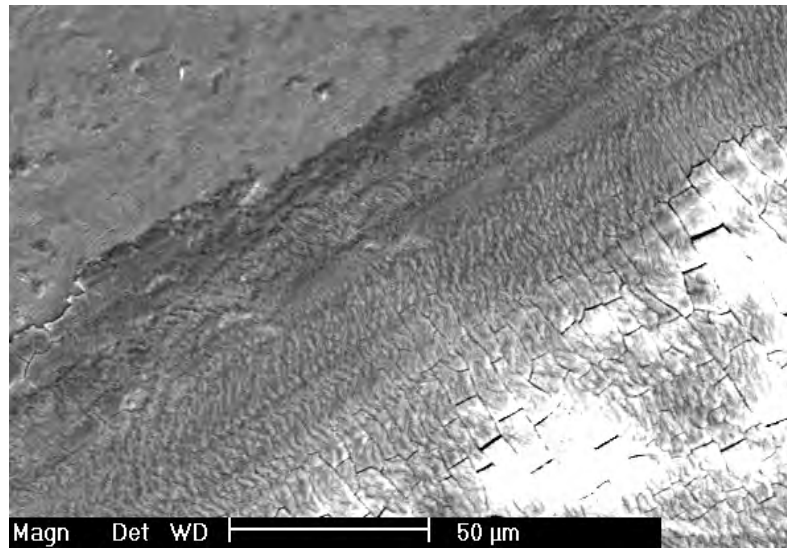
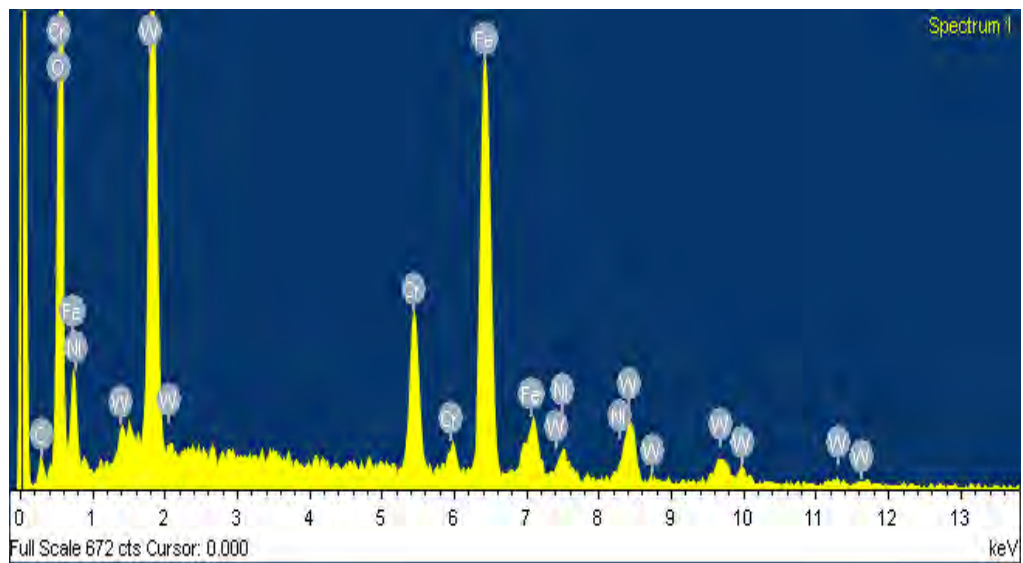


Figure 4.5-8 SEM micrographs of wear tracks on 17-7 PH samples: a) untreated; b) 7PN430 and c) 7PC410



a



b

4.5-9 a) SEM image of a wear track on 7PC410 sample and b) corresponding EDX analysis

4.6 Corrosion Resistance

4.6.1 Salt Spray

After the 100 h salt spray test, surface treated and untreated 17-4PH and 17-7PH stainless steel samples were photographed and weighed to determine the presence of rust and evaluate the weight change before and after corrosion testing.

4.6.1.1 17-4PH

Pictures of before and after salt spray tested 17-4PH samples are presented in Fig. 4.6-1. Compared to the untreated sample, the corrosion resistance of nitrided samples in salt medium was diminished depending on the treatment temperatures. The low-temperature treated 4PN350 showed very mild corrosion (Fig. 4.6-1a) but red rust and severe localized corrosion could be observed in medium- and high-temperature treated 4PN390 (Fig. 4.6-1c) and 4PN430 (Fig. 4.6-1d) samples. As evidenced in Figures 4.6-1 e to g, low-temperature (370°C) plasma carburised 4PC370 sample showed a certain degree of protection against the salt spray corrosion testing, worsening with increasing treatment temperature for 4PC410 and 4PC450 samples (Figs. 4.6-1 f to g).

The weight change of all tested samples during salt spray testing was recorded and the results are summarised in Fig 4.6.1-2. It can be seen that the weight change of low temperature treated samples of 4PC390, 4PC410, 4PN350 and 4PN390 was less than the untreated 17-4PH sample whilst the weight change of the high-temperature treated 4PC450 and 4PN430 was larger than that of the untreated material. The fact that the weight of 4PN430 sample was reduced rather than increased after salt spray test implies that spallation of the corrosion

products may have occurred to this sample. This also indicates that weight change alone is not a good indication of the extent of corrosion during salt spray testing especially when corrosion is severe and some of the corrosion products come off from the surface.

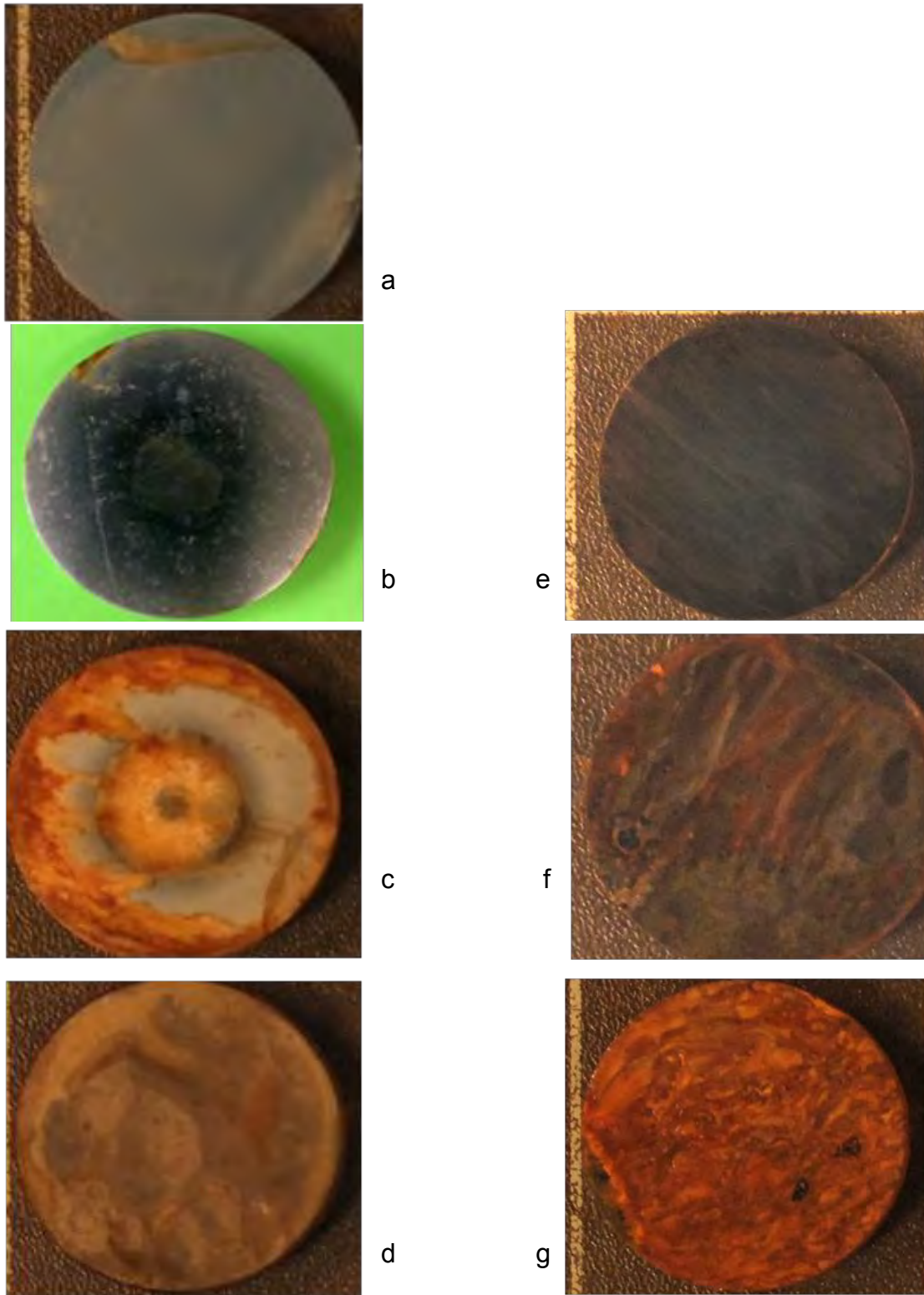


Figure 4.6-1 Photographs of salt spray tested 17-4PH samples: a) untreated (4UNT); plasma nitrided b) 4PN350, c) 4PN390 and d) 4PN430; and plasma carburised e) 4PC370, f) 4PC410 and g) 4PC450.

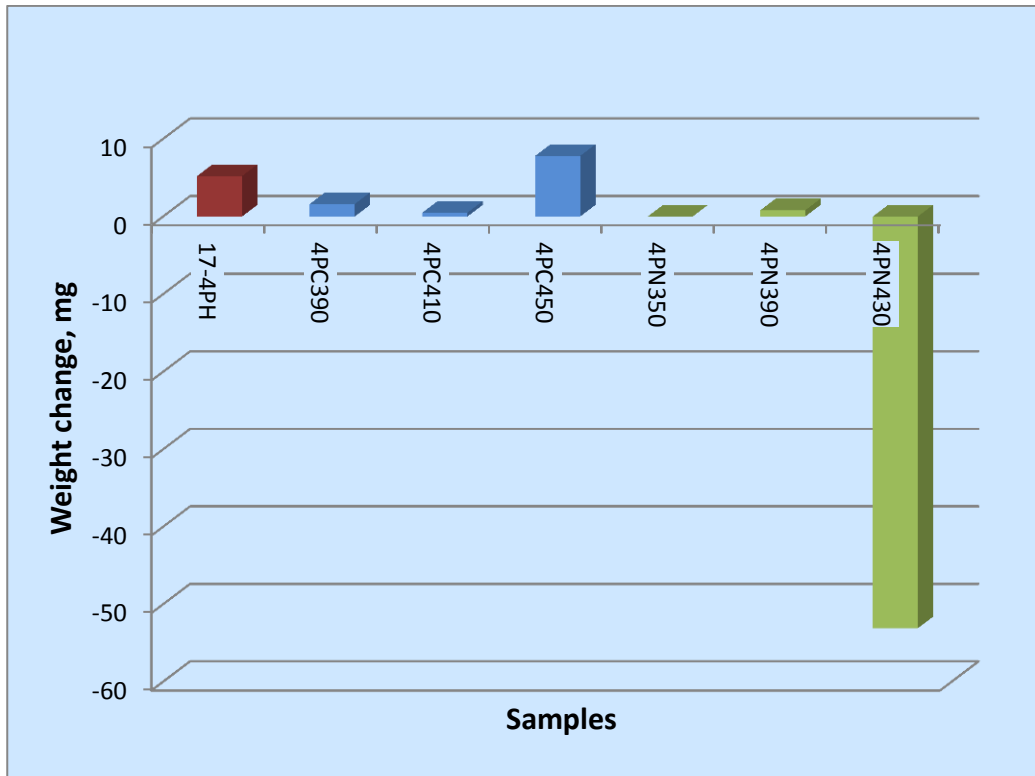


Figure 4.6-2 The weight change of 17-4PH stainless steel samples plasma nitrided (PN) and plasma carburised (PC) at various temperatures

4.6.1.2 17-7PH

In general, plasma nitrided 17-7PH stainless steel samples showed improved corrosion resistance to salt spray, as can be seen in Figure 4.6-3. 430°C plasma nitrided 7PN430 sample showed some colour change in the middle but no rust can be clearly seen (Fig. 4.6-3d).

The corrosion damage suffered by the untreated 17-7PH stainless steel does not appear to be improved through plasma carburising at any temperature. Indeed, the corrosion damage became significantly worse as the plasma carburising treatment temperature increased, as evidenced in Figure 4.6-3.

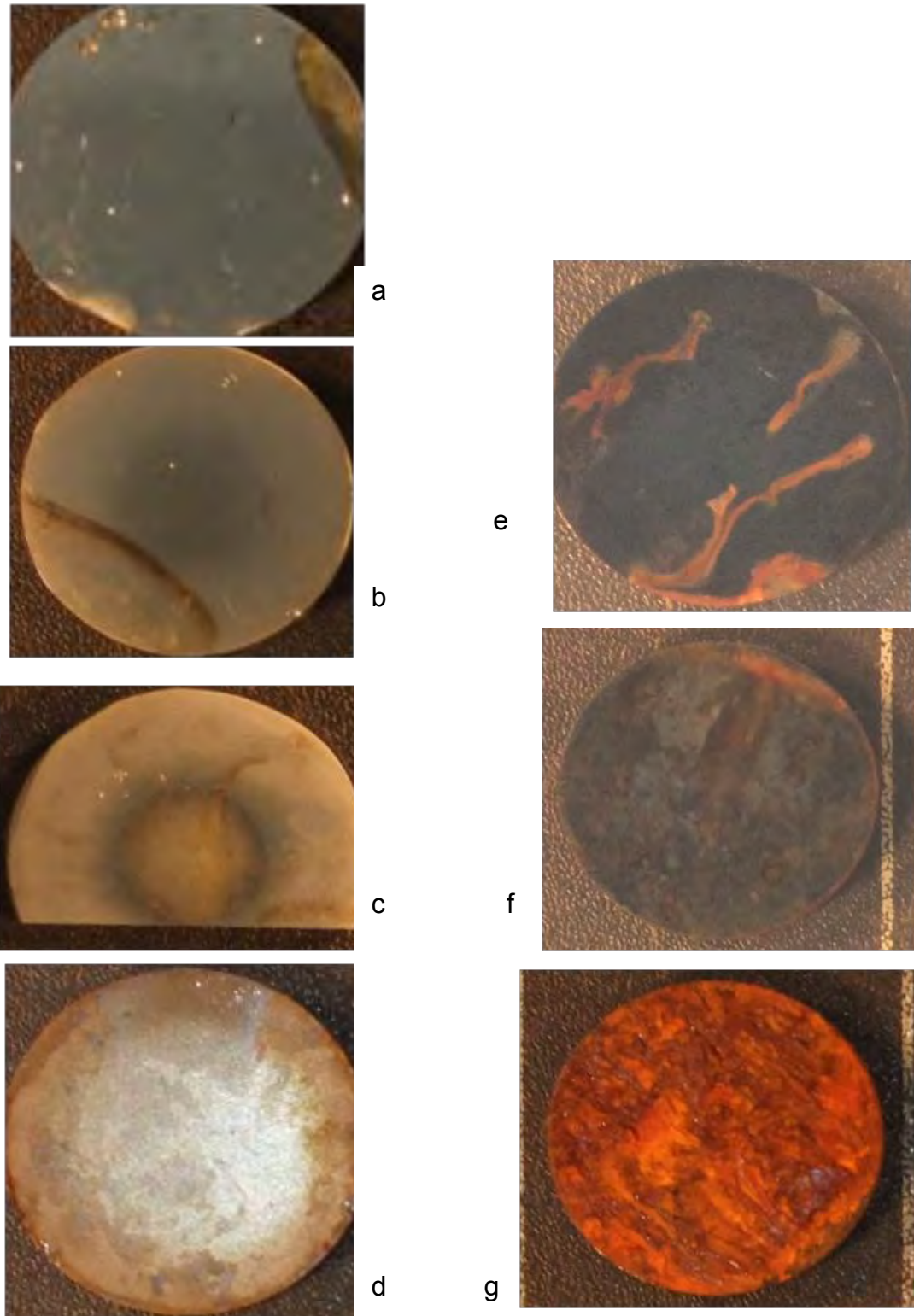


Figure 4.6.3 Photographs of salt sprayed 17-7 PH samples: a) untreated (UT); plasma nitrided b) 7PN350, c) 7PN390 and d) 7PN430; and plasma carburised e) 7PC370, f) 7PC410 and g) 7PC450

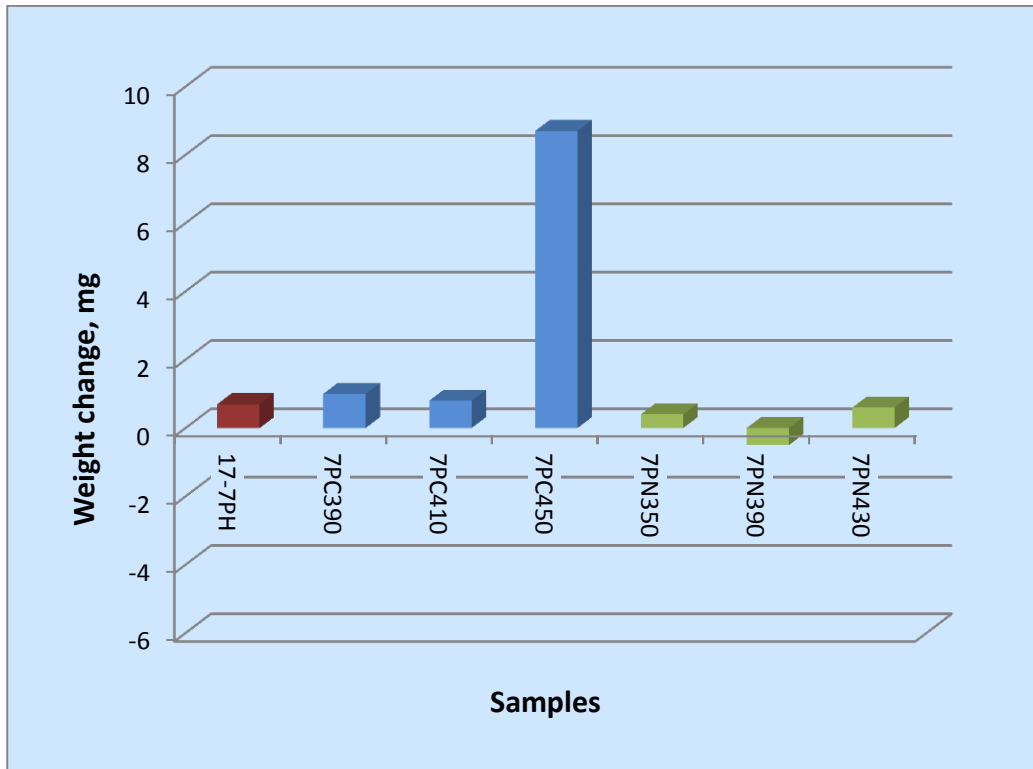


Figure 4.6-4 The weight changes of 17-7PH stainless steel samples plasma nitrided (PN) and plasma carburised (PC) at various temperatures.

The samples nitrided at low treatment temperatures of 350 (7PN350) and 390°C (7PN390) showed less weight change than the as received 17-7PH sample. This suggests that they have low quantity of corrosion products and therefore an improved corrosion resistance when compared to the untreated sample. As shown in Figure 4.6-4, the largest weight change was shown in the 17-7PH stainless steel sample plasma carburised at 450°C (7PC450). This suggests that it has the highest quantity of corrosion products and therefore the poorest corrosion resistance. This is in good agreement with the severe corrosion shown in Figure 4.6-3g.

4.6.2 Electrochemical corrosion

4.6.2.1 17-4PH

Plasma nitriding and carburising 17-4PH stainless steel at various temperatures resulted in changes in electrochemical corrosion resistance compared with untreated sample as can be seen from Figure 4.6-5 and Figure 4.6-6. It can be seen that untreated sample started corrosion at potential -0.12V/SCE ; it had very limited passivation as evidenced by the markedly increased current when potential increased from -0.12 to 0.20 V/SCE . This is an indication of rapid pitting, which is supported by large corrosion pits in the area size of $0.5\mu\text{m}^2$ observed from the corroded surface under SEM (Figure 4.6-7a).

Low temperature plasma nitrided 4PN350 (Fig. 4.6-5) and plasma carburised 4PC370 (Fig. 4.6-6) samples outperformed the untreated material (4UNT) in terms of increased pitting potential and corrosion potential. SEM observation on corrosion tested areas of these two samples revealed very small corrosion pits (Figure 4.6-6b and Figure 4.6-7a). The surface layers wear passivated during the tests and even at the maximum test potential of 1V/SCE the pitting still did not break through.

For samples of 4PN430 (Fig. 4.6-5) and 4PC410(Fig.4.6-6), although their corrosion potentials were lower than untreated sample their pitting potentials were much higher than untreated sample. Some small isolated pits (Fig.4.6-7d) and some connected pits (Fig. 4.6-8b) were found on the corroded surfaces. The high-temperature plasma carburised 4PC450 sample possessed the worst corrosion resistance as indicated by significantly reduced corrosion potential and pitting

potential (Fig. 4.6-6). The tested areas revealed severe pitting and the surface layer was broken through (Fig. 4.6-8c). The corrosion potential and pitting potential of untreated, plasma nitrided and plasma carburised 17-4PH samples are compared in Table 4-1.

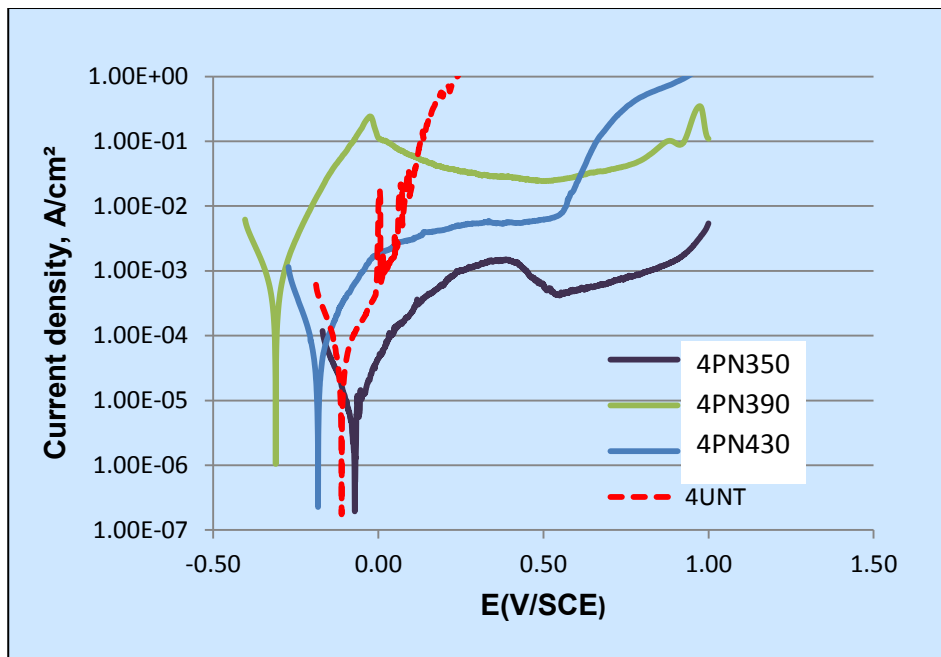


Figure 4.6 -5 The potentiodynamic curves of 17-4PH stainless steel samples, plasma nitrided at various treatment temperatures.

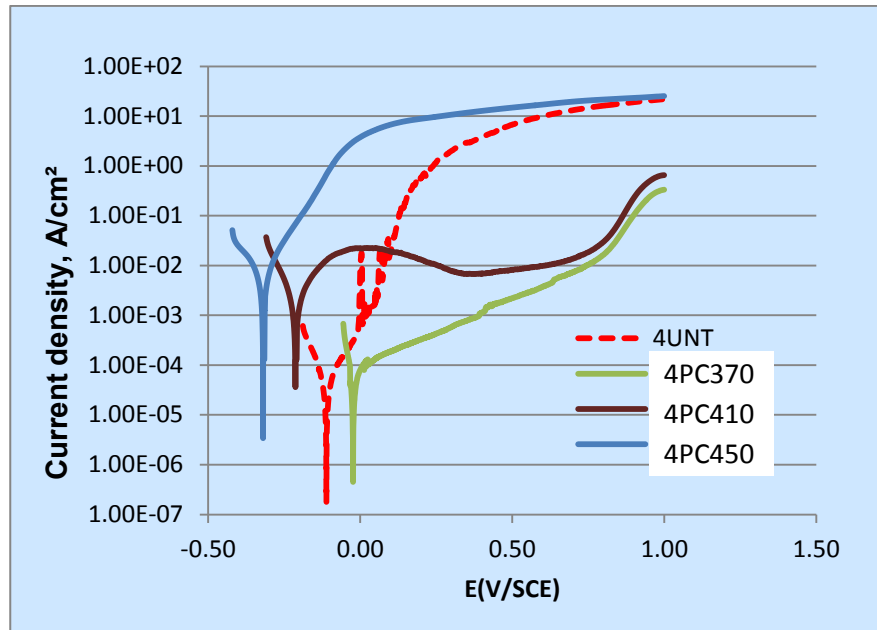
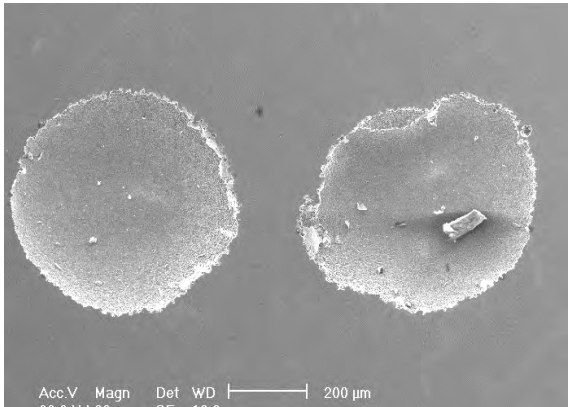


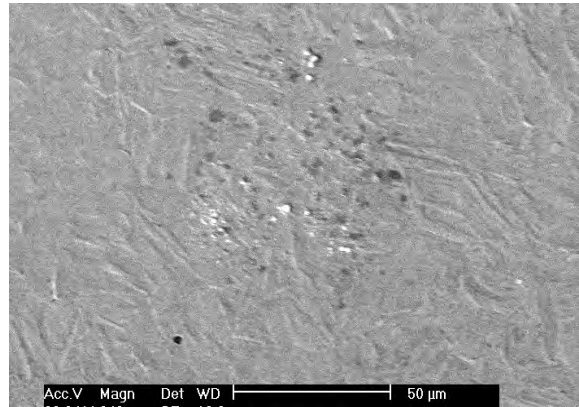
Figure 4.6-6 The potentiodynamic curves of 17-4PH stainless steel samples, plasma carburised using various treatment temperatures.

Table 4-1 The corrosion potential and pitting potential of untreated, plasma nitrided and plasma carburised 17-4PH samples

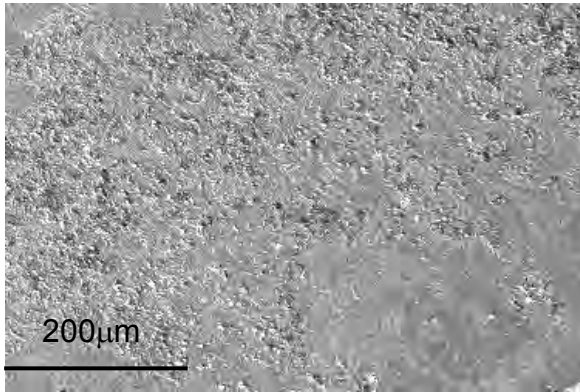
Sample	Corrosion Potential (V/SCE)	Pitting Potential (V/SCE)
UNT	-0.12	-
4PN350	0.08	0.94
4PN390	-0.31	0.92
4PN430	-0.18	0.56
4PC370	-0.02	0.76
4PC410	-0.21	0.77
4PC450	-0.32	-



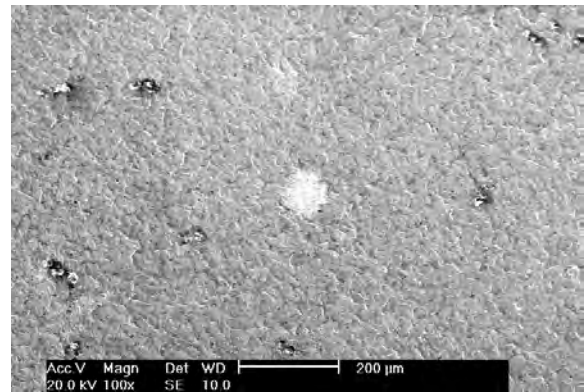
a) Untreated



b) 4PN350

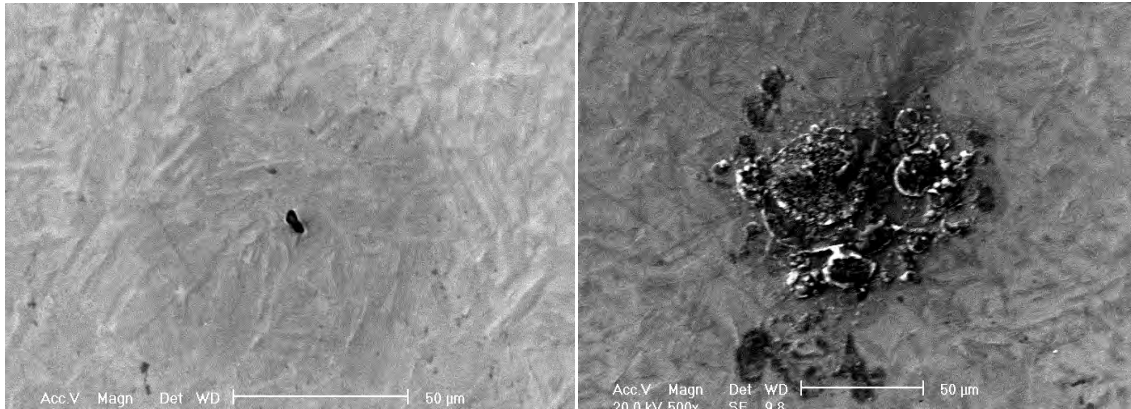


c) 3PN390



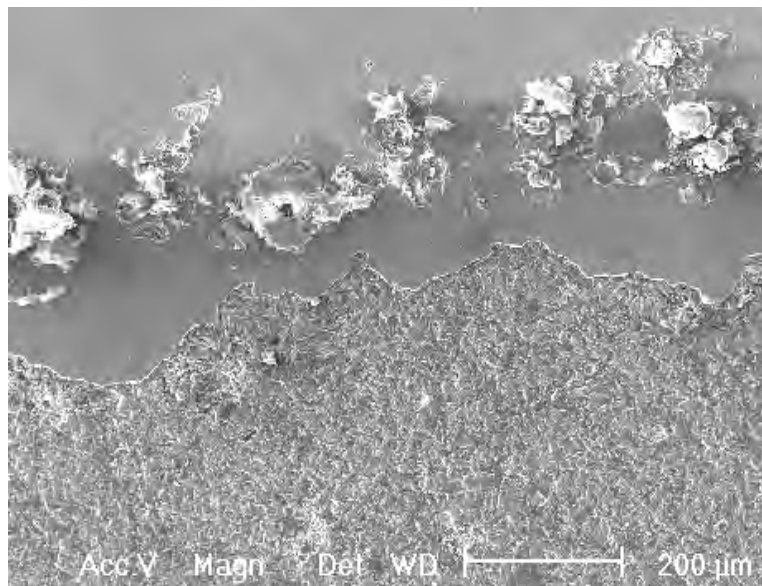
d) 4PN450

Figure 4.6-7 SEM micrographs of corroded areas on untreated: a) UNT and plasma nitrided: b) 4PN350, c) 4PN390 and d) 4PN450.



a) 4PC370

b) 4PC410



c) 4PC450

Figure 4.6-8 SEM micrographs of corroded areas on plasma carburised a) 4PC370, b) 4PC410 and c) 4PC450.

4.6.2.2 17-7PH

The electrochemical corrosion resistance of plasma surface alloyed 17-7PH stainless steel samples was compared with the untreated 17-7PH material. As

shown in Figure 4.6-9, metastable pitting occurred before severe pitting at 0.06V/SCE for the untreated sample. In contrast, although the corrosion potential of all three plasma nitrided samples is the same as that for the untreated material, no pitting was occurred up to the maximum test potential of 1V/SCE. This is supported by the post-tests SEM examination of the corroded surfaces: many large pitting were observed in tested untreated material surface but all the tested plasma nitrided surfaces exhibited features of general rather than localised corrosion (Fig. 4.6-11b).

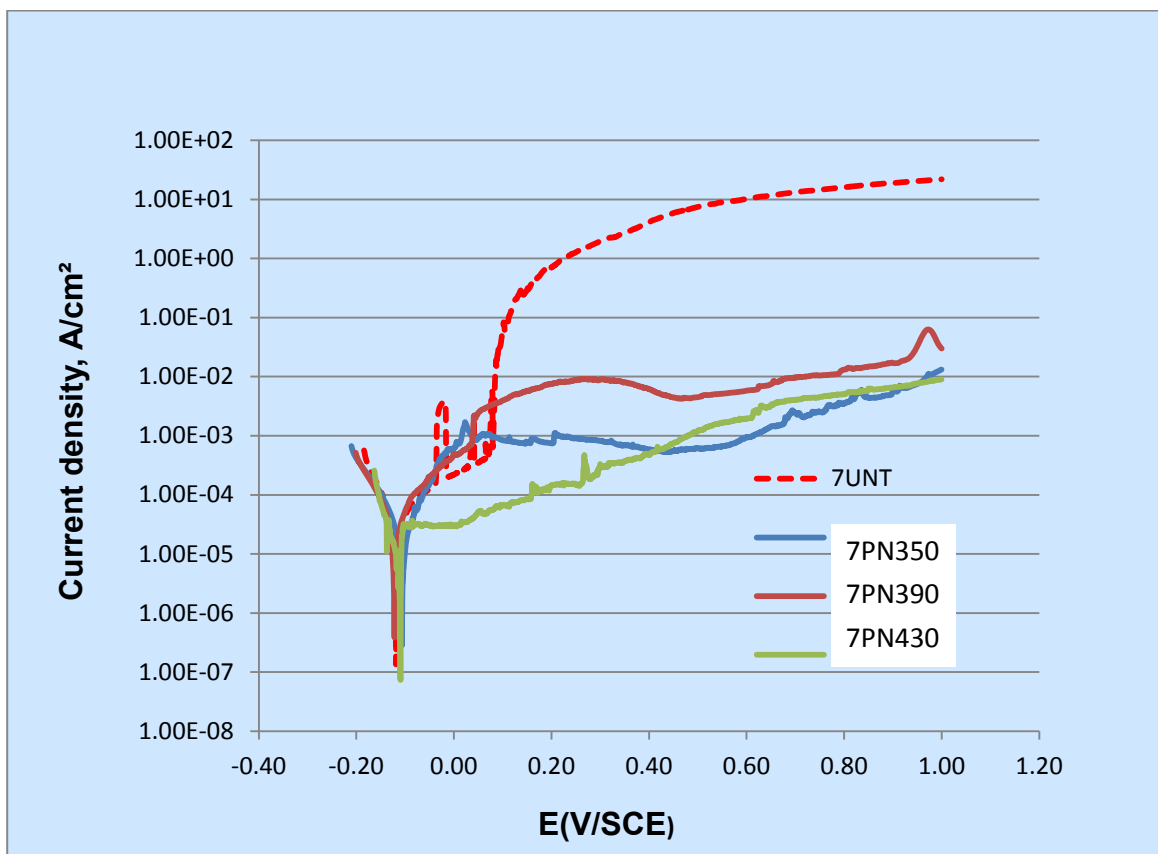
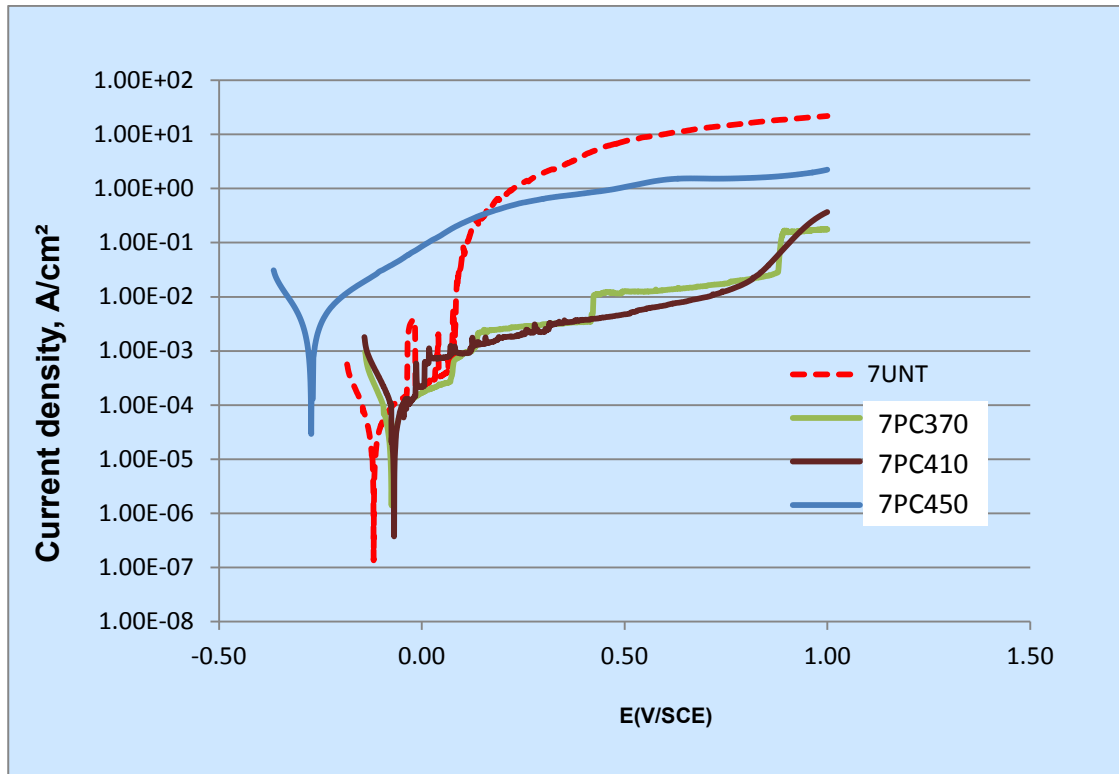


Figure 4.6-9 The potentiodynamic curves of 17-7PH stainless steel samples, plasma nitrided at various treatment temperatures.

As shown in Figure 4.6-10, the corrosion potential of low- and medium-temperature carburised samples 7P370 and 7P410 is marginally higher than that for the untreated material. Metastable pitting was observed but the pitting potential of 7P370 (0.85V/SCE) and 7P410 (0.78V/SCE) is much higher than that (0.06V/SCE) of the untreated material (Table 4.6-2). However, the corrosion performance of the high-temperature (450°C) treated 7PC450 is inferior to the untreated material at potential below about 0.1V/SCE; however, the corrosion current density of 7PC450 is lower than that of untreated materials once the applied potential was above about 0.1V/SCE (Fig. 4.6-10).

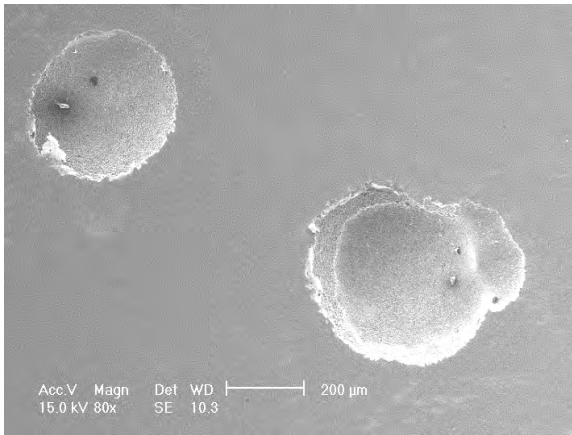
Figure 4.6-12 shows SEM images of the typical corrosion morphologies of plasma carburised 17-7PH stainless steel samples. Few relatively small pits were observed from the corroded 7PC370 and 7PC410 sample surfaces (Figs. 4.6-12 a & b) and 7PC450 showed many larger corroded areas (Fig. 4.6-12c). This fully supports the electrochemical corrosion test results shown in Figure 4.6-10.



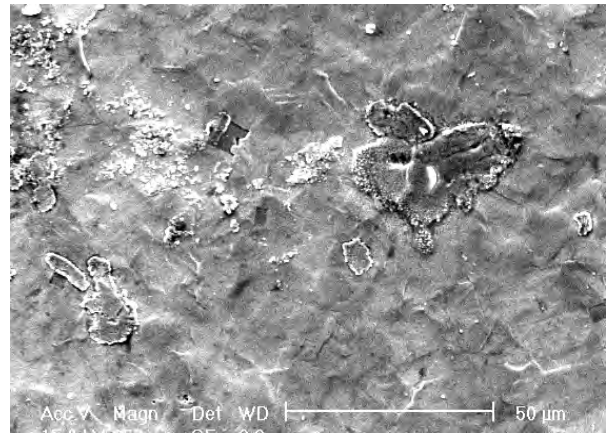
4.6-10 The potentiodynamic curves of 17-7PH stainless steel samples, plasma carburised at various treatment temperatures.

Table 4.6-2 The corrosion potential and pitting potential of untreated, plasma nitrided and plasma carburised 17-7PH samples

Sample	Corrosion Potential (V)	Pitting Potential (V)
UNT	-0.13	-0.06
7PN350	-0.13	-
7PN390	-0.13	-
7PN430	-0.11	-
7PC370	-0.07	0.85
7PC410	-0.07	0.78
7PC450	-0.28	-

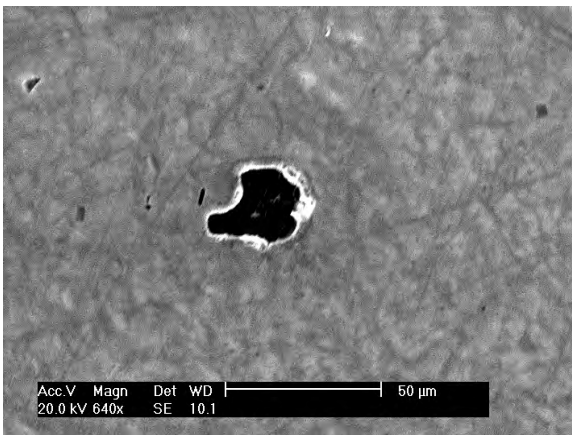


a Untreated

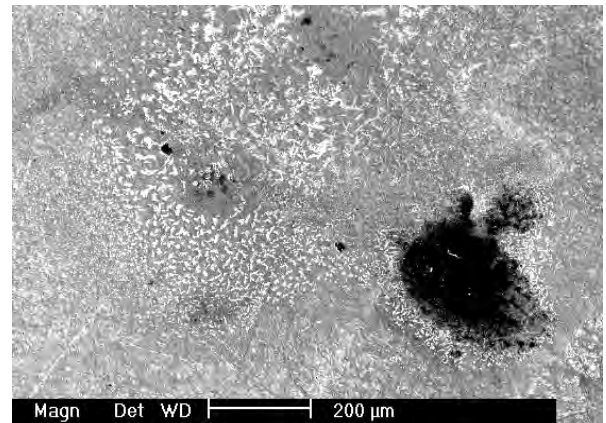


b 7PN350

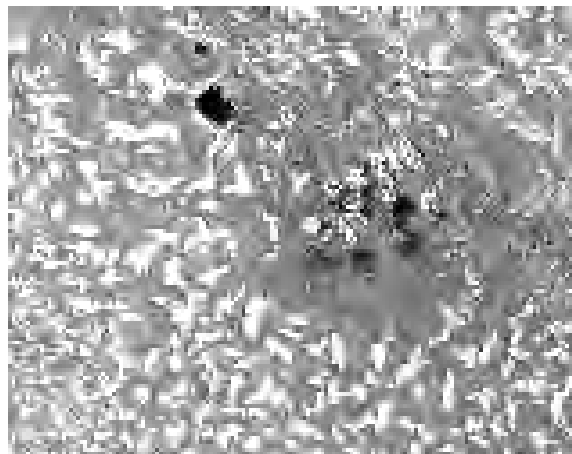
Figure 4.6-11 SEM micrographs of corroded areas on a) untreated and b) plasma nitrided 17-7PH samples



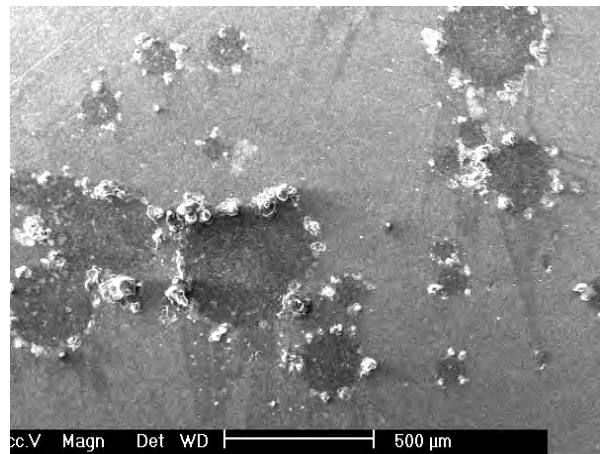
a 7PC370



b 7PC410



(2) c 7PC410



d 7PC450

Figure 4.6-12 SEM observations of corrosion tested areas on a) 7PC370 b) 7PC410 c) 7PC410 d) 7PC450.

Chapter 5 – Interpretation and Discussion

5.1. Response of 17-4PH and 17-7PH to ASP Alloying

Both 17-4 and 17-7 PH steels were active screen plasma (ASP) alloyed with nitrogen and carbon under same conditions. Although both are precipitation hardening steels, they are different in chemical composition and microstructure (see Sections 3.1 and 4.1), thus leading to different responses to active screen plasma alloying treatments.

5.1-1 Hardened layer thickness

Figure 5.1-1 compares the surface layer thickness of 17-4 and 17-7 PH samples after plasma nitriding and carburising treatments. It can be seen that for both steels the thickness of the surface alloyed layer increased with the treatment temperature, in line with Fick's diffusion law.

However, it was observed that a thicker nitrided surface layer was produced in the 17-4PH samples than in the 17-7PH samples after treated at 390 and 450 °C (Fig.5.1-1). This difference could be attributed to the difference in the initial microstructure. As shown in Figure 4.1-1, 17-4PH is of a martensitic structure whilst 7-7PH stainless steel is of a duplex austenitic/martensitic structure. Previous researchers (Bielawski & Baranowska, 2010) have found that the nitride layer is thicker when formed in ferrite than in austenite. This is because the diffusion coefficient of nitrogen is larger in ferrite than in austenite due to the difference in lattice structure and hence the size of interstices for BCC ferrite and FCC austenite. In addition, 17-4PH steel has a martensitic structure and the defects and inter-martensite plates/lathes in the martensitic structure of the 17-

4PH steel can further enhance the diffusion of nitrogen during plasma nitriding. Therefore, a thicker diffusion case was formed in martensitic 17-4PH steel than in duplex (martensite/austenite) 17-7PH steel.

It is of interest or even surprised to note in Figure 5.1-1 that unlike in plasma nitriding, the hardened case created by plasma carburising is thicker in 17-7 PH than in 17-4PH steel. It seems that the above explanation based on the difference in the original microstructures alone would not be applicable for plasma carburising.

The research conducted by Lewis et al, 1993, demonstrated that the maximum solubility of carbon is at least two orders of magnitude higher in austenite than in ferrite at the same temperature. This suggests that during plasma carburising at the same temperature a higher surface carbon concentration would be built up in duplex (martensite/austenite) 17-7PH steel than in martensitic 17-4PH steel. This is mainly because according to Fick's first diffusion law, the carbon diffusion flux J_c depends on the product of carbon diffusion coefficient D_c by the carbon gradient dC/dx (x is the distance from the surface) i.e. $J_c = -D_c \times dC/dx$. Therefore, the high solid solubility of carbon in austenite could effectively increase the carbon gradient and hence the carbon diffusion flux. Consequently, a thick diffusion case could be expected to form in duplex (martensite/austenite) 17-7PH steel than in martensitic 17-4PH steel.

Furthermore, as reported in Section 4.3, carbides formed during plasma carburising of 17-4 PH and 17-7 PH steels. This demonstrates that plasma carburising of 17-4 PH and 17-7 PH steels is not a pure diffusion but a reaction diffusion process. During the plasma carburising, Hägg- Fe_5C_2 (χ) carbide was

formed in both the steels; however, $Cr_{23}C_6$ was also identified from the plasma carburised 17-4 PH steels. This is also reflected by the relatively poor corrosion resistance of carburised 17-4 PH relative to 17-7 PH steel (Section 4.6). Therefore, the relatively shallow diffusion case formed in 17-4 PH than in 17-7 PH steel could be explained by the formation of $Cr_{23}C_6$. This is because the inward diffusion of some carbon atoms could be trapped by Cr atoms, thus stopping or slowing down the further inward diffusion of carbon atoms.

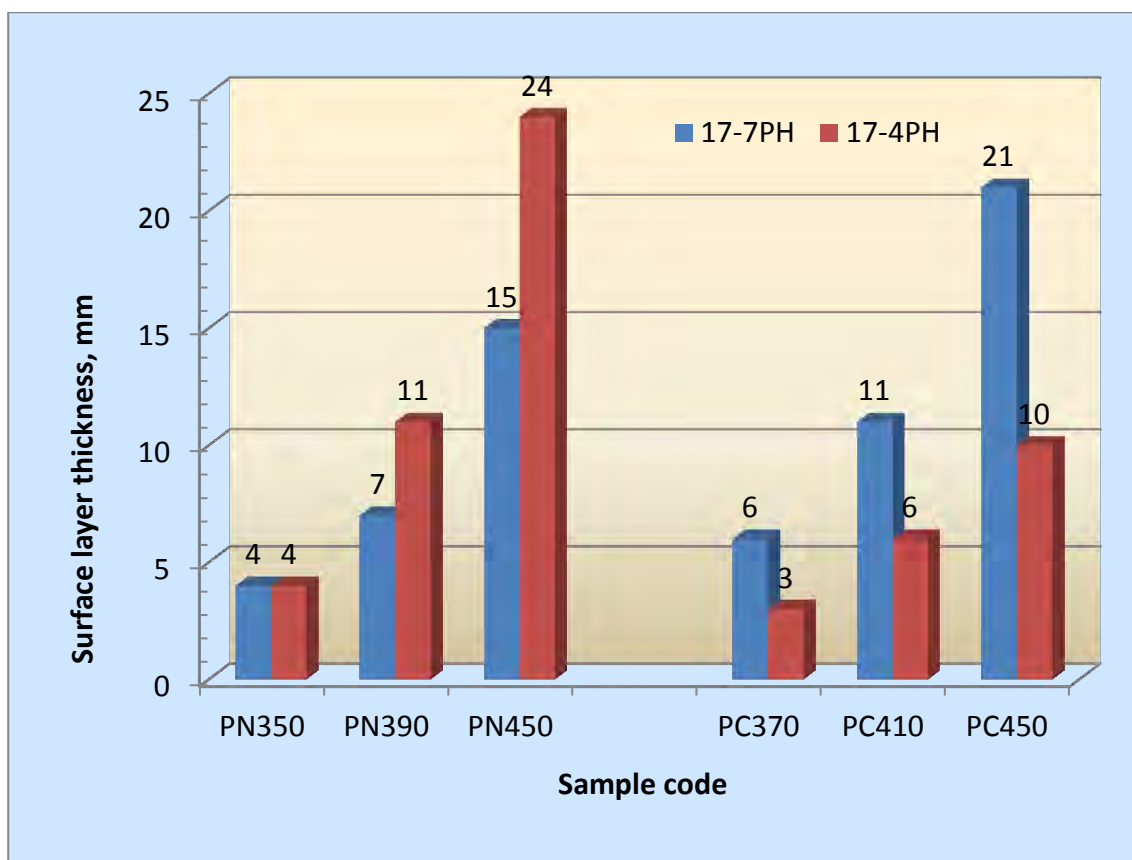


Figure 5.1-1 The thickness of the treated layer on 17-4PH and 17-7PH stainless steel during plasma nitriding and carburising at different temperatures.

5.2 The Nitriding Effect

5.2.1 Effect on wear

As has been shown in Figures 4.5-2 and 4.5-7, plasma nitriding can effectively reduce the wear of both 17-4 PH and 17-7 PH steels. When treated at a very low temperature of 350°C, the improvement is limited for both 17-7 PH (7PN350) and 17-4 PH (7PN350) steels; however, when plasma treated at 390 and 430°C, significant improvement in wear resistance was observed for both steels. In addition, it is also noted that plasma nitriding is more effective in reducing wear when applied to 17-4 PH than to 17-7 PH steel (Figs. 4.5-2 vs 4.5-7) when treated at 390 and 430°C.

Clearly, the wear resistance varies between the two materials and between treatment temperatures because this property is affected by factors such as the surface layer thickness and surface hardness (Esfandiari & Dong 2007). In general, the thickness and the hardness of the plasma nitrided cases increased with increasing plasma nitriding temperature, as did the wear resistance of both stainless steels.

A hard and strong surface layer can provide an increased ability to resist plastic deformation and abrasion, therefore improving the surface damage resistance. It is known that oxide films will form during dry sliding wear due to the friction-induced high flash temperature. A hard and strong surface layer can help the oxide films to retain on the surface of the material (Corengia et al, 2006), thus changing the wear mechanism involved.

This is supported by the experimental observation that the untreated samples were severely worn by delamination and abrasion (Figs. 4.5-3 and 4.5-8a) because of their low hardness (Figs. 4.4-1 and 3). In contrast, mild oxidation wear occurred to plasma nitrided stainless steel steels when treated at 390 and 430°C as exemplified by 4PN390 (Fig. 4.5-4) and 7PN430 (Fig. 4.5-8b) as evidenced by the darkened areas in the wear tracks and the EDX analysis results. The change to oxidation wear mechanism of stainless steel after active-screen plasma nitriding has also been reported by Corengia et al (2006).

The formation of the surface oxide films due to frictional heating can significantly reduce friction (Figs. 4.5-1 & 6). This could effectively reduce the shear stress at the rubbing surfaces and the stress transmitted to the subsurfaces, thus reducing or eliminating delamination wear. In addition, the alloying of nitrogen can cause lattice expansion and introduce extremely high compressive residual stresses (Dong, 2010). These compressive stresses would partially cancel the tensile stresses produced by friction during sliding (Onate, 1990).

Seemingly contradicting wear results was observed for the 350°C plasma nitrided steels. It can be seen from Figures 4.5-2 and 4.5-7 that a slightly lower wear area was observed from the 350°C plasma nitrided 17-7 PH steel (7PN350, Fig. 4.5-7) than from 17-4 PH steel (4PN350, Fig. 4.5-2); however, the surface hardness of the former (~400HV0.05, Fig. 4.4-3) is much lower than that (~1200HV0.05, Fig. 4.4-1) of the latter although the layer thickness is the same for both, ~4 μm. Detailed post-test SEM observations revealed that the wear tracks formed in these two samples were severely damaged showing similar wear morphologies to those of untreated materials (Fig. 4.5-3). Therefore, such seemingly contradicting wear

results could be explained as follows: (1) when loaded under a concentrated load, the nitriding hardened surface layer collapsed because of the very thin hardened case and soft and weak subsurface – ‘thin ice effect’; (2) once broken into fragments, such relatively hard debris became abrasives; and (3) the abrasive wear caused is directly related to the hardness of the abrasives – the harder the abrasives, the severer the abrasive wear. Accordingly, the hard fragments or abrasives formed from 350°C plasma nitrided 17-4 PH steel caused more wear than 17-7 PH steel.

5.2.2 Effect on corrosion

In general, the plasma nitrided 17-7PH stainless steel demonstrated improved corrosion resistance. As evidenced in Figure 4.6-9, plasma nitriding in the temperature range from 350 to 430°C can significantly improve the pitting corrosion resistance of 17-7PH stainless steel. Similar, the plasma nitrided 17-7PH stainless steel showed marginally improved or maintained resistance to salt spray with no or limited rust observed from the tested surfaces (Figs.4.6-3 b, c & d).

This could be attributed to the S-phase formed on the 17-7PH stainless steel (Figs. 4.1-4 and 4.3-3), which provides both improved mechanical properties whilst maintaining and in some cases improving the corrosion resistance of the material. This is because the S-phase formed during plasma nitriding of 17-7PH stainless steel is a nitrogen supersaturated austenite without precipitation of chromium nitrides (Section 2.3.3).

However, as reported in Section 4.6, the effect of plasma nitriding on salt spray and electrochemical corrosion is highly material dependent. Indeed, plasma nitriding had a detrimental effect on the resistance of 17-4PH to salt-spray especially for the 390 and 430°C treated samples. Similarly, these two samples also showed reduced corrosion potentials during electrochemical corrosion tests (Fig. 4.6-5). These results support the work of Bruhl, 2010 who demonstrated that the corrosion resistance of martensitic stainless steel decreased after plasma nitriding, even at a low temperature such as 360°C.

As discussed in Section 2.1, chromium is essential for providing the 'stainlessness' of stainless steels mainly due to the formation of a protective chromium oxide film. The corrosion resistance reduction in the martensitic steel could be related to the chromium depletion that occurs as a result of the formation of Cr₂N (Fig. 4.3-1). This is also supported by the fact that the 350°C plasma nitrided 17-4 PH steel showed only marginally deteriorated resistance to salt spray and even improved electrochemical corrosion behaviour (Fig. 4.6-5). This is probably because precipitation of chromium nitrides at low temperature is very limited due to the low diffusivity of chromium at low temperature.

5.2.3 Combined improvement in wear and corrosion properties

Plasma nitriding 17-4PH stainless steel at 350°C (4PN350) greatly improves the resistance of the sample to localised pitting corrosion, however only slightly increases the wear resistance when compared to the untreated sample. Although the sample treated at 390°C (4PN390) demonstrates the best wear resistance it also demonstrates very poor corrosion resistance. The 17-4PH sample treated at

430°C (4PN430) demonstrates the best combined improvement in both corrosion and wear resistance when compared to the untreated sample.

As shown in Figure 4.6-9, all the plasma nitriding treatments caused a significant improvement to the pitting resistance of 17-7PH stainless steel sample mainly due to the formation of S-phase layer. The plasma nitrided 17-7PH stainless steel sample (in particular 7PN350 and 7PN390) showed improved resistance to salt spray (Fig. 4.6-3). In addition, all the plasma nitriding treatments improved the wear resistance of 17-7PH stainless steel and the improvement becomes greater with increasing temperature (Fig. 4.5-7).

All these plasma nitriding treatments are adequate in producing improvement in both corrosion resistance and wear resistance. Plasma nitriding at 430°C (7PN430) however produced the greatest improvement in wear resistance and therefore would be the optimum treatment to provide a combined improvement in both wear and corrosion resistance of 17-7PH stainless steel.

Although the optimum treatment for 17-4PH stainless steel produces a lower wear loss than that for 17-7PH stainless steel, it is not significantly lower and the excellent corrosion resistance of 17-7PH outweighs this. Therefore in conclusion, the optimum material for a combined requirement of both corrosion resistance and wear resistance would be 17-7PH stainless steel, treated at 430°C (7PN430)

5.3 The Carburising Effect

5.3.1 Effect on wear

In general, plasma carburising produced very similar effect on the tribological properties of both steels in terms of significantly improved wear resistance and effectively reduced friction. As discussed in Section 5.2.1, such improvements could be explained by increased surface hardness, enhanced surface damage resistance and change of wear mechanism from severe adhesive wear to a mild abrasive-oxidative mechanism.

However, some differences in wear resistance were also observed for plasma nitrided and carburised 17-4PH stainless steel. For example, the wear resistance of 17-4PH stainless steel can be improved by plasma carburising but not to the same extent as plasma nitriding. The greatest improvement to the wear resistance of 17-4PH stainless steel during plasma nitriding occurred at a treatment temperature of 390°C which produced a wear area loss of 76.7 μm^2 . The greatest improvement in wear resistance was that of the 450°C treatment that produced a wear area loss of 1.18 x 10² μm^2 . Comparing these results demonstrates that plasma nitriding has a more beneficial effect on the wear resistance of 17-4PH than plasma carburising stainless steel which has a martensitic structure. These results support those found by Li & Bell, 2007, who discovered that plasma nitriding significantly improved the wear resistance whereas plasma carburised only resulted in a small improvement in wear resistance in martensitic stainless steel. For 17-7 PH steel, plasma carburising and nitriding produced similar level of improvement in wear resistance (Fig. 4.5-7).

5.3.2 Effect on corrosion

It can be seen by comparing Figure 4.6-6 with Figure 4.6-5 that plasma carburising and plasma nitriding have similar effect on the electrochemical corrosion of 17-4PH stainless steel. The low-temperature (370°C) treated sample showed improved electrochemical corrosion resistance; however, it became significantly worse when increasing the treatment temperature. Similar trend was observed for the effect of plasma carburising on the salt spray resistance of 17-4PH stainless steel as demonstrated by the relatively good salt spray resistance of low-temperature (370°C) treated sample. Therefore, similar discussion given in Section 5.2.2 is applicable here for plasma carburised 17-4PH stainless steel. The reduced corrosion resistance of 410 and 450°C treated samples could be attributed to the formation of chromium carbides (Fig. 4.3-9), which led to depletion of chromium. However, such precipitation process becomes difficult at such a low-temperature of 370°C.

For 17-7PH stainless steel, plasma carburised at 450°C reduced corrosion resistance when compared to the untreated samples in both the salt-spray testing (Fig. 4.6-3) and electrochemical testing (Fig. 4.6-10). Despite carbon S-phase being formed through treating at 410°C and 450°C, the corrosion resistance has neither been maintained nor improved. This could be attributed to the passive film being more strongly supported on the nitrogen S-phase layer compared to a carbon S-phase layer (Thaiwatthana, 2003). In addition, it is well-known that nitrogen can effectively improve the corrosion resistance of austenitic stainless steel. Hence, it is reasonable to expect that the nitrogen S-phase layer formed

during plasma nitriding should have better corrosion resistance of the carbon S-phase formed during the plasma carburising.

5.3.3 Combined improvement in wear and corrosion properties

The best improvement to wear resistance is shown by the 17-4PH sample treated at 450° but this sample shows very poor corrosion resistance, which despite its superiority in wear resistance means it must be ruled out as an optimum choice of treatment for 17-4PH steel for combined improvement in wear and corrosion.

On the other hand, 370°C carburising confers the greatest resistance to pitting corrosion and salt spray; however, its wear resistance is not so good as 410°C treated samples. Therefore, 410°C could be an optimal treatment temperature for plasma carburising 17-4PH stainless steel to achieve combined enhancement in corrosion and wear resistance. Very similar trade-off was observed for plasma carburising of 17-7PH steel: 370°C carburised samples possess the best corrosion resistance but worst wear resistance; 450°C carburised samples show the best wear resistance but worst corrosion resistance. As a result, the optimum plasma carburising treatment for improving wear resistance and corrosion resistance of 17-7PH steel is that carried out at 410°C.

Chapter 6 – Conclusions

Active –screen plasma surface alloying of 17-7 PH steel

- (1) The present work has shown for the first time that S-phase can be produced in the surface of 17-7PH stainless steel by active screen plasma nitriding at 350, 390 and 430°C in a gas mixture of 25%N₂ and 75%H₂ and by active screen plasma carburising at 370 and 410°C in a gas mixture of 1.5%CH₄ and 98.5%H₂.
- (2) Except for the dual layer structure of 450°C plasma carburised sample, SEM cross-sectional micrographs of all other plasma alloyed samples (i.e. plasma nitriding at 350, 390 and 430°C and plasma carburising at 370 and 410°C) show a single surface modified layer, the thickness of which increases with increasing the treatment temperatures.
- (3) Cross-sectional TEM (XTEM) studies have revealed that the 390°C plasma nitrided layer consists of S-phase, nitrogen containing martensite and Fe₃N, which have a preferred orientation; the 410°C carburised layer is mainly composed of S-phase embedded with carbides.
- (4) Both active screen plasma nitriding and carburising can significantly improve the surface hardness of 17-7PH stainless steel. The hardening effect increases with the increase in the treatment temperature. The highest surface hardness of plasma carburised and nitrided 17-7PH stainless steel can reach about 1200 and 1400HV0.05 respectively, which represents an improvement of about 6-7 times over the untreated material.

- (5) Active-screen plasma surface alloying with carbon and nitrogen can effectively increase the wear resistance and reduce coefficient of friction of 17-7 PH steel mainly due to the change of wear mode from severe adhesive/delamination wear to mild oxidative wear. The 430°C nitriding and 410°C carburising show the best improvement (~ 3.5 times) in wear resistance of 17-7 PH steel.
- (6) The electrochemical corrosion and salt spray resistance of 17-7PH stainless steel can be improved by active screen plasma nitriding at 350, 390 and 430 °C. Plasma carburising at 370 and 410 °C can effectively enhance electrochemical corrosion resistance but their salt spray resistance is similar to or marginally lower than that of the untreated material.
- (7) For 17-7PH stainless steel, plasma carburising at 410°C could be an optimal treatment temperature to achieve combined enhancement in corrosion and wear resistance.

Active –screen plasma surface alloying of 17-4 PH steel

- (8) A single modified layer can be produced in the surface of 17-4 PH martensitic precipitation hardening stainless steel by active-screen plasma surface alloying with nitrogen (i.e. nitriding) or carbon (i.e. carburising).
- (9) Similar for 17-7 PH steel, the thickness of the plasma modified surface layer formed on 17-4 PH steel increases with the treatment temperature. However, when carburised under the same condition, a thicker layer formed on 17-4 PH steel than on 17-7 PH steel; the opposite occurs when plasma carburised under the same condition.

- (10) Both XRD and XTEM studies have revealed that the plasma nitrided layer formed on 17-4 PH steel consists of nitrogen containing martensite together with Fe_3N , Fe_4N and Cr_2N ; carbon containing martensite and carbides (χ - Fe_5C_2 & Cr_{23}C_6) are main phases identified in the plasma carburised layers.
- (11) When plasma surface alloyed under the same conditions, except for 450°C nitriding, a much effective hardening has been observed in 17-4 PH steel than in 17-7 PH steel. The highest surface hardness of plasma carburised and nitrided 17-4PH stainless steel can reach about 1600 and 1400HV0.05 respectively, which represents an improvement of about 7-8 times over the untreated material.
- (12) The tribological properties of 17-4 PH steel can be effectively improved by active-screen plasma surface alloying with carbon and nitrogen in terms of increased wear resistance by more than two orders of magnitude and reduced coefficient of friction owing to the change of wear mode from severe adhesive/delamination wear to mild oxidative wear.
- (13) Only plasma nitriding at 350°C and plasma carburising at 370°C can improve the corrosion resistance of 17-4PH stainless steel. Increasing the temperature has no positive or indeed negative effect mainly due to the precipitation of chromium nitrides or carbides.
- (14) Plasma carburising at 410°C could be an optimal treatment for 17-4PH stainless steel to achieve combined enhancement in corrosion and wear properties.

Chapter 7 – Future Work

The present work has shown that it is feasible to improve the surface hardness, tribological properties and corrosion resistance of both 17-4 PH and 17-7 PH precipitation stainless steels by low-temperature active-screen plasma surface alloying with carbon or nitrogen. However, future study is needed to further optimise the plasma technique and the following topics are suggested.

- ***Corrosion-wear***

The wear and corrosion properties of the plasma surface engineered samples have been evaluated separately. However, in some applications, stainless steel components are subject to wear in corrosive mediums (such as sea water). Therefore, it is necessary to evaluate the performance of the plasma nitrided and plasma carburised samples under corrosion-wear conditions such as sliding wear in simulated sea water or diluted acid solutions.

- ***Plasma surface alloying with both carbon and nitriding***

In the present study, plasma surface alloying with nitrogen (plasma nitriding) or carbon (plasma carburising) have been investigated. It would be scientifically interesting and technologically important to study the synergetic effect of plasma surface alloying with both nitrogen and carbon simultaneously (i.e. plasma carbonitriding).

References

- Abedi, H. R., Salehi, M., Yazdkhasti, M., & Hemmasian, A. (2010). Effect of high temperature post-oxidising on tribological and corrosion behaviour of plasma nitrided AISI 316 austenitic stainless steel. *Surface and Coatings Technology* , 85, 443-447.
- Appleman, B. R., & Campbell, P. G. (1982). Salt-Spray testing for short-term evaluation of coatings. *Journal of Coatings Technology* , 54 (686), 17-25.
- Baba, H., Kodama, T., & Katada, Y. (2002). Role of nitrogen on the corrosion behaviour of austenitic stainless steel. *Corrosion Science* , 44, 2393-2407.
- Bell, T., & Zhang, Z. L. (1985). Structure and corrosion resistance of plasma nitrided stainless steel. *Surface Engineering* , 3, 131-136.
- Bielawski, J., & Baranowska, J. (2010). Formation of nitrided layers on duplex steel - influence of multiphase substrate. *Surface Engineering* , 26 (4), 299-304.
- Blawert, C., Mordike, B. L., Jiraskova, Y., & Schneeweiss, O. (1999). Structure and composition of expanded austenite produced by nitrogen plasma immersion ion implantation of stainless steels X6CrNiTi1810 and X2CrNiMoN2253. *Surface and coatings technology* , 116-119, 189-198.
- Blawert, C., Weisheit, A., Mordike, B. L., & Knoop, R. M. (1996). Plasma immersion ion implantation of stainless steel: austenitic stainless steel in comparison to austenitic-ferritic stainless steel. *Surface and Coatings Technology* , 85 (1-2), 15-27.

Bruhl, S. P., Charadia, R., Simison, S., Lamas, D., & Cabo, A. (2010). Corrosion behaviour of martensitic and precipitation hardening stainless steels treated by plasma nitriding.

Callister, W. D., & Rethwisch, D. G. (2011). *Fundamentals of Materials Science & Engineering: An integrated approach*. John Wiley & Sons.

Campbell. (2008). *Elements of metallurgy and engineering alloys*. ASM international.

Chattopadhyay, R. (2004). *Advanced thermally assisted surface engineering processes*. Norwell, Massachusetts: Springer.

Cobb, H. M. (2010). *The History of Stainless Steel*. Materials Park, OH: AST International.

Corengia, P., Walther, F., Ybarra, G., Sommadossi, S., Cobari, P., & Broitman, E. (2006). Friction and Rolling-sliding wear of DC-pulsed plasma nitrided AISI 410 martensitic stainless steel. *Wear* , 260 (4-5), 479-485.

Corujeira Gallo, S., & Dong, H. (2009). On the fundamental mechanisms of active screen plasma nitriding. *Vacuum* , 84, 321-325.

Czerwiec, T., Renevier, N., & Michel, H. (2000). Low temperature plasma assisted nitriding. *Surface and Coatings Technology* , 131 (1-3), 267-277.

Davis, J. R. (1994). *Stainless steel*. Materials Park, OH: ASM International .

Dong, H. (2010). S-Phase surface engineering of Fe-Cr, Co-Cr and Ni-Cr alloys. *International Materials Review* , 55, 65-98.

- Dong, H., Esfandiari, M., & Li, X. Y. (2008). On the microstructure and phase identification of plasma nitrided 17-4 precipitation hardening stainless steel. *Surface and Coatings Technology* , 202 (13), 2969-2975.
- Esfandiari, M., & Dong, H. (2006). Plasma surface engineering of precipitation hardening stainless steel. *Surface Engineering* , 22 (2), 86-92.
- Esfandiari, M., & Dong, H. (2007). The corrosion and corrosion-wear behaviour of plasma nitrided 17-4 precipitation hardening stainless steels. *Surface and Coatings Technology* . , 202 (3), 466-478.
- Hong, T., & Nagumo, M. (1997). The effect of Chloride concentration on early stages of pitting for type 304 stainless steel revealed by the AS impedance method. *Corrosion Science* , 39 (2), 285-293.
- Ichii, K., Fujimura, K., & Takasa, T. (1986). Structure of the ion-nitrided layer of 18-8 stainless steel. . *Technology reports of the Kansai University. No 27.* , 135-144.
- John, P. I. (2005). *Plasma sciences and the creation of wealth*. New Delhi: Tata McGraw-Hill Education.
- Khatak, H. S. (2002). *Corrosion of austenitic stainless steel: Mechanism, Mitigation and Monitoring* . Cambridge: Woodhead Publishing .
- Krauss, G. (1989). *Steel: Heat Treatment and Processing Principles*. Materials Park: ASM International.
- Kutz, M. (2002). *Handbook of materials selection*. New York: John Wiley.

- Lewis, D. B., Stevenson, P. R., Cawley, J., & Matthews, A. (1993). Metallurgical study of low temperature plasma carbon diffusion treatments for stainless steels. *Surface and Coating Technology* , 60, 416-423.
- Leyland, A., Lewis, D. B., Stevenson, P. R., & Matthews, A. (1993). Low temperature plasma diffusion treatment of stainless steels for improved wear resistance. . *Surface and Coatings Technology* , 62 (1-3), 608.
- Li, C. X., & Bell, T. (2004). Sliding wear properties of active screen plasma nitrided 316 austenitic stainless steel. *Wear* , 256 (11-12), 1144-1152.
- Li, X. Y. (2001). Low temperature plasma nitriding of 316 stainless steel - nature of the S-phase and its thermal stability. *Surface engineering* , 17 (2), 147-152.
- Li, Y., & Bell, T. (2007). A comparative study of low temperature plasma nitriding, carburising and nitrocarburising of AISI 410 martensitic stainless steel. *Materials Science and Technology* , 355-361.
- Liang, W., Bin, X., Zhiwei, Y., & Yaqin, S. (2000). The wear and corrosion properties of stainless steel nitrided by low-pressure plasma-arc source ion nitriding at low temperatures. *Surface and Coatings Technology* , 130 (2-3), 304-308.
- Mannan, S., & Lees, F. P. (2005). *Lee's loss prevention in the process industries: Hazard identification, assessment and control. Volume 1*. Elsevier.
- Manova, D., Thorworth, G., Mandi, S., Newman, H., Stritzker, B., & Rauschenbach, B. (2006). Variable lattice expansion in martensitic stainless steel after nitrogen ion implantation. *Nuclear Instruments and Methods in Physics*

research SectionB: Beam Interactions with Materials & Atoms. , 242 (1-2), 285-288.

Marchev, K., Cooper, C. V., Blucher, J. T., & Giessen, B. C. (1998). Conditions for the formation of a martensitic single-phase compound layer in ion-nitrided 316L austenitic stainless steel. *Surface coatings and technology , 99 (3), 225-228.*

Menthe, E., Bulak, A., Oife, J., Zimmerman, A., & Rie, K. T. (2000). Improvement of the mechanical properties of austenitic stainless steel after plasma nitriding. *Surface and Coatings Technology , 1333, 259-263.*

metals, A. s. (1976). *Source book on stainless steels.* USA: Taylor & Francis.

Nakagawa, H., & Miyazaki, T. (1999). Effect of retained austenite on the microstructure and mechanical properties of martensitic precipitation hardening stainless steel. *Journal of materials science , 34 (16), 3901-3908.*

Onate, J., Dennis, J., & Hamilton, S. (1990). Wear behaviour of nitrogen-implanted AISI 420 martensitic stainless steel. *Surface and Coatings Technology , 42, 199-131.*

Phillip, M., & Bolton, W. (2002). *Technology of engineering materials.* Elsevier.

Pinedo, C. E., & Monterio, W. A. (2004). On the kinetics of plasma nitriding a martensitic stainless steel type AISI 420. *Surface and Coatings Technology , 179 (2-3), 119-123.*

Rahman, M., Haider, J., & Hasmi, M. J. (2005). Low temperature plasma nitriding of 316 stainless steel by a saddle field fast atom beam source. *Surface and Coating Technology , 200 (5-6), 1645-1651.*

- Rajan, T. V., Sharma, C. P., & Sharma, A. (1994). *Heat treatment principles and techniques*. New Delhi: PHI Learning Pvt Ltd.
- Sun, Y., & Bell, T. (2003). Low temperature plasma nitriding characteristics of precipitation hardening stainless steel. *Surface Engineering* , 19 (5), 331-336.
- Sun, Y., & Bell, T. (1998). Sliding Wear characteristics of low temperature plasma nitrided 316 austenitic stainless steel. *Wear* , 218 (1), 34-42.
- Sun, Y., & Bell, T. (1994). Wear behaviour of plasma-nitrided martensitic stainless steel. *Wear* , 178 (1-2), 131-138.
- Thaiwatthana, S., Li, X. Y., Dong, H., & Bell, T. (2003). Corrosion wear behaviour of low temperature plasma alloyed 316 austenitic stainless steel. *Surface Engineering* , 19 (3), 211-216.
- Totten, G. (2006). *Steel Heat Treatment: Metallurgy and technologies*. . Cambridge: CRC press.
- Wang, L., Shijun, J., & Sun, J. (2006). Effect of nitriding time on the nitride layer of AISI 304 austenitic stainless steel. *Surface and Coatings Technology* , 200 (16-17), 5067-5070.
- Xi, Y., Liu, D., & Han, D. (2008). Improvement of corrosion and wear resistances of AISI 420 martensitic stainless steel using plasma nitriding at low temperature. *Surface and Coatings Technology* , 202 (12), 2577-2583.
- Yang, D., He, S., Yang, J., Liu, Y., & Ye, Z. (2011). Microstructural and tribological characterisation of plasma - and gas - nitrided 2Cr13 steel in vacuum. *Materials & Design* , 32 (2), 808-814.

Young, C. A. (2008). Hydrometallurgy. *Proceedings of the Sixth International Symposium* (p. 1039). SME.

Zhang, Z. L., & Bell, T. (1985). Structure and corrosion resistance of plasma nitrided stainless steel. *Surface Engineering* , 1 (2), 131-136.

Zhao, C., Wang, L. Y., & Han, L. (2008). Active screen plasma nitriding of AISI 316L austenitic stainless steel at different potentials. *Minerals and Mining: Institute of Materials* .